University of Puerto Rico
Faculty of Natural Sciences
Department of Environmental Sciences
Rio Piedras, Puerto Rico

The impact of land use and land cover changes and human dynamics in Jobos Bay National Estuarine Research Reserve in Puerto Rico

By

Marianne Cartagena Colón

A Dissertation Submitted in Partial
Fulfillment of Requirements
For the Degree of

Doctor of Philosophy

June 2022

The impact of land use and land cover changes and human dynamics in Jobos Bay National Estuarine Research Reserve in Puerto Rico

Accepted by the Faculty of the Doctoral Program in Environmental Sciences of the University of Puerto Rico in partial fulfillment of the requirements for the degree of

Doctor of Philosophy

_____

Qiong Gao, Ph.D.
Professor of the Department of Environmental Sciences
Thesis Advisor

_____

Loretta Roberson, Ph.D.
Associate Scientist of the Marine Biological Laboratory
Thesis Committee Member

_____

Lorna Jaramillo, Ph.D.
Professor of the Department of Physical Sciences
Thesis Committee Member

_____

Hernando Mattei, Ph.D.
Professor of the Graduate Scholl of Public Health
Thesis Committee Member

_____

Carlos García-Quijano, Ph.D.
Professor of the Sociology, Anthropology and Marine Affairs
Thesis Committee Member

June 13th, 2022

Acknowledgments

First, I want to acknowledge the sponsors that believed in this project and gave funding to fulfill every research phase. This project was supported by the National Science Foundation - IGERT (Grant 0801577) for the first two years. The Centers of Research Excellence in Science and Technology (CREST) this program supports minority-serving institutions' research capabilities. The Ecological Society of America (ESA) for the Hurricane Recovery Grant for materials. During the last four consecutive years, this project was supported by the Puerto Rico NASA Space Grant Consortium (Grant 80NSSC20M0052).

Stepping onto an academic career path is an emotionally complex endeavor work filled with challenges, and difficulties, excitement and happiness while expand beyond the scientific domain. Throughout the writing of this dissertation, I have received a great deal of support and assistance. First, I want to thank my mentor, Professor Qiong Gao, whose expertise was invaluable in formulating the research questions and methodology. Your insightful feedback, especially on my English scientific writing, pushed me to sharpen my thinking and brought my work to a higher level. Also, I want to say big thanks to my dissertation committee members, Dr. Hernando Mattei, Dr. Lorna Jaramillo, Dr. Carlos García-Quijano, and Dr. Loretta Roberson. You have been with me since the beginning of my process and guided me to the best performance.

I want to acknowledge my mentors from my internships at the National Science Foundation (NSF) and NASA Ames Research Center (NASA-ARC) for their wonderful network and research opportunities. First, I would like to single out my mentors at NSF

and NASA-ARC, Mrs. Teresa Davies, and Dr. Juan Torres. Thank you for your patient support and for all the opportunities I was given to further my professional career as a Demographer and Environmental Scientist. I would also like to thank Dr. Jorge Ortiz for his valuable guidance throughout my studies since my undergraduate times. You provided me with the tools to choose the right direction and complete my dissertation with every recommendation letter. To Megan Culler from the U.S. EPA, your assistance in managing the IDM Toolbox created by EnviroAtlas was fundamental to this research. Thank you to the scientists at the USGS – NRCS, Dr. Manuel Matos and Dr. Lizandra Nieves. Your insight on the study area's erosion process was important to wisely tackle the research question.

I want to thank my life partner Dr. Elvis Torres Delgado, who supported me at every stage and was by my side, encouraging me to keep doing it even when things went difficult. Besides, I would like to thank my parents for their unique way of letting me know that we need to have love, respect for everyone, and determination to succeed. Finally, I could not have completed this dissertation without my friends, Dr. Chao Wang, David Torres, Dr. Loderay Bracero, Roselyn Méndez, Laura Fidalgo, Dr. Ose Pauleus, Brenda Santiago, Dr. Romarie Morales, and Dr. Claudia Patricia Ruiz. You all gave me interesting discussions and delighted distractions to rest my mind outside of my research. Also, I want to thank Dr. Marta Rodríguez, IGERT fellows, Grupo Determinados UPR, Mentes Puertorriqueñas en Acción (MAP), Mr. Pedro Carrión from Corredor El Yaguazo, and the community leaders Roberto Thomas, Hery Colón Zayas, Yaminette Rodríguez, Ruth (Tata) Santiago, Nelson Santos, and Héctor Sánchez and all the great people from Iniciativa de Ecodesarrollo de Bahia de Jobos (IDEBAJO) with

whom I will be forever grateful. I hope to have the honor of working with you soon. You are doing great things for the well-being of the people and the environment from solidarity and love. Kira (my dog) and Kumi (my cat), who have accompanied me and served as therapy, thank you.

Table of Contents

List of Tables

List of Figures

List of Abbreviations

JBNERR – Jobos Bay Natural Estuarine Research Reserve

C – Cover and Management Factor

DEM – Digital Elevation Model

GBW – Guánica Bay Watershed

IDM – Intelligent Dasymetric Mapping

JBW – Jobos Bay Watershed

K – Soil Erodibility Factor

L – Slope Length Factor

LS – Topographic Factor

LULC – Land Use and Land Cover

LULCC – Land Use Land Cover Change

NRCS – National Resources Conservation Service

P – Support Practice Factor

R – Rainfall Factor

RUSLE – Revised Universal Soil Loss Equation

S – Steepness Factor

SJBW – San Juan Bay Watershed

Abstract

Globally, the increasing land changes (i.e., urbanization and agricultural practices) in the coastal areas have exacerbated the anthropogenic stress on coastal ecosystems. Human activities on coasts often induce sediments and stressors that degrade the quality of coastal waters throughout the watershed soil erosion process. Specifically, estimates of population size and distribution are also important in allocating resources and managing land cover, and land uses to reduce the erosion impact on coastal areas. Understanding and tackling the impact of human settlements on coastal ecosystems requires interdisciplinary long-term research at a regional and local scale. However, according to land use and land cover profile, precise population data is not always available and needs to be prepared locally.

On the south coast of Puerto Rico, the Jobos Bay National Estuarine Research Reserve has been facing land changes in its watershed since the 1970s, particularly in agriculture activities and urban growth. The Jobos Bay Watershed (JBW) is historically considered an agricultural watershed, even when urban development began in the last four decades. Thus, population and housing estimates were needed to analyze the people residing within the reserve as part of the urban growth analysis and agricultural land conversion. This study assessed the potential impacts of land changes in the estuarine ecosystem thru soil erosion analysis by quantifying land cover changes from 1970 to 2010. Therefore, this work aims to develop a study to link changes in human population and housing units' distribution, and land changes to soil erosion rates to give insights into how these terrestrial processes at a local watershed scale may affect the estuarine waters quality of JBNERR.

Our study suggests that even when the housing settlements and population increased within the JBW, the housing units' densities declined in urban and forest areas from 1990 to 2000. Although it is difficult to explain how housing units reduce their distribution and density, for JBNERR, one reason for this diminution is spatial resolution forest growth. Pasture/grassland increased its population density and the housing unit density from 1990 to 2000. Still, it decreased from 2000 to 2010, contrary in urban areas. In this effort, our methods and results showed that urbanization and sprawl occur mostly from pasture and were continually increasing for the entire study period and in areas closer to the coastal line. Nevertheless, reforestation trends also have a high potential to continue because forest recovery occurred at 44.7% between 1991 and 2000 and 42.4% between 2000 and 2010, especially in the upper east area of JBW.

Respectively to these land changes, the predicted soil erosion rate decreased in cultivated lands between 1977 and 2010. This study illustrated spatiotemporal changes in soil erosion rates based on the Revised Universal Soil Loss Equation (RUSLE) and Hot Spot Analysis. The annual average soil loss was estimated to be 9.8 ton/ha/y in 1977, increasing to 16.0 ton/ha/y in 1991, 11.5 ton/ha/y in 2000, and decreasing to 8.7 ton/ha/y in 2010. The spatiotemporal distribution of soil erosion exposure showed that from 1977 to 2010, more than 40% of the watershed had slight soil loss, around 10% was slight to moderate, more than 13% was moderate, around 5% was moderate and around 11% was very highly exposed. The potential soil erosion risk and severity increase from the mid-upper Northeast to the lowlands reaches of the Jobos Bay Watershed. As evidence from 1977 to 2010, hot spots analysis related to soil loss confirmed that pasture/grass in steep

areas is more vulnerable to soil loss. Cultivated land placed very close to the coast is also susceptible to soil erosion.

This study revealed that the assessment of population and housing distribution linked to land changes provides an insight into the soil erosion process due to economic shift and cultivated land conversion in JBNERR. This finding gives a great base for further research integrating local knowledge from the communities in JBW to track soil erosion related to cultivated land activities in the area and come up with recommendations related to the soil conservation policy.

Biographic Sketch

Mrs. Cartagena attained a Ph.D. in Environmental Sciences at the University of Puerto Rico. Her Master's Degree is in the Science of Demography. She was selected as the Prominent Student of her graduating class in 2011. Her Bachelor's Degree is in Environmental Sciences.

Mrs. Cartagena worked at The Department of Health in Puerto Rico as a Consultant for statistical analysis and demographic issues. She published the Annual Vital Statistics Reports. In addition, Mrs. Cartagena improved the vital statistical analysis quality by providing better definitions for computer programmers to upgrade databases. She was selected to be a Member of the Committee on Infant Death and Maternal Death to identify malpractice trends. Also, she was recognized as a Prominent Professional by the Auxiliary Secretariat of Planning and Development, Department of Health. As a doctoral student, she was awarded an Integrative Graduate Education and Research (IGERT) Fellowship sponsored by the National Science Foundation and a Puerto Rico NASA Space Grant Consortium Fellowship. Besides, she worked as a Professor Assistant, guiding undergraduates' students in their Capstone research projects, and she participated in three graduate internships at National Science Foundation (NSF), Organización Mentes Puertorriqueñas en Acción (MPA), and at NASA Ames Research Center. She is always looking forward to community service integrating socio-environmental science research that involves collaborations with scientists and people in the community.

Introduction

Estuarine environments are the main critical interfaces between land and sea receiving most of the drainage waters coming from land through the fluvial network and also intermittently shallow marine waters through tidal and wave processes (Osei-Twumasi & Falconer, 2014; Traini et al., 2008). Physical alteration of habitats also creates persistent and serious environmental problems, such as large-scale modifications of coastal watersheds (e.g. deforestation and construction, marsh diking and impoundment, bulk-heading and lagoon formation) and estuarine basins (e.g. dredging and dredged material disposal, channel and inlet stabilization, and harbor and marina development), which adversely affect estuarine organisms (Kennish, 2002).

Environmental problems encountered in estuarine environments invariably stem from overpopulation and uncontrolled development in coastal watersheds, as well as human activities in the estuarine embayment themselves (Kennish, 2002). The nature of estuaries, where fresh and marine water ecosystems converge with increasing concentrations of urban development, a fragile balance exists between the needs of coastal cities and communities, and the health of aquatic ecosystems (Lipp et al., 2001). Carter et al. (1973) describe a "short-circuiting" effect of man-made canals that effectively decouples natural estuarine ecological processes from their normal input pathways by shunting overland freshwater drainage directly from the uplands to the estuary.

Coastal urbanization is expanding disproportionally to human population growth (Fabricius, 2005). In just forty years (1970 – 2010) coastal shoreline counties added 125 persons/mi^2, coastal watersheds counties added 99 persons/mi^2 and the United States of

North America as a whole added 36 persons/mi^2 (NOAA, 2013). Regardless of how the coast is defined, it is substantially more densely populated than the U.S. as a whole, and the population density in coastal areas will continue to increase (NOAA, 2013). Accelerated population growth and development in the coastal zone, accompanied by increasing urbanization and industrialization, are closely coupled to these anthropogenic impacts, which have compromised the ecological integrity of many estuaries (Kennish, 2002).

Then, land use / land cover (e.g., urban development, industrial, agriculture) changes, and anthropogenic activities may lead to introduce pollutants to estuary waters. For example, agriculture affects 60% of impaired river miles and in estuaries affects 34% of impaired acres, the third largest source behind the urban run-off and municipal point sources (Parry, 1998). Even relatively small changes in the type of land cover could have major effects on rates of soil erosion. For example, if only 5% of the watershed with the highest erosion rates (bare soil, agriculture on steep slopes) is transformed into closed-canopy forests, erosion in the watershed will decrease by 20% (Grau et al., 2003). Detailed analysis revealed a number of general features including positive relationships of erosion rate with slope and annual precipitation, and a significant effect of land use, with agricultural lands yielding the highest erosion rates, and forest and shrublands yielding the lowest (García-Ruiz et al., 2015). Erosion rates are controlled by rainfall intensity, soil erodibility, slope, land cover, and management practices (Grau et al., 2003). Parts of the stressors that degrade the water quality are erosion and sedimentation accelerated by land-use change, which can alter soil water chemistry with flow-on effects for aquatic ecosystems (Quinn & Stroud, 2002).

Likewise in Puerto Rico the consequences of land clearing and modification, first for agriculture and later for urban development, has increased watershed sediment and nutrient yield, thereby increasing sediment and nutrient discharge to the shelf, which has likely contributed to the widespread degradation of ecosystems that surround the island (Larsen & Webb, 2009; Warne et al., 2005). The effects of river-derived sediment and nutrient discharge on the coral reefs as part of coastal ecosystems are especially apparent in nearshore areas of the north, southwest, and west coasts (Larsen & Webb, 2009). The results of Ryan, Walsh, Corbett, & Winter (2008) study, suggest that modern local terrestrial sediment accumulation approximately doubled the one from the early 20th century, and the cause for this change cannot be unequivocally established, land-use change in the watershed (i.e., coastal development) is hypothesized to play a role in Puerto Rico.

In the coastal plains on Puerto Rico, much of the original flora has been removed to make room for coastal agriculture (especially sugarcane during the 1800s) and development (García-Quijano, Poggie, Pitchon, & Del Pozo, 2015). According to Lal (2001), the type of land use and its management are mainly influenced by social, economic, and policy causes, and by consequence influence the soil erosion rates and the severity of soil degradation. To emphasize, in Puerto Rico, 124,187 ha (306,873 acres), or 14% as well-suited to mechanized agriculture, with slopes under 10% and this land is mainly located in the coastal plains and interior valleys, with the largest patches located in the northwest and south of the island (Gould, Wadsworth, Quiñones, Fain, & Álvarez-Berríos, 2017). Gould et al., (2017) noted the most important impact from agriculture in Puerto Rico:

> *The coastal and interior plains of Puerto Rico encompass 240,000 ha (27% of all land). Of these, 142,292 ha (16%) are classified by the Puerto Rico Department of Agriculture as agricultural reserves, and 98,247 ha (11% of all land) are developed. Within the agricultural reserves, 21,774 ha (15%) are wetlands, and 16,072 ha (11%) are currently forested.*

In the case study area of Jobos Bay, located in the south eastern of Puerto Rico, elements of a physical and biological nature exert influences to create and maintain the dynamics of estuarine ecosystems such as an ecological unit sculpted by natural and anthropic factors, located in the southeastern shore of Puerto Rico (Laboy-Nieves, 2009). All the land adjacent to Jobos Bay National Estuarine Research Reserve (JBNERR) has been impacted by human activities and has suffered modifications in the hydrology, nutrient dynamics, and impediment of the establishment of mangrove species and associated communities in the past three decades (Laboy et al., 2008). Land use at the watershed has gone through changes in growth in urban development and corresponding conversion of agricultural lands to commercial or residential areas, changes in irrigation methods, and the establishment of new industries that can potentially affect the ecosystems (PRWRERI, 2013). These changes or causes (e.g. poverty and illiteracy, political instability, and high demographic pressure), influence the rate of soil erosion which determines the severity of soil degradation (Lal, 2001). Therefore, in terms of land changes and anthropogenic activities, tackling the above-mentioned challenges and drifting the effects requires a great effort to know where intensity changes were shown, how changes occurred and why changes occurred. This is also key to recognize how soil erosion is responding to land changes and reach better soil conservation policy and soil practices in JBNERR. Since soil erosion is the response of the combination of climatic and physical factors, as well as the influence of the topographic factor and land use/land

cover changes (LULCC) aspects, where LULCC might be in part a consequence of human activities.

In this sense, a soil erosion model for JBNERR can be extended to determining soil erosion rates (in units of mass per area and time) under a large range of climatic conditions and land uses, and involving various measurement methods (García-Ruiz et al., 2015). One of the most relevant extensions of erosion and sedimentation analysis is that it can be attached to the watershed unit analysis. Although, data collection is harder for detailed models, by using the GIS extension Revised Universal Soil Loss Equation (RUSLE) erosion rates was calculated.

To analyze and correlate the human settlements distribution to land changes over time 1990 – 2010, the integration of the land cover classification with the Census Blocks were applied to identify the densely populated land and the housing units by means of ArcGIS 10.6.1. The Dasymetric mapping methods is the method used to analyze this relationship. Mapping the distributions of human land uses provides critical information for managing landscapes to sustain their biodiversity and the structure and function of their ecosystems (Helmer, Ramos, López, Quinones, and Diaz, 2002). This method is a geospatial technique that uses information such as land cover classes as ancillary data, and the Digital Elevation Model (DEM) for slope analysis to have a more accurately distributed population data by areal interpolation, that have been assigned to predetermined boundaries (Zandbergen & Ignizio, 2010).

To our knowledge, little research has been done to quantitatively investigate the different and demographic dynamics and biophysical drivers on LULCC and estimate the soil erosion rates over JBNERR area. For better understanding the impact of land

use/land cover change in estuarine ecosystems, we assessed the performance of available erodibility factors through investigating the role of rainfall erosivity (R), topographic factor (LS) soil erodibility (K), and Cover Management (C) on soil erosion in JBNERR from 1991 to 2000 (Figure 1).

Figure 1.

Conceptual Research framework

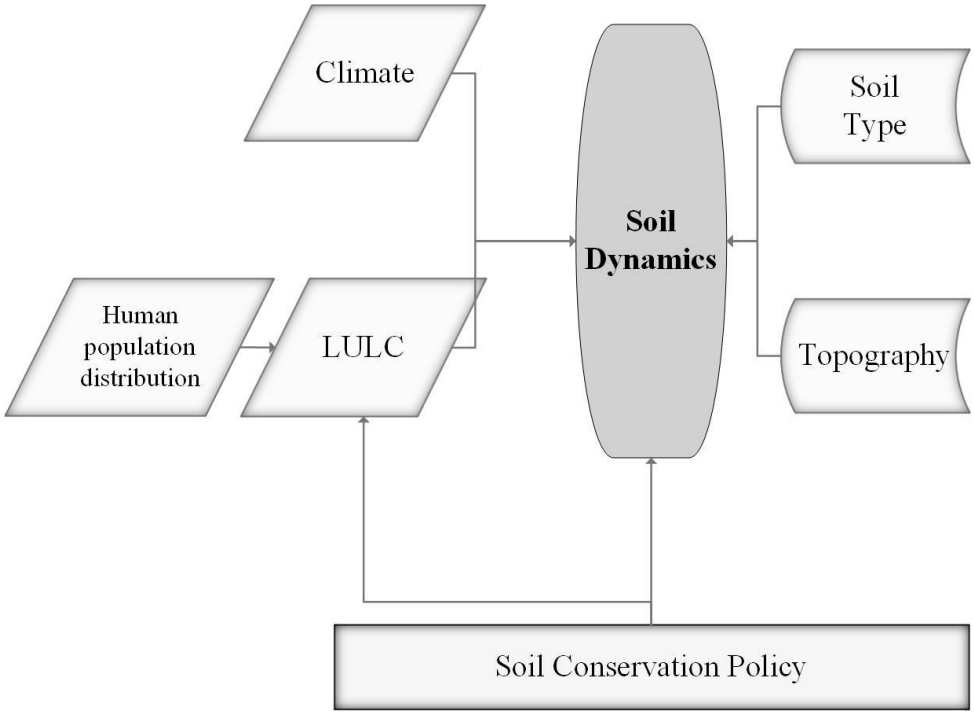

The aim of this work was to develop an analysis to link changes in human population and housing units' distribution, LULCC to soil erosion rates and, describe and give insights about how these terrestrial processes are affected by soil conservation policies and how may affect estuarine waters quality in JBNERR. In sum, the inputs to the analysis are land use and land cover (1977 – 2010), decennial censuses (1990 – 2010), and the results of soil erosion thru the Revised Universal Soil Loss Equation

(RUSLE) (). RUSLE contemplates Daily Rainfall from 1970 – 2015, Soil Properties profile, Topographic analysis, and Conservation of soil (if any), and Agricultural practices in JBNERR.

Figure 2.

Database assessment framework

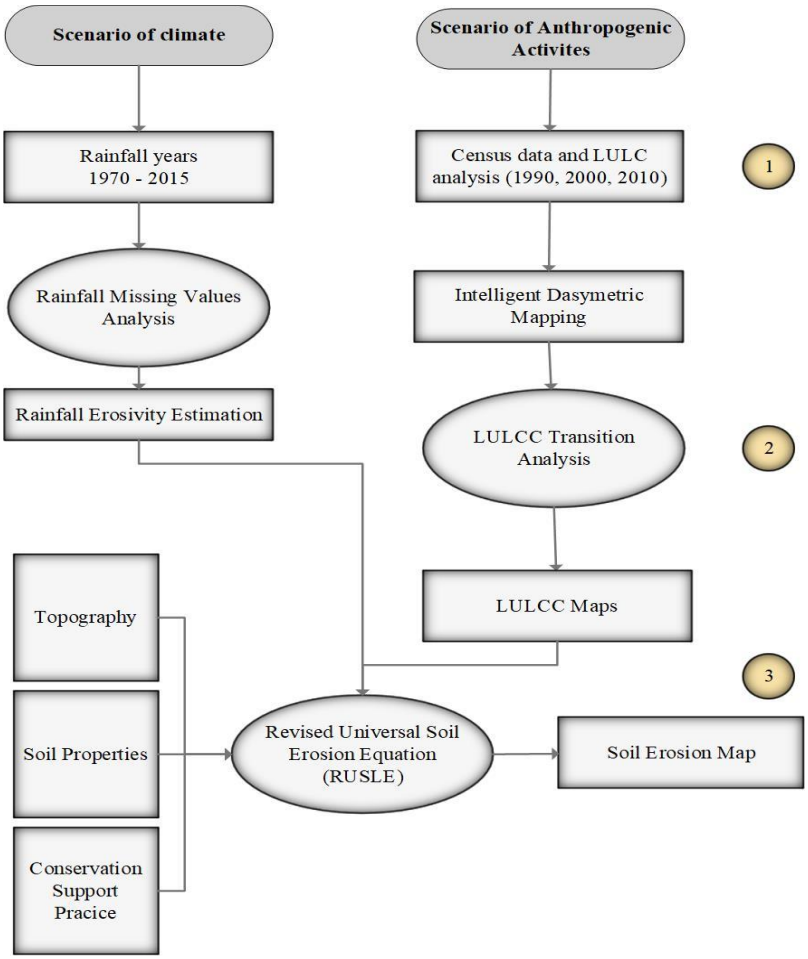

Source: Flowchart adapted from Paroissien, J. B., Darboux, F., Couturier, A., Devillers, B., Mouillot, F., Raclot, D., & Le Bissonnais, Y. (2015). A method for modeling the effects of climate and land use changes on erosion and sustainability of soil in a Mediterranean watershed (Languedoc, France). Journal of Environmental Management, 150 (May), 57–68. https://doi.org/10.1016/j.jenvman.2014.10.034 (Paroissien et al., 2015).

Thesis Composition

The dissertation is composed of three chapters. First, there is an introduction to estuarine ecosystems and how they interact with the terrestrial ecosystems, how estuarine are influenced by anthropogenic activities taking place in its closest watershed. Hence this dissertation seeks to understand the impact of land change and the role of different driving factors (i.e., elevation, slope, soil, rainfall, population density, agriculture, and urban development) working on the LULCC in estuarine ecosystems, to accomplish this goal LULCC, erosion rates, and population distribution at JBNERR from 1977 to 2010 were analyzed. To understand the impact of changes in LULC, particularly agriculture and urban development, the following is structure is presented.

The Chapter II presents a study of how the patterns of land use/land cover depend on human population distribution. By integrating the land cover images derived from objective two and the census blocks, the Intelligent Dasymetric Mapping (IDM) method was applied to identify the densely populated land. The research questions proposed an integrated approach to the watershed management that considers human settlements in areas are built and configured by modifying and/or transforming the land. However, urban development might be characterized as land conversion that is sometimes overestimated or not necessarily follows the population growth rates (Gibson et al., 2014). Using Geographic Information Systems (GIS) was possible to manage and associate information on LULCC and population censuses, by testing the following hypotheses that population density increased from 1990 to 2000, and decreased from 2000 to 2010, which in turn influence LULCC at JBNERR responding to the population trends in Puerto Rico. In Puerto Rico the total population began to decrease after 2000 in

more than 5% because of the poor performance of the Puerto Rican economy for example lack of jobs opportunities (Abel & Deitz, 2014).

Chapter III presents impact of the patterns of land use/land cover changes, particularly on cultivated lands and urban development. In this chapter was based on determine and analyze LULC maps to quantify the changes rates and magnitudes between different LULC classes for the period of 1977 – 2010 to then analyze LULC with urban development and agricultural activities in the watershed. Jobos Bay watershed, still having conflicts in harmonize land use and resource protection, which evolved from sugarcane agriculture to increasingly urban and industrial use in the late 1970's. This changing pattern is raising water quality and quantity concerns which, in turn, could imperil the Reserve's sustainability as a pristine estuarine habitat, a key criterion for National Estuarine Research Reserve (NERRS) (Laboy et al., 2008). It was important to apply a multi-temporal study to detect land changes between two or more reference dates and give insights to plan the appropriate measures to prevent its soil degradation and ensure its best conservation. A Transition Matrix was performed to test the hypotheses that agriculture pattern has been changed because economy has been shifted after 1990 and converted mainly into pasture and urban development whereas forest recovery has mainly occurred in the upper and steepest areas gained from previously pasture/grass land after 1991.

Finally, Chapter IV presents the impact of how the patterns of land use/land cover changes (caused by human settlement distribution, agriculture, and urban development) and climate promote changes of erosion rates from 1977 – 2010 in JBNERR. In Chapter IV the erosion rates were calculated by using the Revised Universal Soil Loss Equation

(RUSLE) to identify and describe how erosion rates relate to changes in land use from 1977 to 2010 and human population settlements in the Jobos Bay watershed. This question leads the use of different datasets to comply the following focal question: (1) how soil erosion was influences by rainfall or topography or LULC over the period of 1977 – 2010 in JBW. The LULC mapping methodology was explored, and the following hypothesis were tested: agricultural land is expected to be related to higher soil erosion and conversion from pasture to forest will result in land less prone to erosive forces in JBW. Particularly, the upper and steeper areas are more prone to erode because of climate variables and the less steep and downhill areas are more prone to erode because of agriculture activities and urban development. Lastly, Chapter V presents the concluding remarks and recommendations for future research projects.

Chapter One. Dasymetric Mapping of Population and Housing Density Using Land Cover Data in JBNERR, Puerto Rico during 1990 – 2010

Abstract

Accurate and precise spatial population data are critical to allocating resources for socioeconomic development and the environmental management decision-making process of any country. However, such data are not always available and need to be prepared. JBNERR is a natural research reserve cover for two municipalities in the southeast of Puerto Rico, threatened by anthropogenic activities. Thus, population and housing estimates are needed to analyze the population residing within the reserve as part of the urban growth analysis. This study proposed a multi-class dasymetric mapping to estimate the housing units and population within JBNERR. The population increased by 19.48% with a growth rate of 0.97%, adding 5,583 new residents from 1990 to 2010. The housing units' estimates revealed that JBNERR watershed experienced an increase of 50.72%, corresponding to a growth rate of 2.54% by adding 5,076 new residents from 1990 to 2010. The highest maximum density corresponds to urban development with 254.8 ± 12.3 persons/900 m^2 in 1990, 71.2 ± 7.1 persons/900 m^2 in 2000, and 94.0 ± 4.8 persons/900 m^2 in 2010. The housing unit density, the highest maximum density corresponds to urban development with 80.3 ± 4.4 houses/900 m^2 in 1990, 21.2 ± 2.5 houses/900 m^2 in 2000, and 46.5 ± 2.1 houses/900 m^2 in 2010. Even when the residential development and population increased within the Jobos watershed, the housing units' densities decline in urban areas from 1990 to 2000 but increases from 2000 to 2010. In pasture/grass as open areas increased its population maximum density and the housing unit density from 1990 to 2000 but decreased from 2000 to 2010 contrary to urban areas. In this effort, our methods and results help to assess areas of major vulnerability for urban

growth since housing development is a critical concern because indirectly threatens ecological and recreational impacts in JBNERR.

Introduction

Accurate and precise spatial population data are critical to assign resources and services for the country's socioeconomic development and environmental management decision-making process. However, such data are not always available and need to be prepared. Specifically, estimates of population size and distribution are vital for socioeconomic planning and management decisions such as allocating food and medical supplies and transportation to analyze and address political, environmental issues, land uses, and regional development (Deng, 2013; Su et al., 2010). The size and distribution of the population, as well as housing units, are often key determinants for resource allocation to establish political boundaries, to monitor the impact of public policies, and to estimate the need for schools, roads, parks, public transportation, etc., for state and local governments (Smith et al., 2002). Considering these wide-reaching impacts, there is a growing demand for fine-resolution and spatially explicit social data that can be used to document how the pattern and extent of the population and housing density changes over time (D. G. Brown et al., 2005). In this context, detailed and contemporary datasets accurately describing the distribution of residential population in the region are required for measuring the impacts of population growth, monitoring changes, supporting environmental and health applications, and planning interventions (Sorichetta et al., 2015).

Censuses are commonly used as the major source for population distribution information (Su et al., 2010). The U.S. Decennial Census data comprises three spatial

aggregation levels based on administrative units and the total population counts (census tract, block group, and block) (Jia & Gaughan, 2016). A census is conducted every ten years at any geographical scale across most of countries (Briggs et al., 2007). The decennial censuses in the United States benefit from bringing aggregate data at finer geographic units such as the census tract or census block. However, even detailed data may be recorded for each person in a census, and privacy concerns prevent these data from being released (Su et al., 2010). To satisfy this demand, researchers are increasingly turning to remotely sensed data and other geospatial data sets to refine the process of producing high-resolution estimates of population density (Stevens et al., 2015).

New methodologies are needed to estimate human population and housing unit distributions more accurately (Deng, 2013; Jeremy Mennis & Hultgren, 2006; Stevens et al., 2015). One concern regarding the census data is that are often only available for administrative units with arbitrary boundaries that convey a wrong impression of homogeneous population density leading to analytical and cartographic problems, and the spatial patterns of population distribution within the aggregated units may be lost or distorted (Fisher & Langford, 1996; Weichselbaum & Papathoma, 2005). The spatial heterogeneity in population distribution exists between natural environments and regional developments (Su et al., 2010). To that land cover provides a useful indicator of where people live as a basis for detailed population mapping. However, it still suffers from a major limitation: how to derive weights for each land cover class or parcel that reflects its population density (Briggs et al., 2007).

Thus, land use and land cover (LULC) change is a key mediator of population-environment interactions. Demographic variables figure prominently among the driving

forces investigated and in which efforts are made to investigate the causal mechanism by which human population changes affect land use environment outcomes (National Research Council, 2005). The population and housing data (e.g., census data) is widely used as an indicator of urban devolvement in LULC change research, demographic factors including population growth, density, and housing growth are known to be important influences on LULC change (Entwisle & Stern, 2005) thru anthropogenic activities. For example, the population totals in a small area are closely related to the number of housing units in that area (Deng, 2013). Housing development has been occurring at unprecedented rates globally, and in the United States (Syphard et al., 2009).

On the other hand, the Latin America and the Caribbean region is one of the most urbanized regions globally, with a total population of around 630 million that is expected to increase by 25% by 2050 (Sorichetta et al., 2015). Though, housing development is growing substantially even when the population size declines and the average household size is declining in the United States (Liu et al., 2003). However, integrating geospatial technology (through GIS) and population census data helps understand how people use and develop the lands (Martinuzzi et al., 2007).

Dasymetric mapping has improved traditional choropleth maps by increasing the spatial variation and accuracy in which data is mapped to a surface. The dasymetric method is a well-known method in assist population interpolation (Wu et al., 2005). Wright, (1936) popularized it out of a concern that choropleth maps do not give a valid representation of population distribution within enumeration units (Wu et al., 2005). Choropleth maps have limited utility for detailed spatial analysis of socioeconomic data, where human populations are concentrated in relatively few towns and cities, found at

lower elevations, and along major river corridors (Holloway et al., 1997). Using satellite remotely sensed imagery to identify settled areas per land cover class, dasymetric mapping can produce an accurate representation (Langford & Unwin, 1994) as a method to estimate population and housing distributions integrating census data and LULC data.

In dasymetric representation, it is assumed that the entire population for each census unit (e.g., ward, block, track) is concentrated within the area as occupied on the classified image (Langford & Unwin, 1994). Dasymetric mapping may therefore be used to generate a surface model that provides a more accurate representation of population within rural block groups or even census block, as well as in urban block groups that contain parks, cemeteries, and other features that may control the within- block group distribution of population (Mennis, 2003). Mennis (2003) also pointed out that census block groups in urban areas may be relatively small and of homogeneous population density, while block groups in rural areas are typically much larger and have a much more heterogeneous population distribution. In this context, the fundamental census units block groups, blocks, or tracts are larger in rural areas than in urban areas increasing the heterogeneity in rural areas.

In sum, Dasymetric mapping refers to a process of disaggregating spatial data to a finer unit of analysis, using additional or "ancillary" data to help refine locations of population or other phenomena (Mennis, 2003). The combination of dasymetric refinement with areal interpolation has been demonstrated as a promising way to improve the precision and accuracy of small area population estimates for temporal analysis (Zoraghein et al., 2016). Dasymetric techniques have recently been examined to refine areal interpolation over multiple periods (Zoraghein et al., 2016). This method, known as

Intelligent Dasymetric Mapping (IDM), is used to assess population growth by land cover classes or land use types over time. Figure 3 shows three types of dasymetric mapping which are the total number of people aggregated by census delineated unit (a); binary (populated versus unpopulated) with populations evenly distributed within the inhabited land use (b); and multi-class weighted that represents an urban 3-class method (Peña, 2012; Sleeter & Gould, 2007). The IDM outcome is a raster representation of population per pixel (Sleeter & Gould, 2007).

Figure 3

Three population distribution techniques for Dasymetric Mapping

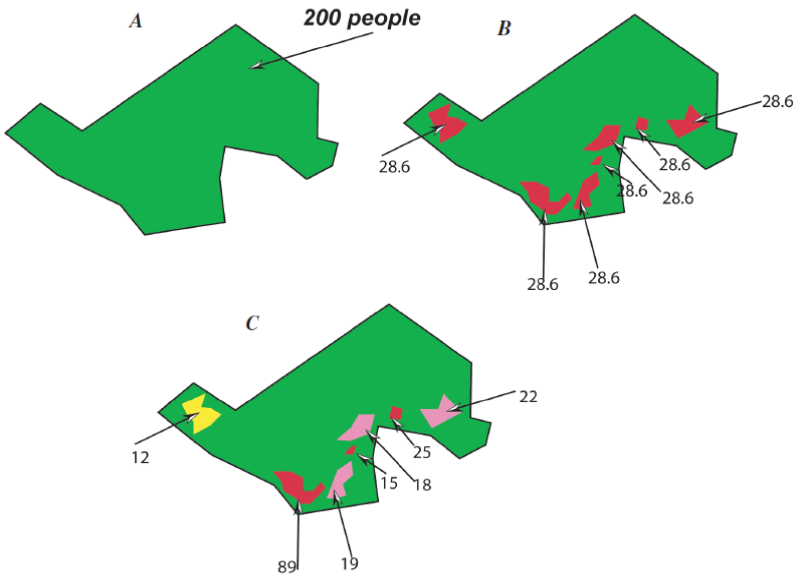

Note. Diagram showing three fundamental approaches to mapping population distribution. **A**, Total number of people, aggregated by census delineated unit; **B**, represents inhabited (red) verses uninhabited (green) with populations evenly distributed within the inhabited land use; and **C**, represents an urban 3-class method, where populations are distributed in high (red), medium (pink), and low (yellow) population class based on LULC-class code and areal weighting.
Source: Sleeter, R., & Gould, M. D. (2007). Geographic information system software to remodel population data using dasymetric-mapping methods. Reston, VA. Retrieved from http://purl.access.gpo.gov/GPO/LPS106635.

The IDM method implemented as a Geographic Information System (GIS) extension facilitates the technique's parameterization and returns a set of statistics that summarize the quality of the resulting dasymetric map (Jeremy Mennis & Hultgren, 2006). The main objective of this extension is to automate the process of taking population data from census enumeration units and transferring the data values to overlaying homogenous zones while (1) maintaining volume preserving properties and (2) using an empirical sampling method for determining relative densities for each homogenous zone (Sleeter & Gould, 2007). The ancillary data can be percent imperviousness, roads, nighttime lights and land cover/land use data (Jeremy Mennis, 2003, 2009, 2016; Jeremy Mennis & Hultgren, 2006; Mitsova et al., 2012; Schroeder, 2017). LULC data is the most frequently used as ancillary data. Overall, total population, total housing units, and land area obtained at the geographic census units are part of IDM inputs by using the land cover images as ancillary data. Besides, using ancillary data, visual interpretation, and expert knowledge of the area through GIS further refines the land cover classification results (Shalaby & Tateishi, 2007).

Housing development and population growth in rural areas have major implications for the region's ecology and forest management practice (Hammer et al., 2004). Asides, data on housing development and population growth can thus be enormously useful in understanding the effects of landscape change and formulating policies to guide future growth (Hammer et al., 2004). This supports why LULC data are commonly used to estimates population and housing distribution. Hence, population data are tied to primary residence and underestimate development in rural areas, especially those affected by significant seasonal and recreational use (Hansen, 2005). Furthermore,

there are important land-use changes at or beyond the urban fringe, including conversion of land in agriculture and forest, which are not well represented in traditional definitions of urbanization (Hansen, 2005). In particular, the agricultural history can focus more explicitly on the history of specific types of agriculture (i.e., cropped vs. pasture) and the demographic history can focus more explicitly on the density of housing units, which more closely relates to landscape changes of interest to ecologists (Hammer et al., 2004; Hansen, 2005; Radeloff et al., 2000).

In this sense, Puerto Rico has served as an interesting land cover transformation and demographic change for many scientists. Dramatic land changes on the Caribbean island of Puerto Rico during the last 70 years, as its economy shifted from agriculture to industry and services (Kennaway & Helmer, 2007). However, more information is needed about how the LULC data impact the housing units and population density within a natural reserve area or small rural areas, as is Jobos Bay National Estuarine Research Reserve (JBNERR) in Puerto Rico. JBNERR is an important area for its local economy, with fishing and tourism being the most common region activity. To illustrate, Pozuelo is the best-known fishing community in Guayama and is located on a peninsula that extends to the sea from Jobos Bay (García-Quijano et al., 2013). Also, the bay has social, cultural, and economic importance for the livelihoods of residents of neighboring coastal communities (García-Quijano et al., 2013).

To know the population and housing distribution is relevant because as the coastal population increases over the next two decades, anthropogenic impacts on estuaries are likely to increase unless effective management strategies are formulated (Kennish, 2002b). Even after being designated as a National Reserve, JBNERR is still threatened by

land use changes, such as urban development and industrial and agricultural activities. Land use in the JBNERR watershed has undergone changes in growing urban development and the corresponding conversion of agricultural land into commercial or residential areas, changes in irrigation methods, and new industries that can affect ecosystems (PRWRERI, 2013). This study aimed to 1) estimate the housing units and population within JBNERR using the land cover land use data as ancillary data, and 2) to estimate the population density and housing units' density thru the dasymetric mapping method. JBNERR is an ideal area to apply dasymetric mapping because this interpolation method outperformed for small study areas, temporal analysis of small-area demographic data commonly relying on areal interpolation methods create temporally consistent and compatible areal units (Zoraghein et al., 2016). The target zone boundaries would also necessarily change over time, and such an approach can also work in cases where the spatial ancillary data vary over time (Mennis, 2016).

The study area and the land cover data as an ancillary source in the mapping process are described in the following sections. Three decennial censuses, 1990, 2000 and 2010 and its variable (total population and total housing units) were used to outline the dasymetric mapping procedure and explain the tested intelligent dasymetric mapping methods. Finally, to assess the map errors in the mapping analysis, the Root Mean Square Error (RMSE), and the Mean Absolute Error (MAE) are presented in this chapter. The error assessment is critical since the most troubling issue for this particular project is that certain regions, such as industrial complexes, that are sparsely populated (in terms of residence) may be classified as high urbanization due to their dense road networks and

large areas of impervious surface, the spectral signature of which in T.M. imagery may resemble residential and commercial areas (Mennis, 2003).

Methodology

This paper applies the IDM methodology proposed by Mennis & Hultgren, 2006 since they emphasize that IDM is not restricted to use with U.S. Census data or even population data, but it can be applied to the estimation of any spatially aggregated count data like housing units. This method is demonstrated by dasymetric mapping for the total population and total housing units derived from the U.S. Census Bureau 1990, 2000, and 2010 at block level geographic level. The chosen study area is appropriate because it contained various LULC classes and covered several major landforms, including the coastal plain. Therefore, these classes' different population patterns are expected due to the large area lands classified as forest, pasture, and cultivated lands but small land extension as urban development.

Study area

The study area of JBNERR covers 137.3 km^2 where encompasses parts of Guayama and Salinas, two municipalities in Southern Puerto Rico (Figure 4). The land area of JBW contain the 38.9 % of both Guayama and Salinas total area. JBNERR is designated as part of the NOAA - National Estuarine Research Reserves System since 1981, serving as a living laboratory for scientists, communities, and other professionals from different academic backgrounds to conduct research. This reserve is protected and managed by the Puerto Rico Department of Natural Resources and the Environment and collaborates with universities in Puerto Rico and the United States, with input from local community organizations. The JBNERR is also known as Jobos Bay; its watershed belongs to the Rio Coamo watershed and is divided into four sub-watersheds: Rio Nigua,

Rio Seco, Quebrada Aguas Verdes, Rio Seco West, and East. Jobos Bay watershed is considered an agricultural watershed because of the high cropland activity close to the coastal plain.

Figure 4

Study area JBNERR watershed delimitation.

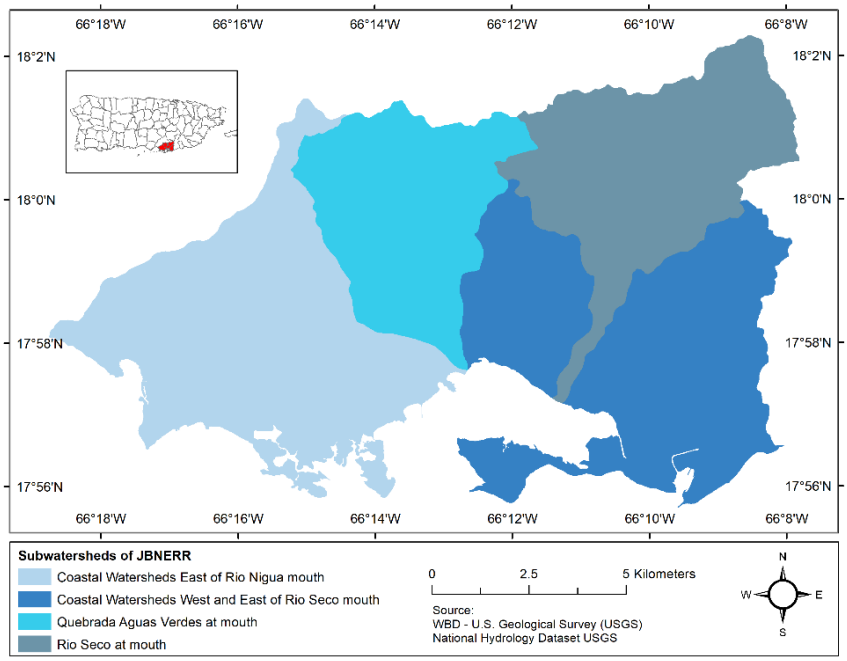

Databases

Dasymetric mapping can be considered a type of areal interpolation (Mennis, 2015). Dasymetric mapping methods is the geospatial technique that uses land cover classes as ancillary data to calculate accurately distribute count data through areal interpolation that have been assigned to predetermined boundaries (Zandbergen & Ignizio, 2010). The census block selection is to provide count data as a set of geographic units that cover JBNERR. The census block is the smallest geographic unit bounded by visible features, such as streets, roads, streams, and railroad tracks, and by nonvisible boundaries, such as selected property lines and city, township, school district, and county

boundaries in which population data is collected (United States Census Bureau 2018). In this study the total population and the total housing units per census blocks are the count data selected to apply the IDM method. According to the US Census Bureau (2018), the housing unit is defined as a house, an apartment, a mobile home or trailer, a group of rooms, or a single room occupied as separate living quarters, or if vacant, intended for occupancy as separate living quarters. It is important to point out that the housing unit statistics also exclude group quarters (such as dormitories and rooming houses), transient accommodations (such as transient hotels, motels, and tourist courts), moved or relocated buildings, and housing units created in an existing residential or non-residential structure. Units in assisted living facilities are housing units, however, units in nursing homes are not considered to be housing units.

Land cover has been the most widely used type of ancillary data for dasymetric mapping (Eicher & Brewer, 2001a; Holt et al., 2004; Jeremy Mennis, 2003; Jeremy Mennis & Hultgren, 2006; Zandbergen & Ignizio, 2010). The idea of using ancillary data in the spatial interpolation of population data originates with the work of John Wright (1936), who used USGS quadrangle maps to eliminate uninhabited areas and recalculate and adjust population densities for the populated areas (Mitsova et al., 2012). It is important to note that there is no "best/one-fits-all" scenario, and the ancillary data chosen should correspond to the spatial scale and particular research applications (Mitsova et al., 2012).

To test the dasymetric mapping performance for JBNERR, the ancillary data used for this study area are classified land-cover data set as raster format created by the USDA Forest Service for 1991, and 2000 and another classified land-cover raster made by the

NOAA-CCAP for 2010 to calculate the population and residential densities (Figure 5). The LULC raster's for JBNERR are reclassified with five land-cover classes following the classification system made by Kennaway and Helmer (2007) for Puerto Rico. The land cover classes are identified as forest, cultivated lands, pasture/grass, urban development, and non-forest (Figure 6). Using these population and housing and land cover data, a map series was generated using IDM, areal weighting, and the multi-class dasymetric mapping technique. This assumes the population density within each dasymetric zone is uniform, but since these zones are typically much smaller than the source areas, the result is a more accurate estimate of the population in the target areas compared to the estimate based on areal weighting without ancillary data (Zandbergen & Ignizio, 2010).

Figure 5

Census data analysis to create a dasymetric map.

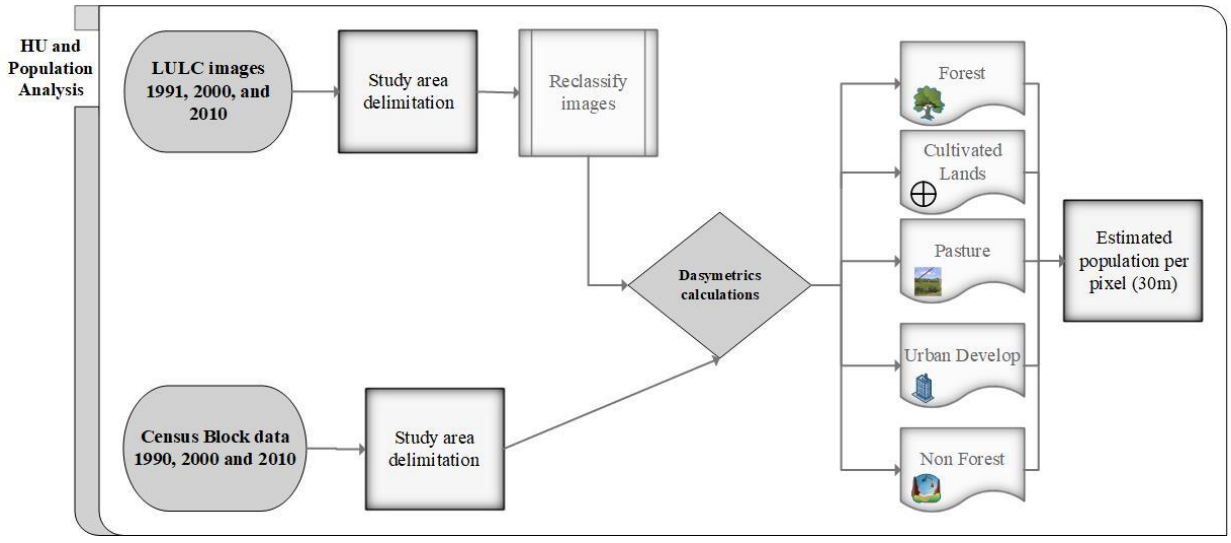

Figure 6

Land use/cover maps based on the classification system made by Kennaway and Helmer (2007) by year, 1991, 2000 and 2010.

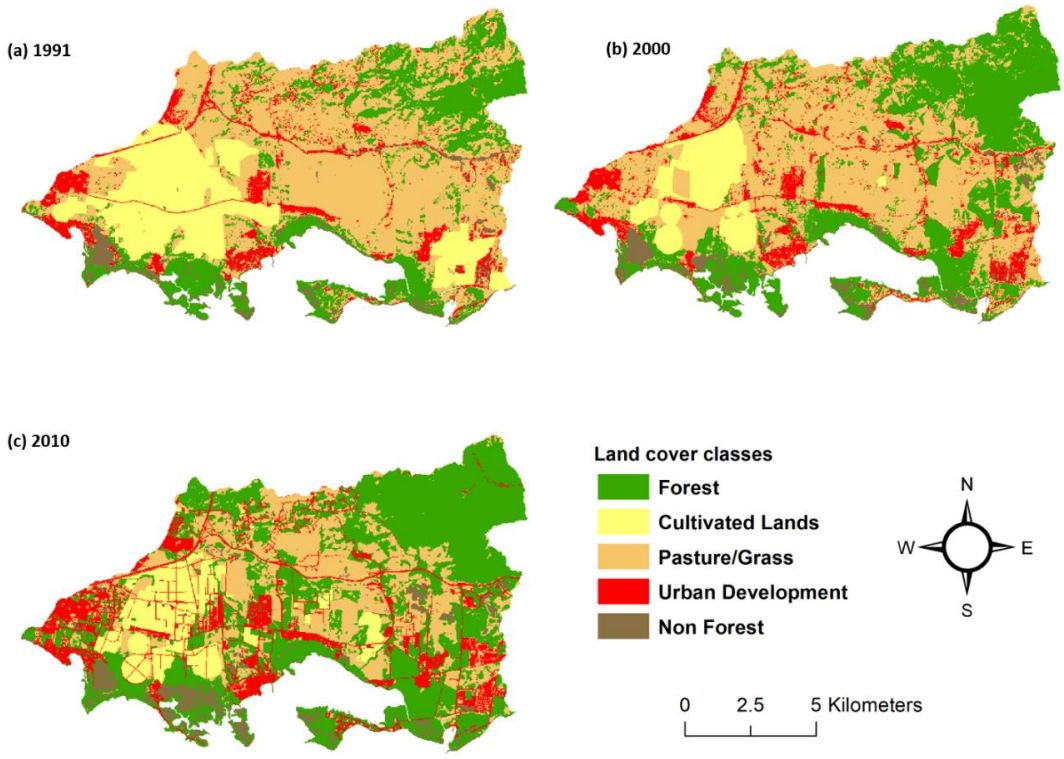

Dasymetric Mapping Statistical Approach

The original spatial units that contain the data are referred to as the source zones and the spatial units to which the data are to be transformed are referred to as the target zones (Mennis, 2016). In dasymetric mapping, the target zones are created from the source zones overlay with some ancillary spatial data layer, such that the target zones nest perfectly within the source zones (Mennis, 2016). Intelligent dasymetric mapping takes input count data mapped to a set of source zones and a categorical ancillary data set. It redistributes the data to a set of target zones formed from the source's intersection and ancillary zones (Mennis & Hultgren, 2006). Data are redistributed based on a

combination of areal weighting and ancillary classes' relative densities (Mennis, 2003). Thus, consider the population and the housing units in the block unit. The source zone s and ancillary data are zone **z,** where **z** is associated with ancillary class **c**. Then the target zone t is the area where **s** and **z** overlap. The estimated count for a given target zone is calculated as:

Equation 1. Target Zone Estimation

$$\hat{y} = y_s \left(\frac{A_t \, \widehat{D}_c}{\sum_{t \in s} \left(A_t \widehat{D}_c \right)} \right)$$

Where $\hat{y}$ is the estimated count of the target zone, y_s is the count of the source zone, $\widehat{D}_c$ is the estimated density of ancillary class c, A_t refers only to the areas of target zones associated with ancillary classes inhabited, i.e., for which the analyst has not enforced a data density of zero. The $\widehat{D}_c$ refers only to the densities of ancillary classes that are populated. This method can employ three sampling options, the containment method, centroid method, and the percent cover method. In this research, the sampling method chosen is centroid method because guarantees a high sample rate, as each source zone centroid falls within an ancillary class zone, but it is vulnerable to outliers (Mennis & Hultgren, 2006). After a sample of source zones has been selected as representative of a particular ancillary class, $\widehat{D}_c$ may be calculated as:

Equation 2. Estimated density of ancillary class

$$\widehat{D}_c = \frac{\sum_{s=1}^{m} y_s}{\sum_{s=1}^{m} A_s}$$

Where m is the number of sampled source zones associated with ancillary class c and, A_s is the area of the source zone. In the case where one or more ancillary classes are assigned a data density of zero by the researcher, the term A_t in Equation 1 refers only to the areas of target zones associated with ancillary classes populated, i.e., for which a data density of zero has not been enforced by the analyst (Mennis & Hultgren, 2006). Additionally, the term $\widehat{D}_c$ in Equation 2 refers only to the densities of ancillary classes that are inhabited. In addition, the term A_s Equation 2 is replaced by the area of the source zone occupied by inhabited ancillary classes.

However, the possibility that a particular ancillary class may go unsampled can occur using the percent cover sampling method. In this case, the unsampled class's density is estimated using "refined" areal weighting (Mennis & Hultgren, 2006). They exposed that first, the count assigned to each target zone associated with an unsampled class is estimated based on the previously estimated densities of the other ancillary classes that occupy that target zone's host source zone. For example, consider a source zone that overlaps multiple ancillary zones. Some ancillary zones are associated with an ancillary class that has gone unsampled (denoted ancillary class u and whose density estimate is unknown. The other ancillary zones are associated with an ancillary class whose density estimate is known (denoted ancillary class k). It was derived from sampling or a preset density value assigned by the researcher. Then the count of a target zone associated with u is calculated as:

Equation 3. Target Zone Estimation Associated with $\boldsymbol{u}$

$$\hat{y}_{t(u)} = \left(y_s - \sum_{t(k)\in s} \left(\widehat{D}_k A_{t(k)}\right)\right)\left(A_{t(u)} \Big/ \sum_{t(u)\in s} A_{t(u)}\right)$$

Where $\hat{y}_{t(u)}$ is the estimated count of the target zone associated with u, $\widehat{D}_k$ is the estimated density of k, $A_{t(k)}$is the area of the target zone associated with k, and $A_{t(u)}$ is the area of the target zone associated with u. Note that $\hat{y}_{t(u)}$ is a temporary estimate, used only to estimate the ancillary class's density whose density estimate is unknown; it is not the final estimated count for that target zone. Once the value of $\hat{y}_{t(u)}$ is found, the estimated density of ancillary class u can be calculated using the formula:

Equation 4. Estimated density of u

$$\widehat{D}_u = \sum_{t(u)=1}^{p} \hat{y}_{t(u)} \Big/ \sum_{t(u)=1}^{p} A_{t(u)}$$

Where $\widehat{D}_u$ is the estimated density of u, and p is the number of target zones in the entire data set associated with u.

In the next session, the IDM computational steps are discussed. This method is implemented as a geographic information system (GIS) extension that facilitates the parameterization of the technique and returns a set of statistics that summarize the quality of the resulting Dasymetric (raster) map (Mennis & Hultgren, 2006).

Intelligent Dasymetric Mapping Computational Steps

IDM takes input count data mapped to a set of source zones and a categorical ancillary data set and redistributes the data to a group of target zones formed from the

intersection of the source and ancillary zones (Mennis & Hultgren, 2006). In this study, the total population and the total housing units were redistributed based on a combination of areal weighting and the relative densities of LULC classes as an ancillary class. A Visual Basic performed the IDM method for Applications (VBA) script encoded within the ArcGIS software as a package, known as Intelligent Dasymetric Mapping (IDM) Toolbox developed by Torrin Hultgren. The IDM process of this tool integrates the equations discussed by Mennis and Hultgren (2006).

The script prompts a series of dialog boxes to put the census blocks' layers as the source zone and the LULC raster as the ancillary data as the first step. The first three steps prepare the data to further calculations and dasymetric mapping creation. The first step essentially converts the census blocks polygon feature class to an integer raster, population raster or raster housing units. This process was completed overlay operations in ArcGIS. The overlay operation can select only those polygons in one layer that fall completely within polygons of another layer as one parametrization option and is used to support containment sampling, where the script loops through a series of selection functions that identify those source polygons that are wholly contained within polygons or grid cell of each ancillary class (Mennis & Hultgren, 2006). Another spatial selection parameterization option supports centroid sampling, in which script loops through a series of selection functions that identify those source polygons whose centroids fall within each ancillary class, essentially a point-in-polygon search (though the analytical geometry is handled internally by the software) (Mennis & Hultgren, 2006).

The second step combines the population or housing enumeration units' raster and the LULC ancillary raster to create another raster corresponding to the population or

housing data and the ancillary class. This raster will have a column in its attribute table that serves as an indicator value for each combination of population units and ancillary classes. A standalone table is created to redistribute the population or the housing units within each source unit according to the ancillary classes. The calculations done on a standalone table in the next steps are more predictable than do the math directly on the raster value attribute table.

The third step creates a separate table containing preset density values for all the unique LULC classes in the ancillary dataset. Once the table is created, it is manually filled with preset density values, and the LULC classes should be preset to zero because they are considered uninhabited and removed from the table. The LULC class removed from the preset table is the non-forest class because this land cover class consider emergent wetland, salt or mud flats, tidally flooded evergreen dwarf-shrubland and forb vegetation, water bodies, bare soil, coastal sand and rock which implies the uninhabited class. Even when estimating the population density fraction for more than one inhabited class is not a trivial matter from the onset of dasymetric mapping, researchers have been challenged to identify, test, and assess various methods of partitioning the available population counts into population density fractions (Mitsova et al., 2012).

The population of each block group was distributed to each grid cell in the population surface based on two factors: (1) the relative difference in population densities among the three urbanization classes; and (2) the percentage of total area of each block occupied by each of the LULC classes. Factor one concerns that a grid cell with a high urbanization class has a higher population density than a grid cell with a low or non-urban urbanization class (as derived from empirical measurement, described below)

(Mennis, 2003). Thus, the high-urbanization grid cell should receive a greater share of the total population assigned to a block or block group than a low or non-urban urbanization grid cell in the same block or block group (Mennis, 2003).

The fourth step was where the script generates two tables with the dasymetric calculations. For each LULC ancillary class, the representative population density was calculated by using areal weight for the selected housing or population units. For each ancillary class, the preliminary population estimate was calculated by multiplying the relative population or housing density (sampled or preset) by the area of each output unit (an output unit is a row in the table, representing a unique combination of population unit and ancillary class). In the first table named Sampling Summary Table that contains statistics for the source housing or population units regarded as representative of each LULC ancillary class. The second table is the Final Summary Table, including the statistics for the final density values. The second table presents a secondary population estimate by multiplying all relative population or housing densities (sampled or preset) by each output unit's area.

Though, to ensures that the original value of the source units was preserved in the transformation to the target units the pycnophylactic integrity or property proposed by (Tobler, 1979) or the volume preserving requirement explained by (Lam, 1983) should be implemented. This means that when the population count of a source zone was disaggregated and summed back into the source zone, the total should equal that of the original value (Qiu et al., 2012). Subsequently, in this step, to maintain pycnophylactic integrity for each population unit, find the sum of the secondary population estimates and

calculate a distribution ratio that was the output unit secondary population estimate divided by the total estimated population for the specified population unit.

The final step creates the final floating-point population density raster by joining the calculated population density with the combined population and ancillary raster created in step two. When the IDM script finished, it returns a dasymetric raster layer with a data count and density estimates for the target zones. This population surface simultaneously describes the number of persons stored within each grid cell and population density (persons/900 m^2, the area of each grid cell) (Mennis, 2003).

Error Assessment

The root mean squared error (RMSE) to quantify the error introduced by different areal interpolation methods was used by Fisher and Langford (1995). They concluded that area-weighting performed poorly compared with intelligent models that utilized ancillary data and that better accuracy was achieved as the number of target zones declines (Qiu et al., 2012). Meanwhile, Mennis (2015) applied dasymetric mapping principles to spatiotemporal interpolation, indicating that the accuracy of estimates was significantly improved. Therefore, it is important to assess the accuracy of this method because high estimation errors were discovered in fast-growing subregions, in areas that were more fully developed for both the source and target periods, and in rural settings where land-cover data is known to underestimate developed residential land (Zoraghein et al., 2016). Several assessment error measures can be considered based on the difference between the observed count data and the estimated data in the dataset to assess the housing units' accuracy and population estimation models derived from the census blocks. The most common error assessments used are mean absolute error (MAE), root

mean square error (RMSE), and the adjusted percent error (P.E.) (Eicher & Brewer, 2001b; Jeremy Mennis & Hultgren, 2006; Mitsova et al., 2012; Qiu et al., 2012).

The accuracy of the derived population surface was estimated using RMSE and MAE to know the number of misplaced persons either overestimate or underestimate. The root mean square error (RMSE) is a measure of statistical error calculated as the square root of the sum of squared errors, where the error is the difference between an estimate and the actual value; if the mean error is zero, it also equals the standard deviation of the error (Titus, J.G et al., 2009).

Equation 5 Root Mean Square Error

$$RMSE = \sqrt{\frac{\sum_{i=1}^{n}(P_i - E_i)^2}{n}}$$

Where P_i is the observed population in areal unit i, E_i is the estimated population for the same areal unit, and n is the number of observations. RMSE has the disadvantage of producing large estimation errors for blocks with large population counts (Qiu et al., 2010). Fisher and Langford (1995) noted that if the population of the blocks varies greatly, the blocks with high populations tend to have large estimation errors and therefore will heavily affect the RMSE measure, while blocks with low people tend to have small estimation errors and less influence on the RMSE measure. Thus, Means and medians were used in preference to root mean square averages because of the latter's lack of robustness to the distorting influence of a few extreme outlying values (Harvey, 2002).

To avoid the possibility of accuracy overestimation due to canceling out of negative and positive errors, the Mean Absolute Error (MAE) was calculated. An average

of the absolute values is an indicator of overall accuracy, including variability/consistency and bias (Harvey, 2002). MAE is a measure of precision calculating the numeric variation between the predicted value and the 'true' value indicating how close the estimated values to the actual values (Deng, 2013).

Equation 6. Mean Absolute Error

$$MAE = \frac{1}{n}\sum_{i=1}^{n}|\hat{y}_i - y_i|$$

Where $\hat{y}_i$ is the estimated population count in block *i*, y_i is the actual population count in block *i*, and *n* is the total number of census blocks.

Results

Population and Housing Units Estimates General Findings

Table 1 provides a summary of the population and housing unit growth for JBNERR and Guayama and Salinas municipalities. JBNERR has an estimated population of 28,667 in 1990, 32,489 in 2000, and 34,250 inhabitants in 2010 (Table 1, Figure **7**). These population estimates range between 41.0% and 44.9% of the population of both municipalities, Guayama and Salinas, from 1990 and 2010, respectively (Table 1). The study area's population growth rate increased by 1.33% from the 1990s to 2000 but increased slightly from 2000 – 2010 by 0.54%. The number of new residents increased from one decade to the next, adding 3,822 and 1,761 new residents in each period from 1990 – 2000, and 2000 – 2010, respectively. The study site presents from 1990 to 2000, and 2000 to 2010 the population increased double the population increased in each municipality. While Guayama increased 6.5% and Salinas increased

9.8% from 1990 to 2000. Similarly, from 2000 to 2010, JBNERR increased 5.42%, while Guayama increased by 2.39%, and Salinas decreased by 0.11%.

A comparable trend is related to the housing unit estimates, which range from 42.4%, 42.9%, and 43.7% of both municipalities' housing units respectively to 1990, 2000, and 2010. JBNERR has an estimated housing unit of 10,007 in 1990, 12,116 in 2000, and 15,083 in 2010 (Table 1 and Figure 7). These housing units' estimates range between 42.4% and 43.7% of the municipalities' population. Specifically, the number of new housing units increased from one decade to the next, 21.08% (2,109 new houses) from 1990 to 2000, and 24.49% (2,967 new houses) from 2000 – 2010. However, the increase in housing in the study area from 1990 - 2000 compares with the rise in Guayama at 20.40%, whereas in Salinas, it was 18.80%. The contrary happened from 2000 to 2010, where the increase in housing units is similar with the Salinas trends in 24.87% but Guayama increase in 20.42%.

Table 1

Total population and housing units' comparison between the study area and Guayama and Salinas municipalities.

JBNERR						
	POP			**HU**		
Census	**Total***	**Δ%**	**Growth Rate**	**Total***	**Δ%**	**Growth Rate**
1990	28,667	-	-	10,007		
2000	32,489	13.33	1.33	12,116	21.08	2.11
2010	34,250	5.42	0.54	15,083	24.49	2.45
Guayama						
	POP			**HU**		
Census	**Total**	**Δ%**	**Growth Rate**	**Total**	**Δ%**	**Growth Rate**
1990	41,588			13,595		
2000	44,301	6.52	0.65	16,368	20.40	2.04
2010	45,362	2.39	0.24	19,711	20.42	2.04

Salinas						
	POP			HU		
Census	Total	**Δ%**	**Growth Rate**	Total	**Δ%**	**Growth Rate**
1990	28,335			9,997		
2000	31,113	9.80	0.98	11,876	18.80	1.88
2010	31,078	(0.11)	(0.01)	14,830	24.87	2.49

Figure 7

Population and housing units counts in the study area and Guayama and Salinas municipalities.

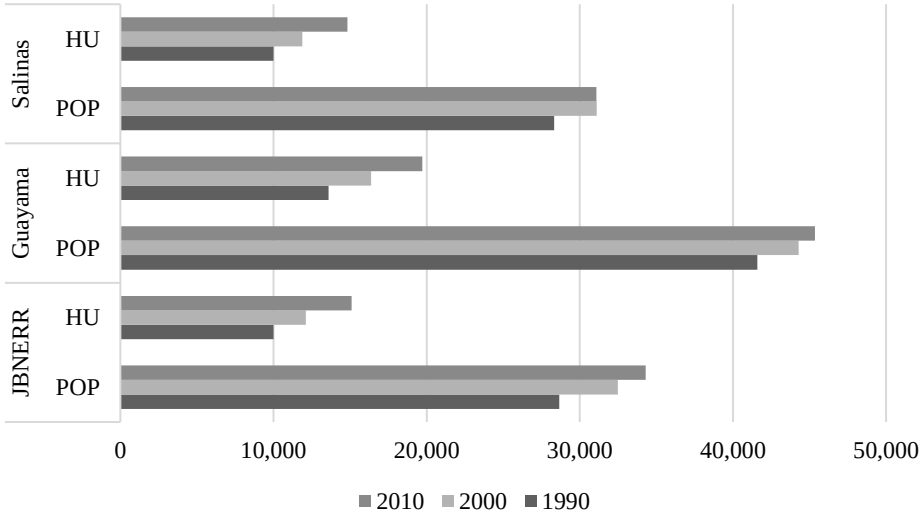

Overall, a review of census data for twenty years revealed that the JBNERR watershed population increased from 1990 to 2010. The population increased by 19.48% with a growth rate of 0.97%, adding 5,583 new residents from 1990 to 2010. Similar trends were found for housing unit estimates for the whole study period. The housing units increased from one decade to the other by adding 5,076 new housing, corresponding to an increment of 50.72% at a growth rate of 2.54% in twenty years. In JBNERR, it is important to point out that the number of census blocks increased from one decennial

census to the other, respectively, to 829 blocks in 1990, 1,118 in 2000, and 1,551 blocks in 2010.

Intelligent Dasymetric Mapping Error Assessment

The density of the population and housing units was redistributed to 30 by 30 meters cell-size scale by each decennial census. This research indicated that 1990 and 2000 censuses had a root mean squared error (RMSE) of misplaced persons of 2.85 persons/m^2 and 3.01 persons/m^2, respectively. Meanwhile, for 2010 the RMSE was 96.52, indicating that the overestimation or underestimation of people is around 96 persons per block in this census. Related to housing units, the error assessment presented a better estimation fit done by the IDM method. Particularly, in 1990 the RMSE was very close to 0, with 0.83 houses that might be misplaced per block. While 2000 and 2010, the RMSE were 1.09 and 1.10, respectively, indicating a good housing estimation done by the IDM method. According to previous studies in rural blocks, as is the case of JBNERR, relatively large rural blocks tend to be overestimated, while small urban blocks tend to be underestimated (Eicher & Brewer, 2001b; Harvey, 2002; Jeremy Mennis & Hultgren, 2006).

Table 2

Error Assessment of IDM method (meter unit).

Source data	1990		2000		2010	
	RMSE	MAE	RMSE	MAE	RMSE	MAE
POP	2.85	0.10	3.01	0.11	96.52	33.21
HU	0.83	0.03	1.09	0.04	1.10	0.05

Regarding the MAE, the population estimation with this approach is 0.10 in 1990, 0.11 in 2000, and 33.21 in 2010, illustrating that the population in 2010 is overestimated, particularly the blocks with larger geographical areas (e.g., blocks in the forest or pasture cover classes). The MAE for the housing units estimate was 0.03 in 1990, 0.04 in 2000, and 0.05 in 2010, showing the same situation in population estimates. To sum up, it is reasonable to expect that higher accuracy of predicted values at the administrative unit level results in a higher accuracy of the final gridded population distribution datasets (Stevens et al., 2015). Another explanation is that as far as the missing blocks, these might be very small. If they are small enough, there might be no pixels in the LULC raster with centroids in that block, and therefore no centroids in the final population or housing density raster. Nevertheless, in this study, most of these blocks had 0 population or a very small population.

In other words, the sum of the estimated population of the dasymetric zones that compose a single original choropleth zone should equal the original encoded population of that choropleth zone (J Mennis, 2009). Because the available census data are fine, the dasymetric mapping approach for the final end-user product will still have high accuracy as the census counts "anchor" the end-user product predictions to observed values at a smaller spatial scale (Stevens et al., 2015). This "anchor" effect minimizes the bias introduced by the "Ecological Fallacy" by redistributing population data within each census unit to predicted population density; estimates are guaranteed to at least be accurate when aggregated back to the census unit level (Stevens et al., 2015).

Dasymetric Population Mapping

Population estimates, and population density attributes were assigned to each LULC class within each census block using weighted aerial interpolation.

Figure 8 shows the suitability of dasymetric mapping to map population density compared to choropleth mapping more accurately. The visual comparison indicates that dasymetric mapping provided a better representation of population density's spatial orientation, particularly in outlying census blocks that encompass much-uninhabited land. Indeed, the use of LULC images as ancillary data was performed positively because these data have a direct interpretation as population density estimates over 30m x 30m of land. This supplied means of modeling population density as a continuous surface (Langford & Unwin, 1994).

Figure 8

Visual comparison of the choropleth and the dasymetric map of population density for JBNERR, Census blocks.

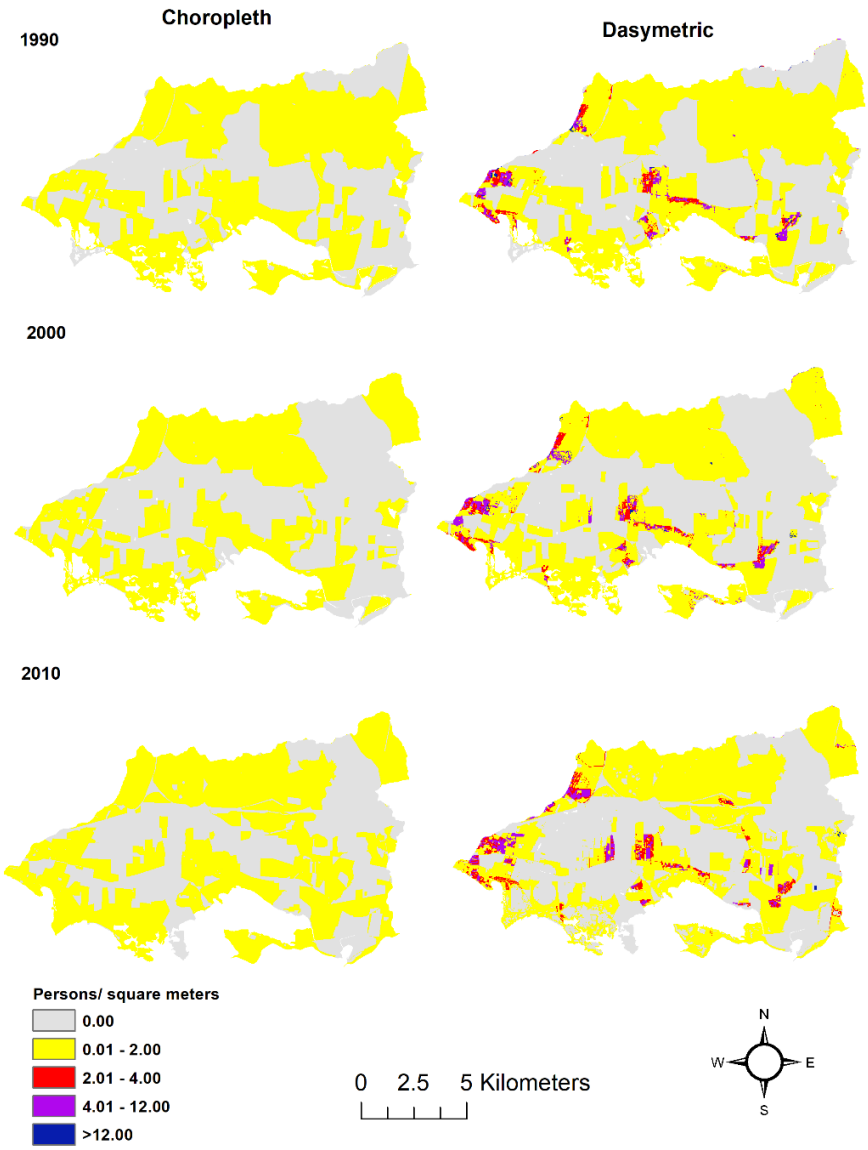

Table 3 provides the general results of the aerial interpolation for each land cover class for each year. Results indicate the population estimates increased steadily for urban development over the period.

Table 3 shows that the urban development class has the highest population, estimated 26,321 inhabitants in 1990, 29,167 in 2000, and 33,161 inhabitants in 2010. In every census urban development represented 90% or higher from the total population in the study area. They were followed by pasture/grass with 1,069, 2,561, and 853 inhabitants in 1990, 2000, and 2010. Forest ranked the third place with more population and followed with 959, 514 and 236 inhabitants. The less populated land cover classes were cultivated lands and non-forest with 292 and 26 persons in 1990, 22 and 225 persons in 2000, and 0 and 0 persons in 2010 were estimated respectively to these two land cover classes. Comparing the aerial interpolation of the population for each census provides further insight into the type of urban growth throughout JBNERR. Also, the results show that the population estimates in cultivated lands decreased from one census to the other. Contrary occurred to forest land cover.

In terms of population density, we found that the highest maximum density corresponds to urban development with 254.8 ± 12.3 persons/900 m^2 in 1990, 71.2 ± 7.1 persons/900 m^2 in 2000, and 94.0 ± 4.8 persons/900 m^2 in 2010. Followed by forest 22.0 ± 1.9 persons/900 m^2 in 1990, by pasture with 20.8 ± 1.4 persons/900 m^2 in 2000, and 7.9 ± 0.5 persons/900 m^2 in 2010. However, the population density in forest were significantly decreasing from one census to the other. While the population density increased from 1990 to 2000 but decreased in 2010 in pasture lands.

Table 3

Dasymetric Mapping Population Statistics Summary in JBNERR by Census blocks level.

			1990				
Land cover classes	**Frequency**	**New Pop.**	**Percentage**	**Mean density**	**Min density**	**Max density**	**Std density**
Forest	231	959	3.35	0.309	0.000	22.03	1.876
Cultivated Lands	188	292	1.02	0.033	0.000	2.58	0.236
Pasture/Grass	519	1,069	3.73	0.107	0.000	13.86	0.770
Urban development	616	26,321	91.82	4.425	0.000	254.76	12.325
Non-Forest	137	26	0.09	0.011	0.000	0.35	0.037
		28,667	100				
			2000				
Forest	409	514	1.58	0.085	0.000	9.000	0.644
Cultivated Lands	115	22	0.07	0.001	0.000	0.088	0.009
Pasture/Grass	836	2,561	7.88	0.259	0.000	20.810	1.362
Urban development	927	29,167	89.78	3.725	0.000	71.212	7.068
Non-Forest	181	225	0.69	0.178	0.000	15.914	1.206
		32,489	100				
			2010				
Forest	803	236	0.69	0.008	0.000	1.364	0.066
Cultivated Lands	157	0	0.00	0.000	0.000	0.000	0.000
Pasture/Grass	747	853	2.49	0.054	0.000	7.938	0.479
Urban development	1305	33,161	96.65	2.091	0.000	94.000	4.787
Non-Forest	195	0	0.00	0.000	0.000	0.000	0.000
Totals		34,250	100				

Note. Frequency is the number of output units (census blocks) that correspond to this ancillary class. New Pop is the total dasymetrically calculated population for this ancillary class. New Population is the population resulted from the IDM method.

The IDM tool's output provided a population density raster layer for each decennial census (Figure 9). The dasymetric map of population densities for JBNERR

depicted areas with higher population densities within the watershed. These generally correspond to small urban areas, especially in new higher-density housing (Holt et al., 2004). Hence, the lowest population densities were found in the north and northeast of the watershed, while the highest population densities are along the east boundary and close to the coast. Similarly, it was observed that in the range of 4 to more than 12 persons per pixel were intensifying from 1990 to 2010. It was also observed that in areas where the IDM estimated zero population per pixel (grey color) in 1990, those areas presented 2.0 persons per pixel like the northeast in 2000 and 2010. These two observations show that population were sparsely redistribute according to the land cover areas and in other parts the population were intensified.

Figure 9

Dasymetric Map of Population Density in JBNERR

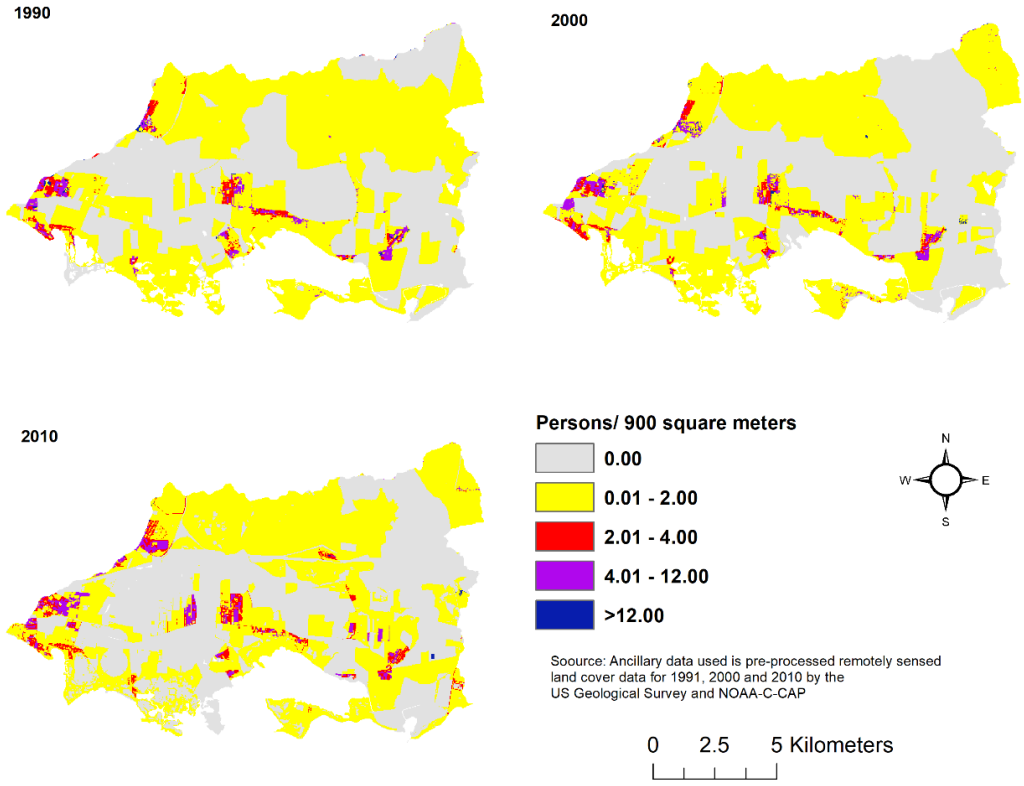

Dasymetric Housing Units Mapping

The IDM tool's output provided a housing density raster layer for each decennial census (Figure 10). The housing estimates and housing density attributes were assigned to each land cover class within each census block using weighted aerial interpolation, equally to population estimates and population density. The figure shows the visual comparison clearly between dasymetric mapping representation of the spatial orientation of population density, particularly in outlying census blocks that encompass much-uninhabited land. Since the dasymetric map using LULC images as ancillary data performed positively better than choropleth maps.

Figure 10

Visual comparison of the choropleth and the dasymetric map of housing unit density for JBNERR, Census blocks.

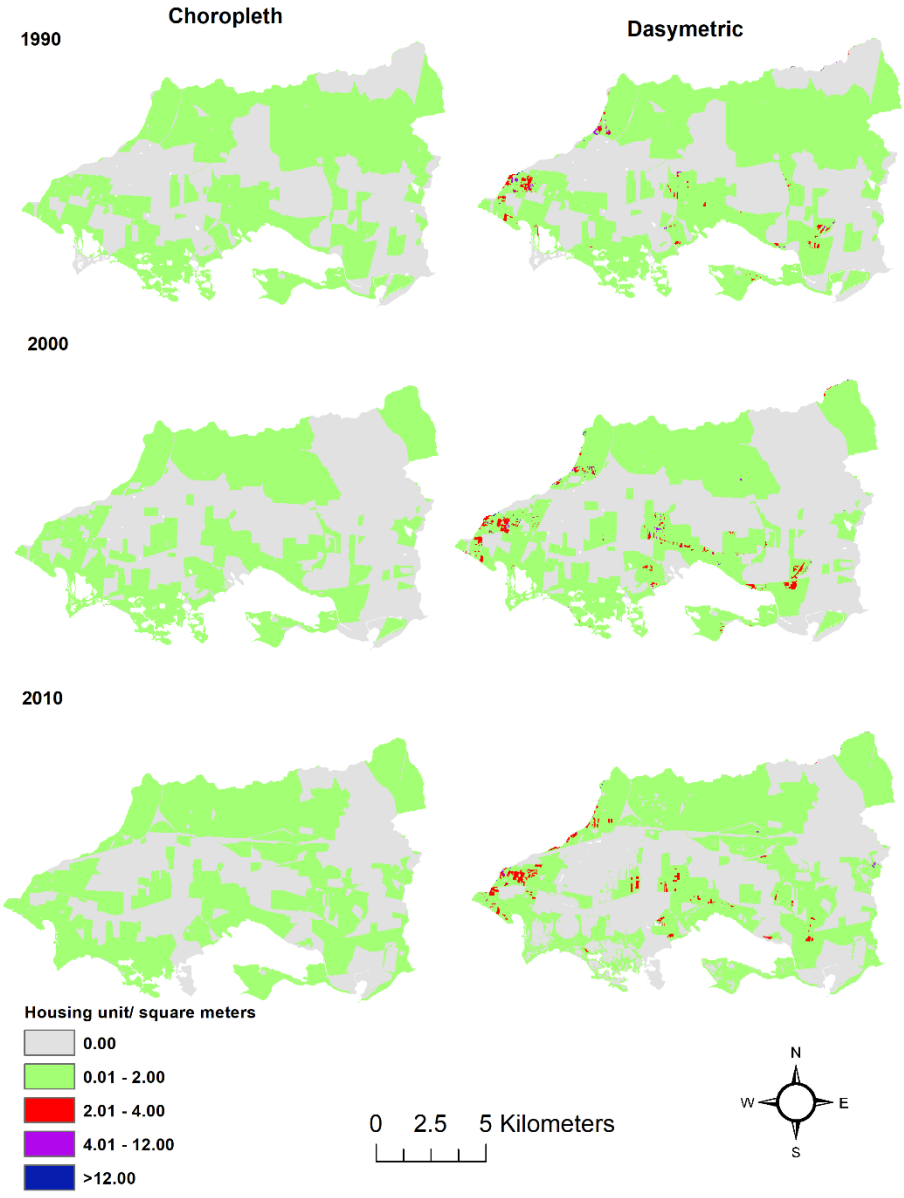

Table 4 Table 4 lists the dasymetric housing densities per land cover class for each census in JBNERR. Results indicate that the housing units' estimates increased gradually for urban development over time, the same as the population estimates. The urban development class has the highest housing units estimated at 9,132 in 1990, 10,931 in 2000, and 14,460 houses in 2010. Like population estimates, the housing units' estimates presented the same trends per land cover classes. Pasture/Grass followed them with 432, 897, and 431 houses in 1990, 2000, and 2010. Forest rated third place with more housing units and followed with 306, 216, and 192 houses. The less populated land cover classes were cultivated lands, and non-forest with 123 and 15 in 1990, 9 and 63 persons in 2000, and 0 and 0 houses in 2010 were estimated respectively to these two land cover classes.

Table 4

Dasymetric Mapping Housing units Statistics Summary in JBNERR by Census blocks level.

Land cover classes	Frequency	New H.U.	Percentage	Mean density	Min density	Max density	Std density
			1990				
Forest	231	306	3.06	0.098	0	6.32	0.567
Cultivated Lands	188	123	1.23	0.012	0	1.05	0.088
Pasture/Grass	519	432	4.31	0.042	0	4.71	0.276
Urban development	616	9,132	91.26	1.555	0	80.30	4.429
Non-Forest	137	15	0.15	0.008	0	0.37	0.043
		10,007	100				
			2000				
Forest	409	216	1.78	0.032	0.000	3.000	0.229
Cultivated Lands	115	9	0.07	0.000	0.000	0.016	0.002
Pasture/Grass	836	897	7.41	0.091	0.000	6.864	0.462
Urban development	927	10,931	90.22	1.429	0.000	21.211	2.496
Non-Forest	181	63	0.52	0.048	0.000	3.777	0.289
		12,116	100				
			2010				
Forest	803	192	1.27	0.006	0.000	1.033	0.045
Cultivated Lands	157	0	0.00	0.000	0.000	0.000	0.000
Pasture/Grass	747	431	2.86	0.023	0.000	3.935	0.188
Urban development	1305	14,460	95.87	0.987	0.000	46.500	2.060
Non-Forest	195	0	0.00	0.000	0.000	0.000	0.000
Totals		15,083	100				

Note. Frequency is the number of output units (census blocks) that correspond to this ancillary class. New HU is the total dasymetrically calculated housing units for this ancillary class.

Generally, results indicate that much of the population resides in urban developments, those areas that are contributing most to population and housing units' growth. Respecting to housing unit density, the highest maximum density corresponds to

urban development with 80.3 ± 4.4 houses/900 m^2 in 1990, 21.2 ± 2.5 houses/900 m^2 in 2000, and 46.5 ± 2.1 houses/900 m^2 in 2010. Followed by forest 6.3 ± 0.6 houses/900 m^2 in 1990, by pasture with 6.9 ± 0.5 houses/900 m^2 and 3.9 ± 0.2 houses/900 m^2 in 2000 and 2010, respectively. Therefore, both the housing unit and the population density as a continuous surface serve as a predictor variable to further analysis. Even when the dasymetric approach calculated conservative estimates of housing change, the population data are compared over time. The initial and final populations' distributions are often independent because people are dynamic and migrate (Syphard et al., 2009). Houses remain in place over time, and their final distribution depends on their initial distribution; thus the dasymetric approach was slightly more complex (Syphard et al., 2009).

Figure 11 presents the dasymetric map for housing units and provides more precision in differentiating areas of higher and lower housing density within the watershed. Likewise, the lowest housing densities are found at the north and northeast of the watershed to the population density dasymetric map. The highest population densities are along the east boundary and close to the coast. Also, it is observed that in the range of 4 to more than 12 houses per pixel were intensifying from 1990 to 2010 in the east. Besides, it is also observed that in areas where the IDM estimate zero population per pixel (grey color) in 1990, those areas present 2.0 persons per pixel in 2000 and 2010.

Figure 11

Dasymetric Map of Housing units Density in JBNERR.

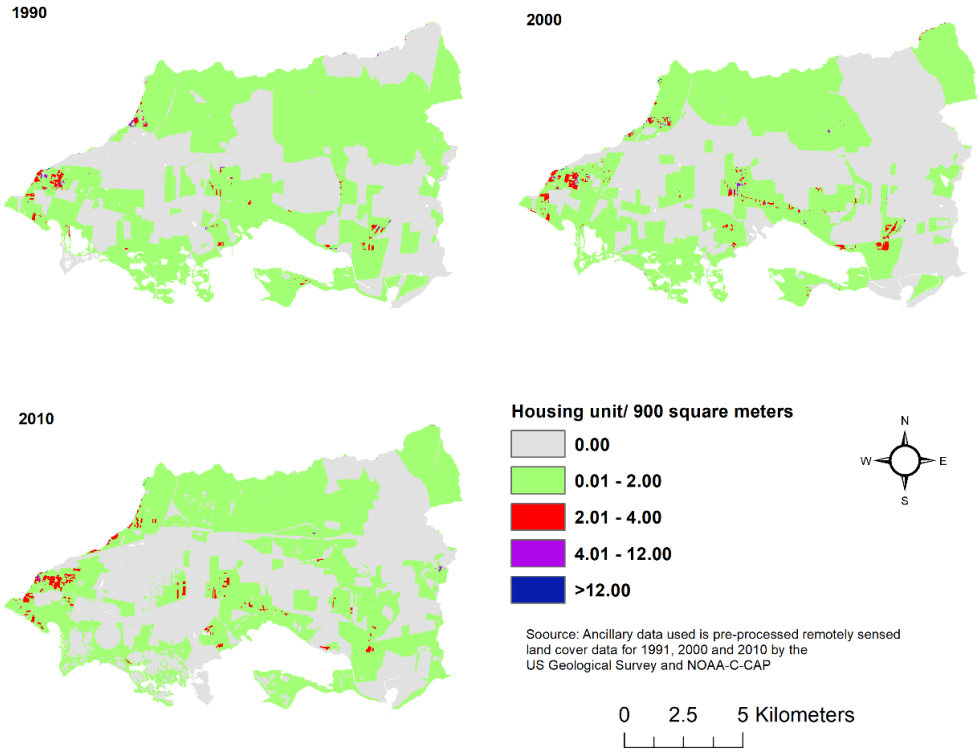

Table 5

Estimated population and housing units and LULC classes changes, 1990 to 2010

LULC class	Pixels		Population		Housing unit	
	$\Delta_{1\%}$	$\Delta_{2\%}$	$\Delta_{1\%}$	$\Delta_{2\%}$	$\Delta_{1\%}$	$\Delta_{2\%}$
Forest	77.06	96.33	-46.40	-54.09	-29.41	-11.11
Cultivated Lands	-38.83	36.52	-92.47	-100.00	-92.68	-100.00
Pasture/Grass	61.08	-10.65	139.57	-66.69	93.52	-48.44
Urban development	50.49	40.78	10.81	13.69	19.70	32.28
Non-Forest	32.12	7.73	765.38	-100.00	320.00	-100.00

Note. $\Delta_{1\%}$ is the net change from 1990 to 2000, and $\Delta_{2\%}$ is the net change from 2000 and 2010.

Discussion

JBNERR watershed can be defined as a rural agricultural small area of 137 km^2 with population and housing units located within census blocks with a population density

of ranges from 209, 237 to 250 people per km^2, from 1990 to 2010. While housing density ranges from 73, 88 to 110 housing units per km^2 from 1990 to 2010. This compares to previous studies where the average population density in Jobos Bay is maintained at a comparatively low 234 people/km^2 by large areas of open space among communities in 2000 (Whitall et al., 2011). Recent studies revealed that population density is closely related to residential area or dwelling area thus, much previous research for population estimation was based on housing or dwelling units using high spatial resolution images (Li & Lu, 2016).

For example, Castro-Prieto et al. (2017) demonstrated that lands around protected areas in Puerto Rico like JBNERR are extremely vulnerable to development and that residential development can continue to grow despite the human population declines. More than 500 housing units have been constructed from 2000 to 2010 in the Jobos bay watershed area (Laboy et al., 2008). Supported by our findings, even when the residential development increased within the Jobos watershed, the housing units' densities decline in urban areas from 1990 to 2000 the censuses. According to our findings, the housing unit's density, where the maximum housing density decreased in urban areas from 1990 (80.3 ± 4.4 houses/m^2) to 2000 (21.2 ± 2.5 persons/m^2) and increased to 46.5 ± 2.1 houses/m^2 in 2010. According to Syphard et al. (2009), widespread housing density decline is unrealistic, except for cases of, for example, natural disasters, the effects of which tend to be limited in space or time (e.g., wildfires and hurricanes are almost always followed by rebuilding). This chapter does not analyze how the land change trends and major environmental events like hurricane disturbance interact to determine the structure and composition of population and housing unit density.

Future work is recommended to explore how environmental events like hurricanes and land changes impact the population and housing density in JBNERR. For example, in Puerto Rico, from 1991 to 2000, the island faced the following hurricanes: Hurricane Marilyn in 1995, Hurricane Hortense in 1996, and Hurricane Georges in 1998 (Metro Puerto Rico, 2017). From 2000 to 2010, hurricanes Frances in 2004, and Earl in 2010. Meanwhile, Lee and Leigh (2005) disclosed that recent analyses have shown that the only places where sustained, substantial loss of housing occurs are in areas that are decentralizing because of widespread property abandonment at the center of large urban areas in the U.S. Similarly occurred in Puerto Rico because of an economic shift from agriculture to the industry that pulled a migration from rural to urban areas increasing the demand of new housing outside from the existing urban areas, industrial facilities and roads at the beginning of the century (Lopez Marrero, 2003).

Another explanation for housing density decline is likely due to the increase in spatial resolution of the census blocks combined with the assumption that housing data were homogeneously distributed within the source and target zones (Syphard et al., 2009). For example, some of the 2000 block boundaries may have been updated to delineate small neighborhoods located within large, sparsely populated areas (Syphard et al., 2009). Thus, when a large polygon with low housing density in 1990 was split into two polygons in 2000, one of the 2000 polygons would be comparatively densely populated with houses, whether there was any change in houses on the ground, while the other would have no houses in the area that was formerly represented as populated with low-density housing (Syphard et al., 2009). A simple solution to verify is doing an overlay of the 1990 and 2000 boundaries in the second polygon. Therefore, it would

show a false decline in housing density (when in reality, it was probably undeveloped in both 1990 and 2000) (Syphard et al., 2009). Therefore, it will continue to be important for scientists to understand where and how housing growth is occurring so that land-use planners and conservation biologists can work together to plan for change on a regional scale and can aggregate larger areas protected from development, there will be more potential for effective land conservation and stewardship (Lenth et al., 2006).

All methods involved some trade-off level, including analytical difficulty, data resolution, magnitude, or bias in the direction of change (Syphard et al., 2009). Analysts need to recognize that housing density change estimates are sensitive to the method of interpolation and to choose between the trade-offs following their specific objectives and research questions (Syphard et al., 2009). The quality of the interpolation estimates relies heavily on (1) how to source zone, and target zone boundaries are defined, (2) the LULC classification accuracy, (3) the degree of generalization in the interpolation process, and (4) the characteristics of the partitioned surface (Lam, 1983).

For its part, population maximum density decreased in urban areas from 254.8 ± 12.3 persons/m^2 to 71.2 ± 7.1 persons/m^2 and increased to 94.0 ± 4.8 persons/m^2 in 2010. During this decade, in Salinas, only Barrio Aguirre, located within the Jobos watershed, reflected an increase in its population by 15.5% (Junta de Planificación de Puerto Rico, 2019). Even when Aguirre experienced a population gain, the Salinas municipality experienced a population loss from 2000 to 2010. This population loss in the Salinas neighborhood represents a trend that has been experienced in most of the urban centers of the municipalities of Puerto Rico (Junta de Planificación de Puerto Rico, 2019). This phenomenon of emigration, as studied in previous research from urban centers in Salinas,

occurs due to various factors, among which are: (1) the development of new residential developments; (2) the housing shortage in urban centers; (3) the deterioration and abandonment of existing residences; (4) the scarcity of parking spaces; (5) traffic congestion; and (6) the loss from commercial, service, educational, and other job-generating activities (Junta de Planificación de Puerto Rico, 2019).

For its part in Guayama, where to the west is JBNERR, the area industrial area, and the floodplain area of the Guamaní River and the Caribbean Sea to the south (Junta de Planificación de Puerto Rico, 2020), experienced population growth from 2000 to 2010. To illustrate, the Jobos barrio, located within the Jobos watershed, also presented an increase in population of 7.53% and its housing units by 17.8% from 2000 to 2010 (U.S. Census Bureau, 2012). Nonetheless, these new areas might affect a small proportion of the landscape compared to areas where houses remain or are becoming more numerous (Syphard et al., 2009), like the not new residential areas, Jobos and Aguirre barrios, or neighborhoods in the JBNERR watershed. Pasture/grass as open spaces increased its population maximum density and the housing unit density from 1990 to 2000 but decreased from 2000 to 2010, contrary to urban areas in our study area. This means that pasture areas became urbanized as urban sprawl with dispersed and density in population and housing development over the study period.

However, according to Census 2020, total population in Puerto Rico decreased 11.8% from 2010 to 2020 (U.S. Census Bureau, 2020). All the municipalities of Puerto Rico reflected loss of their resident population with percentage changes ranging from -0.1% to 29.0% (Red State Data Center de Puerto Rico (SDC-PR), 2021). To that Guayama and Salinas experienced a population decreased around 5 and 10 percent. In

terms of the Housing Units in Puerto Rico the percent of change is negative in 2.4% (U.S. Census Bureau, 2020). Only 15 out of 78 municipalities experience an increase in its total housing units from 2010 to 2020. From the remaining 62 municipalities that experiences a decrease in its total housing units, Guayama and Salinas are categorized as those municipalities with the most noticeable decrease in 6.0% and 6.1%, respectively. As mentioned before, this does not mean that there is no new residential development occurring in those municipalities, this reduction might be explained by the habitable housing losses due to the passage of hurricanes during the decade, for example Hurricane Maria and Hurricane Irma in 2020.

Therefore, even when the total population and total housing units are not yet available by at the barrio levels in the Decennial Census 2020, we can make inferences by using the 5 years Puerto Rico Community Survey estimates for 2020. According to the 5 years Puerto Rico Community Survey population estimates five of six barrios loss population in Salinas, including Aguirre. Likewise, in Guayama nine of ten barrios loss population, including Jobos barrio (US Census Bureau, 2022). Then, it is expected to see a population decreased within Jobos Bay Watershed because Guayama is the seventh municipality with the highest population loss with 9.7% between 2010 and 2020 (Red State Data Center de Puerto Rico (SDC-PR), 2021). Likewise, Salinas ranked nineteenth with a negative population change of 5.9% (Red State Data Center de Puerto Rico (SDC-PR), 2021). To that it is highly recommended to analyze the sociodemographic characteristics and housing type and vacancy status to have a better understanding on anthropogenic activities taking place in the study area.

The sociodemographic and housing type and vacancy status should help to a better understanding on anthropogenic activities taking place in the study area. In this sense, even when at an island wide scale, urbanization may reinforce forest expansion, at a local scale, in areas adjacent to the most intensively urbanized areas, an opposite pattern emerged: Low-density residential use invades forest (Grau et al., 2003). In addition, urban expansions occur over the most productive agricultural areas, a process that greatly reduces the island's capacity to re-adapt to an economy less dependent on external food sources (Grau et al., 2003). JBNERR is considered not only a research reserve due to its ecological richness, but its watershed also has soils of high agricultural value. Likewise, JBNERR is being threating by urban development because of its high landscape value.

Consequently, before 2015 deforestation, landfilling and illegal construction (in the community of Las Mareas and Camino del Indio), some with sanitary discharges directly into the sea, continued for another 34 years, until in 2015 the former Secretary of Natural and Environmental Resources and today regional director of the Federal Agency for Environmental Protection (EPA), filed a cease and desist order, which imposed hundreds of thousands of dollars in fines and mitigation actions on three individuals for non-compliance with various environmental laws (Rodríguez-Velázquez & Sosa-Pascual, 2022, Figure 12). They denounce the construction of houses with pools and docks in the Estuarine Reserve in Salinas, causing the destruction of mangroves, as well as the development of illegal homes that even have legal power energy and water supply services (Telemundo Puerto Rico, 2022). As well, in the 2018 Annual Report of the United States National Oceanic and Atmospheric Administration (NOAA), the DNRA has even been pointed out in its negligence by the federal authorities, it is specified that

the agency failed to comply with the protection of the area, allowing the illegal invasion of the land and the construction of summer homes (Noticias Salinas, 2022). They also pointed out that they were not complying with everything related to navigation and fishing in the area (Noticias Salinas, 2022). At least 29 illegal houses were constructed and an area for trailer houses or camper is also found in Camino del Indio (Pérez, 2022, Figure 13 and Figure 14.). The ongoing investigation of illegally built homes in the Puerto Rico's second-largest estuary, where more than 3,600 trees were clear-cut, according to authorities, has led to public hearings and the launch of a criminal investigation by the island's Department of Justice while drawing attention to other similar cases (Coto & Los Angeles Times, 2022). Thus, physical alteration of habitats also creates persistent and serious environmental problems, such as large-scale modifications of coastal watersheds (e.g., deforestation and construction) and estuarine basins (e.g., dredging and dredged material disposal, channel and inlet stabilization, and harbor and marina development), which adversely affect estuarine organisms (Kennish, 2002). During the last 200 years, human activities in Puerto Rico have had negative and positive impacts on the mangroves (Martinuzzi et al., 2009).

Figure 12

Recursos Naturales sabía de las irregularidades en Bahía de Jobos en Salinas.

Source: Noticias Salinas, March 24, 2022.

Figure 13

DRNA sabe del desastre ambiental en la Reserva Jobos de Salinas desde el 2019.

Note. Casas rodantes / Trailer homes. *Source*: Redacción, March 24, 2022.

Figure 14

Vivienda en construcción en la Reserva Nacional de Investigación Estuarina de la Bahía de Jobos en Salinas (Puerto Rico). Date: May 3, 2022. By Carlos Giusti / Associated Press.

Source: Carlos Giusti, Associated Press, May 3, 2022.

The environmental consequences of the mangrove deforestation for urban development is manifested by an array of damaging cascading changes in ecosystem structure and function (Kennish, 2016) such as flooding due to tides, part of the most productive ecosystems in the world because is a refuge for fish and invertebrate species, reduce the effects of hurricanes and tsunamis, serve to clean the waters that flow from the rivers before reaching marine waters, and has great relevance in the terrestrial fauna (Kennish, 2002b). According to Martinuzzi et al. (2009) the future of the mangroves in Puerto Rico depends on human decisions, and on the legal and social attitude aimed to conserve them argued based on their study of 200 years of conversion and recovery of Puerto Rican mangroves. Although the law protects the mangroves anywhere they occur, this approach has not prevented negative effects of human decisions and activities related to mangroves and coastal ecosystems in general (Martinuzzi et al., 2009). In addition, it seems that the Law Num. 33 known as the Ley de Mitigación, Adaptación y Resiliencia al Cambio Climático de Puerto Rico (Puerto Rico Climate Change Mitigation, Adaptation and Resilience Act) establish states that coastal planning must be implemented to address rising seas while directing new development away from shoreline is not being consider to grant urban development permits, increasing in 29% by 2021 (Centro de Periodismo Investigativo, 2022, Figure 15). From forty four (44) coastal municipalities, Guayama and Salinas has 293 and 183 of building permits that have been approved between 2015 and 2021, respectively (Centro de Periodismo Investigativo, 2022, Figure 16).

Figure 15

Concesión de permisos de construcción en el litoral.

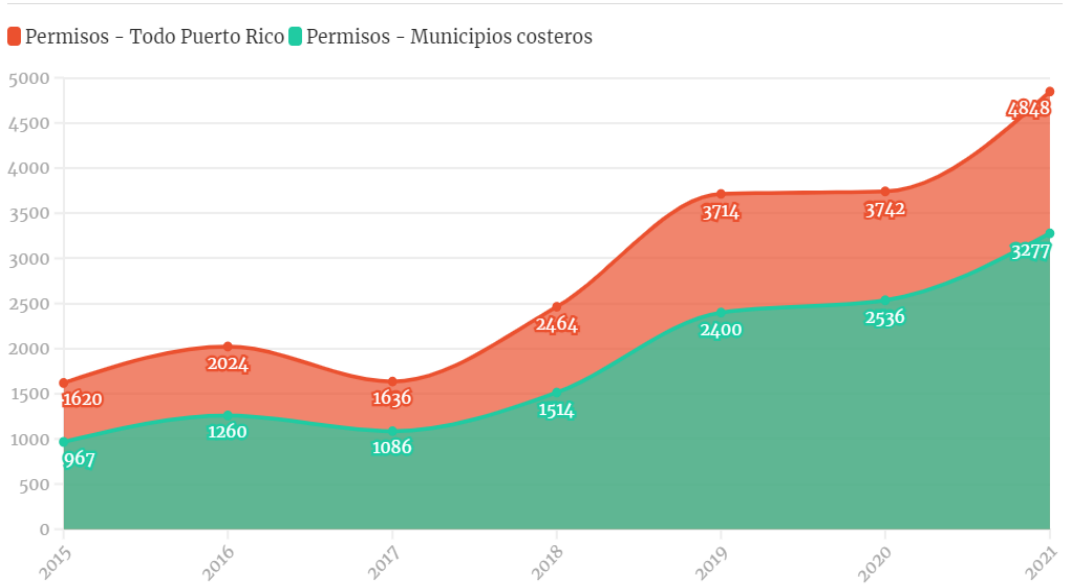

Note. Cantidad de permisos de construcción aprobados por la Oficina de Gerencia de Permisos para el desarrollo de proyectos en los pueblos costeros de Puerto Rico entre 2015 y 2021.
Source: Oficina de Gerencia y Presupuesto. Graph created by Gabriela Carrasquillo Piñeiro, 2022.

Figure 16

Zonas con más construcciones costeras.

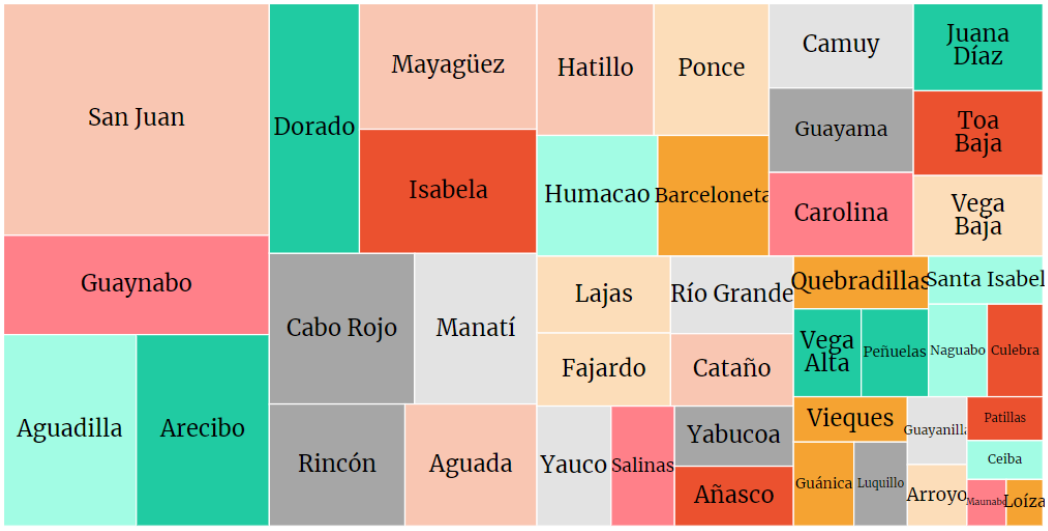

Note. Número de permisos de construcción que se han aprobado para cada uno de los 44 pueblos costeros entre 2015 y 2021.
Source: Oficina de Gerencia y Presupuesto. Graph created by Gabriela Carrasquillo Piñeiro, 2022.

In sum, this chapter contribute to the advancement of knowledge on how population densities have been increasing along the urban expansion in JBW, and to the comprehensive on the critique umbral among housing distribution, human population, land uses and land changes when forest mangroves has been cut due to illegal urban development. In short, the JBW will continue facing anthropogenic threats and the solutions to mitigate and stop new construction on the coast relies on the partnership between local communities and the academic community.

Conclusion

This research provides a new approach to map population density distribution in JBNERR at a $30m^2$ cell size scale, based on the established relationship between population density and LULC data. This approach was applied for the first time in JBNERR and provided the potential to update population density using LULC data. The

estimates derived from LULC classification by applying the IDM provide a timely resource for measuring several concerns in the study area 1) population growth impacts, 2) housing development closer to natural reserve boundaries, and 3) urban sprawl trends. According to our results, urban development in JBNERR presented that the maximum population density decreased from ~ 255 to ~71 persons/900m^2 during 1990 – 2000 and increased into 94 persons/900m^2 in 2010. The same trend was shown for housing density, decreasing from ~80 to ~21 hu/900m^2 from 1990 to 2000 and increasing by ~47 hu/900m^2 in the urban developments.

On the contrary, the results for population and housing estimates and densities in forest land cover in JBNERR. The population estimate decreased from one census to the other, 959 residents in 1990 to 236 residents in 2010. The population density in this land cover also decreased from ~22 to ~1 persons/900m^2 from 1990 to 2010. In the same way, in Figure 4, the forest was the land cover with significant increase during the same period, which might affect the density calculations because major areas are considered to calculate how many inhabitants or houses are found per land cover class. Moreover, both trends for population and housing in urban areas are mainly located at the border, particularly the west boundary, and closer to the coast of the study area. Housing programs need to be integrated with land use and urban planning policies. From an environmental and ecological perspective, concerns arose in JBNERR related to habitat loss and degradation in its watershed.

According to Estudios Técnicos Inc., (2017), habitat loss and degradation occur in the reserve and its watershed as a result of nutrient inputs to surface and ground water, cutting and filling of mangroves, and land use impacts such as sedimentation from

development and groundwater withdrawal to support agriculture and communities. In this effort, our methods and results help to assess areas of major vulnerability for urban growth since housing development is a critical concern because it indirectly threatens ecological and recreational impacts in JBNERR. In Puerto Rico, the absence of this integration through the decades leading to a very negative urban sprawl situation on the one hand and, on the other, to siting of affordable housing projects away from urban centers and job locations (Estudios Tecnicos Inc, 2014). In addition, an economy shifted from agriculture to an industrial economy, particularly in a land closer to the coasts, leaving space for forest recovery, population migration from the most rural areas to urban areas are some of the explanations to our results (López Marrero, 2003; C. Wang et al., 2016, 2017). Thus, the housing units' estimates decreased from 1990 to 2010 in the forest cover area and the housing unit density, which declined from ~6 in 1990, ~3 in 2000, and ~1 housing units/900m^2. It is more difficult to explain how housing units reduce their distribution and density; for JBNERR, one reason to explain this diminution is spatial resolution forest growth.

Furthermore, many planning decisions in JBNEER may impact the local development and the conservation of the reserve. The local community knowledge of JBNERR serves as an important information source to integrate with the dasymetric method to help planners, geographers, and every stakeholder who seek to link population and housing distribution and its density with other environmental aspects like agriculture and recreation. Especially after 2010, for Puerto Rico, the population declined over the next decade due to economic conditions and emigration (SDC-PR, 2021). In turn, a population decline in JBNERR will be expected. Therefore, much of the existing

infrastructure is underused as population declines and future conversion from permeable to impermeable surfaces may relate to the reduced cost of building on existing open space vs. redeveloping the urban area, desired ambiance of non-urban settings for development, proximity to existing development, or other reasons (Gould et al., 2017).

Chapter Two. Understanding Land Changes in Jobos Bay Watershed, Puerto Rico during 1977-2010: Urban Expansion and Agriculture Conversion

Abstract

In 1981, Jobos Bay on the south coast of Puerto Rico was designated as a National Estuarine Research Reserve (JBNERR). However, increasing land changes (i.e., urbanization and agricultural practices) in the nearest watershed of JBNERR has exacerbated the anthropogenic stress on local coastal ecosystems. To quantify land cover changes and to assess the potential impacts of land changes in the estuarine ecosystem, we applied the methodology of Pontius et al. (2004) to detect the landscape transformation in the tropical watershed of JBNERR in terms of four land cover categories for 1977, 1991, 2000, and 2010. We derived the land cover transition matrix to show each transition's magnitude and the amount of gain and loss in each land cover class. The results showed that urbanization and sprawl occur mostly from pasture and were continually increasing for the entire study period. Specifically, the highest urban expansion was found from 2000 and 2010 (46.7%), in 1977 to 1991 (25.2%), and around 18% between 1991 and 2000. Nevertheless, land change trends of reforestation also have a high potential to continue because forest recovery occurred at 44.7% during 1991 and 2000 and 42.4% between 2000 and 2010. In sum, this research provides an insight into the understanding of urban growth and cultivated lands reduction, which support the prediction, assessment, tracking of land changes related to the conservation policy.

Introduction

Land use/land cover change (LULCC) is one of the most critical components and driving factors of global climate and environmental change (Grau et al., 2003; Han et al., 2015; Turner et al., 1995). The terms 'land use' and 'land cover' are often used interchangeably (Rawat & Kumar, 2015), but each term has its definition. Land cover considers the attributes of the earth's land surface and immediate subsurface, including

biota, soil, topography, surface and groundwater, and human structures (Lambin et al., 2003). On the other hand, land use refers to the functional dimension corresponding to the description of the socioeconomic purposes (e.g., areas used for residential, industrial or commercial, farming or forestry, recreational or conservation purposes, etc.) which links to land cover (European Communities, 2001; Turner et al., 1995). Land cover changes is often a result of land-use change, climate change, and vegetation succession. However, used together, the phrase Land Use / Land Cover refers to Land change science that has emerged as a fundamental component of global environmental change and sustainability research (Turner, Lambin, & Reenberg, 2007). Timely and accurate change detection of land provides a better understanding of relationships and interactions between the human and natural environment and provides insights for better management and resource use (Lu et al., 2004).

Nonetheless, despite the societal need to thoroughly understand the land change in our rapidly changing world, there is a surprising lack of LULC data produced with sufficient accuracy, consistency, and spatiotemporal coverage (Clark et al., 2012). Better data alone are insufficient for improved models and projections of land-use and land-cover change (Lambin et al., 2001). Proper change detection research should provide the following information: (1) area change and change rate; (2) spatial distribution of changed types; (3) change trajectories for land-cover kinds; and (4) accuracy assessment of change detection results (Lu et al., 2004). Remote sensing and geographic information science capabilities to map and monitor land change emerged as tools to measure the spatial and temporal patterns at different geographic scales (Alo & Pontius, 2008). Geographical Information Systems (GIS) are the systematic introduction of additional

disciplinary spatial and statistical data to inventory the environment, observation of change and constituent processes, and prediction based on current practices and management plans (Ramachandra & Kumar, 2004). GIS also has proved to be a useful tool in many change detection applications and has become an essential tool to improve change detection accuracy (Lu et al., 2004). A common method about land changes metrics is the use of a land use/cover transition matrix, which provides a cross-tabulation matrix used to quantify and analyzed the trends and causes for those changes, including socioeconomic factors and agricultural policies (Pôças et al., 2011; Zhang et al., 2017). LULC transitions can be detected by statistical evaluation by comparing different temporal pattern maps (Zhang et al., 2017).

The tropical islands of Puerto Rico have been used as a land cover transformation model for many scientists interested in land cover change (Arce-Nazario, 2016). For example, the land cover change and land fragmentation has significantly altered the watershed hydrology (Gao & Yu, 2017). It was found that much of the original flora in most of the coastal plains has been removed to make room for coastal agriculture (especially sugarcane during the 1800s) and development (C. G. García-Quijano et al., 2015). Another study of the potential effect of land-use changes on water quality at watershed-scales are essential to minimizing water pollution (Yuan et al., 2015) and make better decisions on environmental resources management. This study aimed to detect LULCC and to identify the trajectory of cultivated land changes with regard to the state and local economy and the environmental conservation of the tropical estuary at Jobos Bay National Estuarine Research Reserve (JBNERR) in Puerto Rico.

During the last three decades, all the land around JBNERR has been impacted by human activities, and has experienced modifications in hydrology, nutrient dynamics, and impediment of establishing mangrove species and associated communities (Laboy et al., 2008). These changes are part of the dramatic land changes on the Caribbean island of Puerto Rico during the last 70 years, as economy shifted from agriculture to industry and services (Kennaway & Helmer, 2007). The increasing industrial and commercial growth in the watershed has been recognized as a concern to Jobos Bay's ecosystem health (Whitall et al., 2011). Therefore, the land changing pattern in JBNERR aroused concerns for water quality and quantity, which could imperil the reserve's sustainability as a pristine estuarine habitat, a key criterion for National Estuarine Research Reserve System (NERRS) (Laboy, Capellla, Robles, & González, 2008). Therefore, three specific objectives of this study were to (1) analyze the spatial and temporal dynamics of land change patterns from 1977 to 2010; (2) to quantify land cover changes thru Land Cover Transition Matrix; and (3) illustrate the trajectory of agriculture change and the driving factors.

Methodology

Study Area

JBNERR is in the southeast of Puerto Rico. It is the second widest estuary in the island, only surpassed by the San Juan Bay estuary. NOAA designated the JBNERR as a National Estuarine Research Reserve in the 1980s (Figure 17). Estuarine environments are the transitional zones between rivers and sea, receiving most of the drainage waters from the land through the fluvial network and are important ecosystems where oceans and rivers contribute to specific biodiversity (Osei-Twumasi & Falconer, 2014; Ratnayake et al., 2005). They are important water bodies for human food sources and

recreational activities (Ratnayake et al., 2005). Then, the watershed land-use changes (e.g., urban development, industrial, agriculture) and anthropogenic activities may lead to introduce pollutants to estuary waters.

The Jobos Bay watershed (JBW) covers 137.3 km² (34,000-acres) of the southern coastal plain, and two perennial rivers, Río Nigua to the west and Río Guamaní to the east form the stream network (Whitall et al., 2011). JBNERR belongs to the Rio Coamo watershed and is divided into four sub-watersheds: Rio Nigua, Rio Seco, Quebrada Aguas Verdes, and Rio Seco. Every sub-watershed has a unique set of surface water drainage and land cover, and land use conditions. Moreover, the Canal de Patillas (Patillas'channel) and Canal de Guamaní (Guamaní's channel) was built primarily for irrigation of agriculture. Consequently, the JBNERR watershed does not contain one single river network that accumulates surface water flow throughout the basin (Estudios Técnicos Inc., 2017). This watershed includes various distinct pathways by which surface waters are contributed to Jobos Bay, which provides for perennial stream discharges, intermittent stream discharges that join and flow directly into the bay, and diffuse overland runoff (Estudios Técnicos Inc., 2017; Whitall et al., 2011).

Figure 17

JBNERR watershed delimitation.

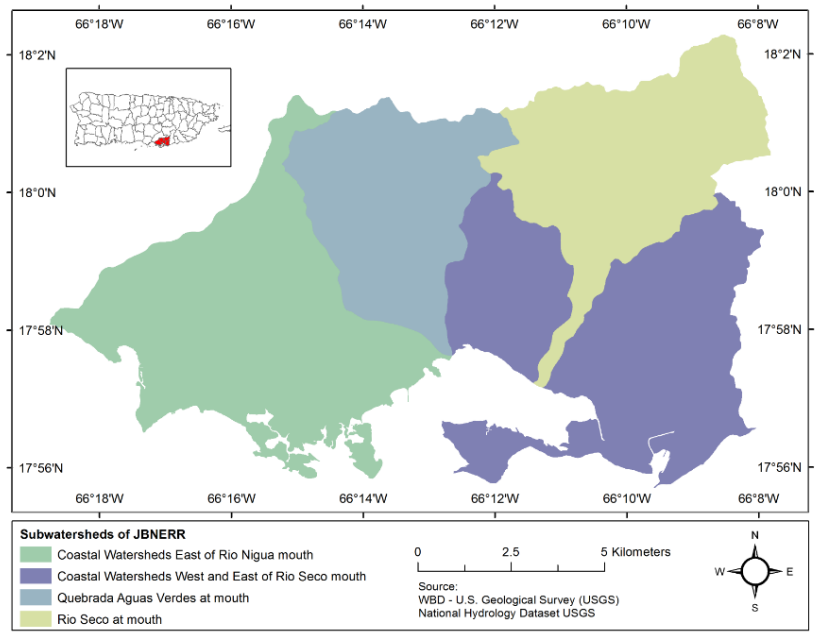

This paper applies Pontius et al. (2004) methodology to derive and analyze the transition matrix and detect strong land transformation signals in JBW based on four land cover maps of 1977, 1991, 2000, and 2010. The transition matrix reveals the magnitude of each transition and the amount of gain and loss in each land cover type. The land uses at the watershed have gone through urban development and conversion of agricultural lands to commercial or residential areas. Changes in irrigation methods and the growing industries tend to impact the ecosystems (PRWRERI, 2013). According to Zitello et al. (2008), cultivated lands in JBNERR comprise 11% of the total land cover, and the bay area also hosts two electric power generation plants, a petroleum refinery, and several major chemical and pharmaceutical facilities. Contaminants from the industries, agriculture pesticides and herbicides, household sewage, and illegal or conflictive

recreational practices may potentially threaten the ecosystems (Estudios Técnicos Inc., 2017; Laboy et al., 2008; Zitello et al., 2008).

Databases

This study used classified images provided by the USDA Forest Service and NOAA Office for Coastal Management. The classified images have been classified as analyzing the Landsat TM+ satellite images with 30 by 30 meters high resolution from 1977, 1991, and 2000 to detect the spatial distribution created by Gould et al. 2007 and Helmer and Kennaway 2007. The classification system applied for 1977 was a time series that include a digitized paper maps of land cover in 1977 based on photo interpretation, but the quantitative information on the accuracy of the maps for 1977 is not available (Kennaway & Helmer, 2007). The data from 1977 was co-registered to the Landsat image mosaic from about the year 2000, and then converted to raster format with a pixel size of 30 meters (Kennaway & Helmer, 2007). The other two maps are of forest type and land cover and are based on decision regression tree classification of Landsat image mosaics dated 1991 and 2000 (Helmer & Ruefenacht, 2005; Kennaway & Helmer, 2007). Another image classified by the NOAA Office for Coastal Management (NOAA/OCM) was considered in the study, respectively, to the year 2010. However, the NOAA/OCM created a 30-meter land cover map from the 2-meter product by performing a majority focal analysis and incorporating the percent impervious values following the C-CAP 30 meter class definitions (High Intensity Developed > 79% impervious, Medium Intensity Developed > 49% impervious, and Low Intensity Developed > 19% impervious) (NOAA Office for Coastal Management (NOAA/OCM), 2009, 2017).

This study mostly seeks to analyze the cultivated land reduction into coastal areas to pasture, and afforestation has been the common forms of transitions in JBNERR. In this sense, the sequence periods of 1977, 1991, 2000, and 2010 were selected with at least ten years span between one data image to the other because it represents an economic shift in Puerto Rico from agriculture to industry activities. For this study, a reclassification process was done to LULC maps to calculate the transition matrix. The five land cover maps were reclassified, followed by the classification system made by Kennaway and Helmer (2007) for Puerto Rico. The LULC maps for JBNERR were prepared with five land-cover classes named Forest, Cultivated lands, Pasture/Grass, Urban development, and Non-Forest.

Conventional Transition Matrix

Map comparison is a fundamental procedure in geographical analysis (Kuzera & Pontius, 2008). Transition matrices have often been used in landscape ecology and GIS studies of land use to estimate the rate of change (Takada et al., 2010). The land transition matrix comes from system analysis seeking the quantitative description of the system state and state transition, and it is the most common approach used to compare maps of different sources, as it provides detailed "from-to" change class information (Teferi et al., 2013; Zhang et al., 2017). Thus, an analysis of multi-temporal LULCC through enhanced transition matrix and spatial statistical modeling improved the identification, quantification, and understanding of determinants of most systematic transitions in an area (Teferi et al., 2013).

Land changes analysis was obtained from maps of times one and two, examining the changes with a transition matrix to identify the most important transitions and

investigate the processes generating the shifts (Pontius, Shusas, & Mceachern, 2004). This method disaggregates the process of LULCC in the different resulting land covers so that the response is not the total change in land use/cover, but rather an approximation to the surface converted, for example, from forest to a different land use/cover (Torres-Rojo et al., 2016). In conventional land cover transition models, the probability P_{ij} for a land cover change from *i* to *j* is exemplified by the following illustration (Osaragi & Aoki, 2006, Figure 18):

Figure 18

Illustration of the geometric union operation combines the information of two land-cover maps into a transition map and how the transition matrices are obtained from this map.

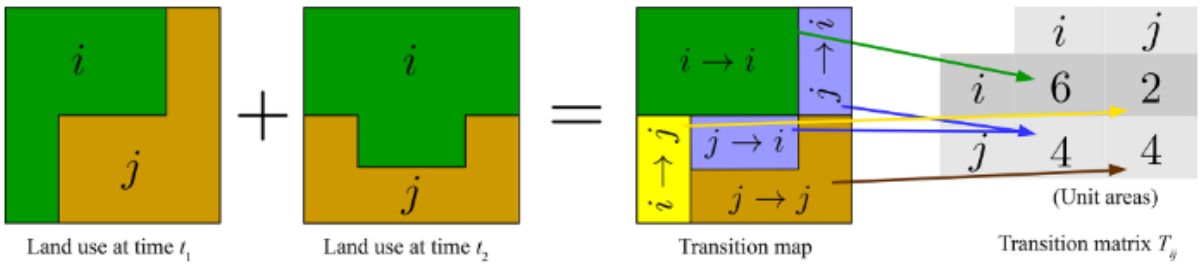

Source: Müller-Hansen, F., Cardoso, M. F., Dalla-Nora, E. L., Donges, J. F., Heitzig, J., Kurths, J., & Thonicke, K. (2017). A matrix clustering method to explore patterns of land-cover transitions in satellite-derived maps of the Brazilian Amazon. Nonlin. Processes Geophys, 24, 113–123. https://doi.org/10.5194/npg-24-113-2017.

In this study, Pontius' methodology (2004) was used to compute the transition matrix and net changes for the Jobos Bay watershed at 30 meters resolution. The conventional cross-tabulation matrix or transition matrix follows (Table 6).

Table 6

Land use/cover transition matrix for comparing two maps from different points in time.

		Time$_2$						**Total time 1 (P_{i+})**	**Loss**
	LULC class	**L_1**	**L_2**	**L_3**	**L_4**	**L_5**	**L_n**		
Time$_1$	**L_1**	P_{11}	P_{12}	.		.	P_{1n}	P_{1+}	P_{1+} - P_{11}
	L_2	P_{21}	P_{22}	.		.	P_{2n}	P_{2+}	P_{2+} - P_{22}
	L_3	P_{31}	P_{22}	.		.	.	.	.
	L_4	P_{41}	P_{22}	.		.	.	.	.
	L_5	P_{51}	P_{22}	.		.	.	.	.
	L_n	P_{n1}	P_{n2}	.		.	P_{nn}	P_{n+}	P_{n+} - P_{nn}
Total time 2 (P_{+i})		P_{+1}	P_{+2}				P_{+n}		
Gain		P_{+1} - P_{11}	P_{+2} - P_{22}	P_{+3} – P_{33}	.	.	P_{+n} - P_{nn}		

Source: Illustration adapted from Zhang, B., Zhang, Q., Feng, C., Feng, Q., & Zhang, S. (2017). Understanding land use and land cover dynamics from 1976 to 2014 in Yellow River Delta. Land, 6(1), 1–20. https://doi.org/10.3390/land6010020

Where the rows display the classes of time one, and the columns show the classes of time two (Robert G Pontius et al., 2004). P_{i+} denotes the proportion of the landscape in class *i* in time one, which is the sum over all *j* of P_{ij}. The notation P_{+j} represents the proportion of the landscape in class *j* in time two, which is the sum over all *i* of P_{ij}. The notation P_{ij} denotes the proportion of the landscape that experiences a transition from class *i* to class *j*, and J is the total number of classes (Alo & Pontius, 2008; Pontius et al., 2004). Unchanged areas occupy the diagonal of the matrix while changed areas are represented in the off-diagonal elements of the matrix (Bhatta, 2010), indicating a transition from category *i* to a different category *j* (Teferi et al., 2013). Hence the diagonal entries indicate no change, then P_{jj} denotes the proportion of the landscape that

shows unchanged land class *j* (Pontius et al., 2004). The *N* is the number of grid cells in the maps.

Gross gains, gross losses, and net changes

The land cover change rate reflects the severity of land cover change in the study area in a given time (Liping et al., 2018). The diagonal data in the transition matrix is useful to calculate the gains and losses (Table 6). The gains are the differences between the land area from time two and the unchanged area per land cover class ($P_{+i} - P_{ii}$). The losses are the differences between totals in time one and the unchanged land area per land cover class ($P_{i+} - P_{ii}$). The "net change" is the difference between the total in time two and time one per land cover class ($P_{+i} - P_{i+}$). An essential contribution of these calculations is that a class-by-class paired comparison between the totals from time one and the totals from time two allows scientists to see how the two maps relate to the quantity of each land class (Pontius & Cheuk, 2006).

Land use Land Cover Annual Rate of Change

The annual rate of change is calculated by comparing the area under a land cover class in the same region at two different times (FAO, 1995; Puyravaud, 2003). The annual rate of change for each land cover class was calculated using the following equation proposed by Puyravaud (2003).

$$r = \left(\frac{1}{t_2 - t_1}\right) \times \ln\left(\frac{A_2}{A_1}\right)$$

Where r is the change for each class per year, A_2 and A_1 are the class area in time t_2 and time t_1, respectively, for the period being evaluated, and t is the number of years spanning that period (Batar et al., 2017). The proposed equation is commonly used to analyze forest land changes (Batar et al., 2017; Tripathi et al., 2020) because r is more

meaningful to biologists and gives higher values when the deforestation is high (Puyravaud, 2003).

Results

Land use Land Cover classification analysis

The LULC reclassification maps of 1977, 1991, 2000, and 2010 (Figure 19) indicated the visible land transformation involving significant changes of cultivated lands and an increase in a forest, pasture/grass, and urban development land. A detailed observation emphasizes that landscape change is relevant, with a significant decrease in the agriculture areas from 1977 to 1991 and 1991 to 2000.

Figure 19

Land use/cover maps based on image classifications by year: (a) 1977; (b) 1991; (c) 2000; (d) 2010.

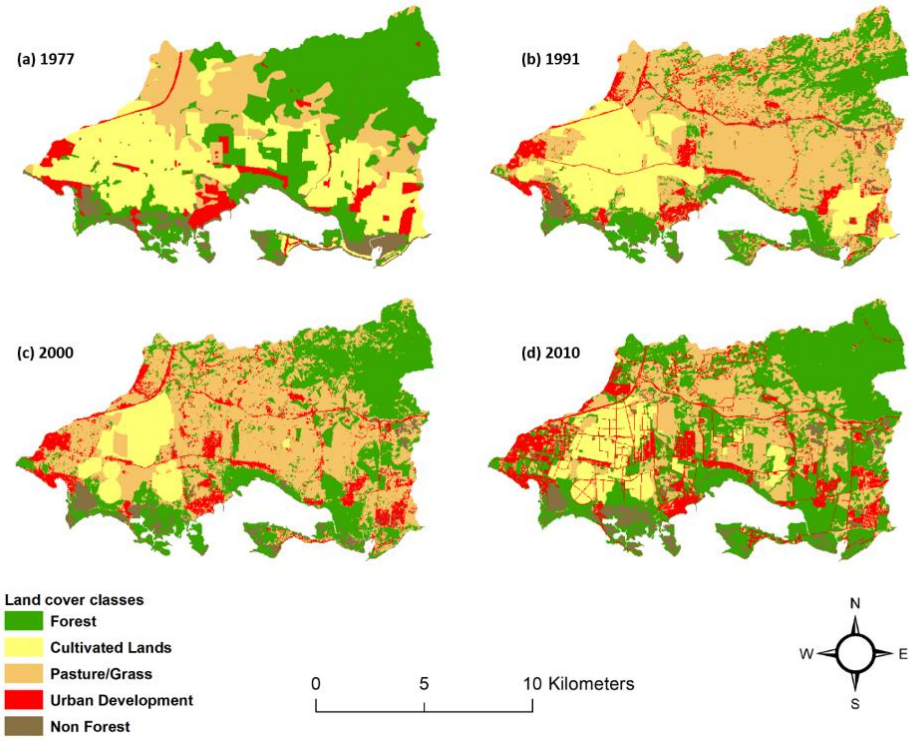

According to the reclassification results, the statistics profile represents the increases and decreases in different per land cover classes from 1977 to 2010 (Table 7 and Figure 20). In 1977, forest areas covered 52.1 km^2, ranking first with 38.1%. Forest was constantly the dominant land cover in the watershed's upper area, including 38.1% in 1977 and 45.4% in 2010. The significant increase in forest areas in 2000 and 2010 arose because of a considerable transformation from pasture/grass to the forest. Cultivated lands were mostly dominant in 1977 in sugarcane fields by covering 31.6%, second only to the forest. Cultivated lands considerably decreased to 8.3% in 2000 but then slightly increased to 9.6% in 2010. Meanwhile, the pasture/grass encompassed 17.8% of the Jobos watershed, ranking third of the total area in 1977.

In 2010 pasture/grass ranked second, covering 25.4% of the basin. However, in 1991 and 2000, pasture/grass ranked first, occupying 47.5% and 46.1%, respectively, of the total land area. Despite the pasture/grass declined from 46.1% in 2000 to 25.4% in 2010 due to primarily forest recovery, gains reverse this land cover class during other periods. Urban development land gradually increased during the 33 years from 1977 to 2010, which is characteristic of the urbanization process in Puerto Rico during that time. In 1977, the urban development areas represented 6.5% of the total area, ranking the fourth within the watershed. During the other periods, urban development increased up to 19.2 km^2 or 14.0% in 2010. The non-forest areas decreased during the 33 years from 6.0% (8.2 km^2) in 1977 to 5.5% (7.5 km^2) in 2010. These results compare with a previous study in JBNERR, where vegetated lands cover 70% of the landscape with grassland, forest, and scrub/shrub, accounting for 42%, 15%, and 13%, respectively to 2008 (Whitall et al., 2011).

Table 7

Land cover statistics profile from 1977 to 2010.

LULC classes	1977		1991		2000		2010	
	Area (km^2)	%	Area (km^2)	%	Area (km^2)	%	Area (km^2)	%
Forest	52.1	38.1	29.9	21.9	43.6	31.9	62.1	45.4
Cultivated Lands	43.3	31.6	25.5	18.7	11.3	8.3	13.2	9.6
Pasture	24.3	17.8	65.0	47.5	63.0	46.1	34.8	25.4
Urban Development	8.9	6.5	11.1	8.1	13.1	9.6	19.2	14.0
**Non Forest	8.2	6.0	5.2	3.8	5.7	4.2	7.5	5.5
Totals	136.8	100.0	136.8	100.0	136.8	100.0	136.8	100.0

Note. *Square kilometers values extracted from ArcGIS Summarize of Land Cover shapefile polygons.
**Barren lands and Water bodies are consolidated into Non Forest class.
Source data from the Landsat TM+ satellite images, US Department of Agriculture (USDA) and US Geological Survey (USGS).

Figure 20

Percentage of land cover classes distribution within JBNERR watershed, 1977 - 2010.

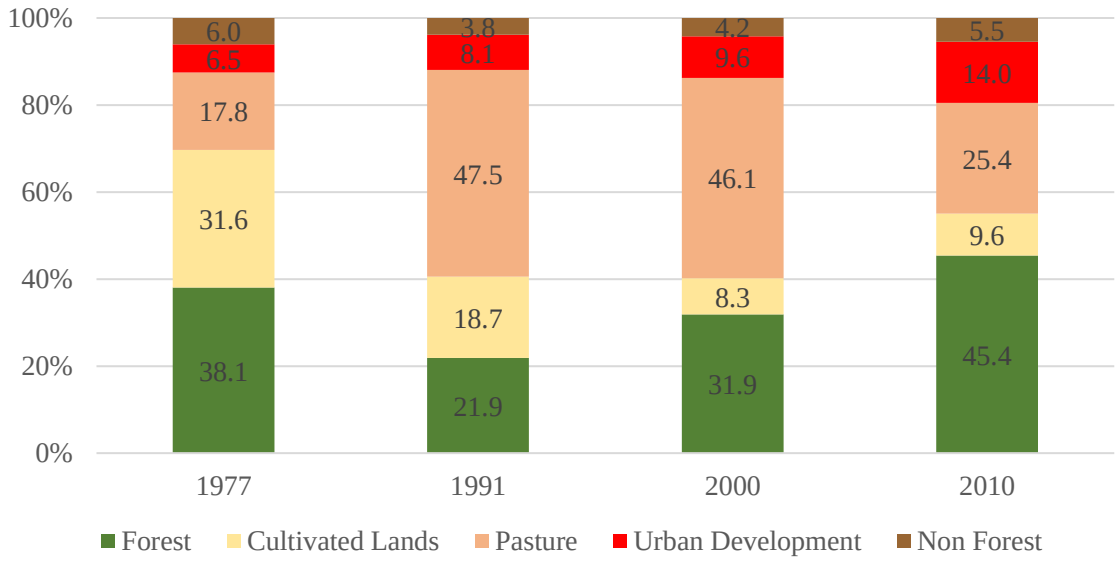

Land changes trends

This section presents the net change expressed as net change percentages, gross gain, gross loss, and the unchanged land area results by each land cover class and three-time periods. Figure 21 shows the net change percentage of each land class per period. The transitions were that forest increased 45.7% in the periods of 1991–2000 and 42.4% in 2000–2010 and decreased 42.5% in the first period 1977–1991. Urban development kept increasing from 1977 to 2010, but the third period, 2000 – 2010, presented a more considerable increase of 46.7%. In 1977–1991, pasture/grass land almost tripled the size with a total net change of 167.3%. Contrary to the period 2000–2010, that pasture decreased by 44.7%, reducing its total land area three times. Regarding cultivated land, a noticeable decrease of 41.0% and 55.5% to the periods 1977–1991 and 1991-2000 respectively but increased 16.2% in 2000-2010.

Figure 21

LULC net change percentage from 1977 to 2010.

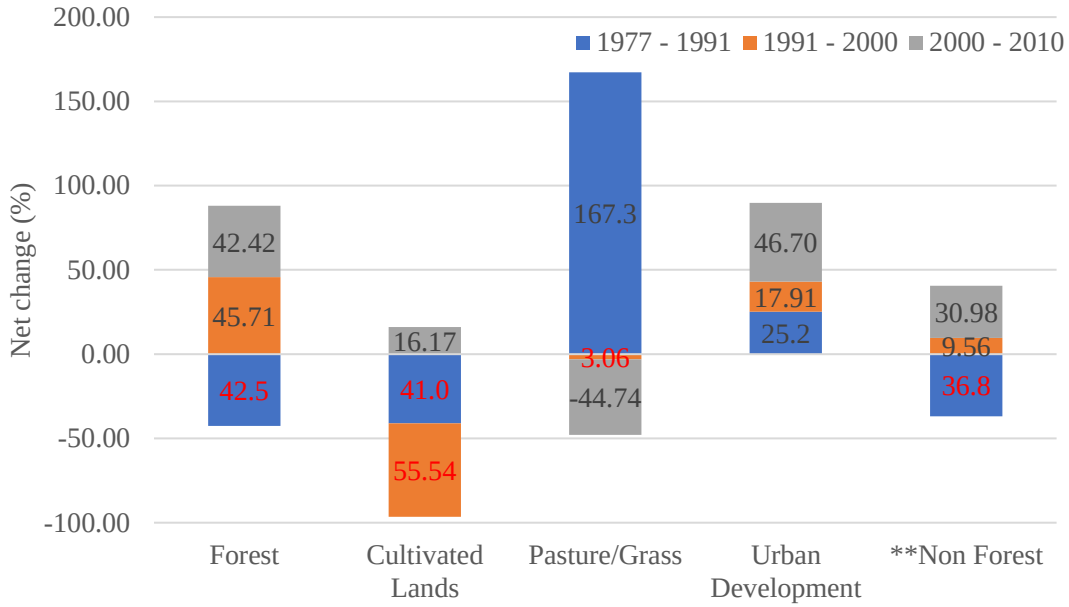

Note. **Non Forest include Barren lands and Water bodies are consolidated into Non Forest class.

Land changes trends

This section presents the net change, net change percentages, gross gain, gross loss, the unchanged land area, and the percentage of the annual rate of change results by each land cover class (Table 8). For better comprehension of the land changes, this section was discussed per period, 1977 – 1991, 1991 – 2000, and 2000 – 2010.

Land changes 1977 - 1991

The most significant negative net changes of 22.1 km^2 and 17.8 km^2 respectively to the forest and cultivated land with a negative annual change rate of 3.88% and 3.70% were noticed in the first period. During this period, forest land decreased by 42.5%, with a gross loss of 29.5 km^2. The cultivated land area had a gross loss and gross gain rate of 20.8 km^2 and 3.0 km^2, respectively, showing a noticeable decrease of 41.0% in 14 years. Another significant net change of 40.7 km^2 in pasture/grassland was found, which almost

tripled its area extension to 65.0km^2, and its gross gain was 47.1 km^2, with an increase of 167.3%. Whitall et al. (2011) explained these land cover trends indicating that land use and land cover in the Jobos watershed has evolved from predominantly sugarcane cultivation in the early 1900s to increasingly urban and industrial use in the late 1970s. Besides our results compared to Puerto Rico land changes, a 64% decrease in agricultural lands of about 1,190 km^2 is the most substantial land-cover change on the island between 1977 and 1991 (Helmer, 2004). In sum, in Puerto Rico, the urban areas increased around 32% and 7.2%, from 1977 and 1991, and from 1991 to 2000, respectively (Helmer, 2004; Helmer & Ruefenacht, 2005).

Land changes 1991 - 2000

The forest and urban development areas increased by 13.7km^2 (45.7%) and 2.0km^2 (17.9%), respectively, indicating a gain gross of 19.7km^2 and 3.1km^2. The positive annual change rate of 4.27% and 1.85%, respectively, to the forest and urban development. However, the cultivated lands decreased by 55.5%, and its gross loss was 15.3km^2, being the second-highest gross loss, followed by pasture. Our findings compare with the land changes trend in Puerto Rico, where urban areas increased 32% in 1977 - 1991 and 7.2% in 1991 - 2000 (Helmer, 2004; Helmer & Ruefenacht, 2005). While pasture and urban areas were displacing cultivated lands in JBNERR, Forest was displacing Pasture areas. Forest (18.9km2) gross gain was significantly greater than the net gain of cultivated lands (1.1km^2). Therefore, the negative net change of cultivated lands in JBNERR between 1991 and 2000 (14.2km^2) was significantly smaller than the Pasture net change (2.0 km^2). The principal finding from this change analysis for 1991-2000 is that Forest net change has greatly increased (13.7km^2) while urban development net change has increased very fragmented as urban sprawl (2.0km^2). According to our

land changes results during this period in JBNERR compare to the land changes in the island, as a result of an economic shift, intensively cultivated lands have transitioned to hay or intermittently grazed pasture, and if left unmanaged, regenerate to the forest (Kennaway and Helmer, 2007).

Land changes 2000 - 2010

From 2000 to 2010, the net changes in Forest land presented a significant increase of 42.4% (18.5 km^2). Forest and urban areas have the highest gross gain with 25.3 km^2 and 10.7 km^2, respectively, while pasture land has a major gross loss of 34.9 km^2. The pasture areas decreased by 28.2 km^2 (44.7%), putting this land cover change with the highest reduction in the entire study period. The cultivated lands increased by 16.2% (1.8km^2), ranking the fourth land class with a noticeable increase, and its gross gain is 4.4km^2. Meanwhile, urban areas listed second, increasing at 46.7% (6.1km^2). In terms of the annual rate of change, forest annually increased by 3.60%, urban areas by 3.91%, cultivated lands by 1.51%, but pasture annually decreased by 5.76%. In Puerto Rico during 2000 – 2010, the net change rates of forest were positive (C. Wang et al., 2017), comparable to our results in the last two periods. Besides, our results align with Wang, Yu, & Gao, (2017) land changes trends result for Puerto Rico, where Herbaceous agriculture/pasture has a net loss (624.4 km2, 21.7%) in this period, giving rise mostly to the expansions of forests (311.5 km_2, 7.8%) and woodland (197.3 km2, 18.7%) during 2000 - 2010.

Table 8

Statistical table of the land cover dynamic changes in JBNERR from 1977 to 2010.

1977 - 1991								
Class	**Area (km^2) 1977**	**No change**	**Gross Loss**	**Gross Gain**	**Area (km^2) 1991**	**Net change**	**Δ%**	**r (% per year)**
Forest	52.1	22.6	29.5	7.4	29.9	(22.1)	-42.5%	-3.88
Cultivated Lands	43.3	22.5	20.8	3.0	25.5	(17.8)	-41.0%	-3.70
Pasture	24.3	17.9	6.4	47.1	65.0	40.7	167.3 %	7.28
Urban Development	8.9	4.8	4.0	6.3	11.1	2.2	25.2%	1.62
****Non Forest**	8.2	2.6	5.6	2.6	5.2	(3.0)	-36.8%	-3.23
Total	136.8	70.4	66.4	66.4	136.8	-	-	-
1991 - 2000								
Class	**Area 1991**	**No change**	**Gross Loss**	**Gross Gain**	**Area 2000**	**Net change**	**Δ%**	**r (% per year)**
Forest	29.9	23.9	6.0	19.7	43.6	13.7	45.7%	4.27
Cultivated Lands	25.5	10.2	15.3	1.1	11.3	(14.2)	-55.5%	-8.61
Pasture	65.0	44.1	20.9	18.9	63.0	(2.0)	-3.1%	-0.35
Urban Development	11.1	7.6	3.5	5.5	13.1	2.0	17.9%	1.85
Non Forest	5.2	2.6	2.6	3.1	5.7	0.5	9.6%	1.02
Total	136.8	88.5	48.2	48.2	136.8	-	-	-
2000 - 2010								
Class	**Area 2000**	**No change**	**Gross Loss**	**Gross Gain**	**Area 2010**	**Net change**	**Δ%**	**r (% per year)**
Forest	43.6	36.8	6.8	25.3	62.1	18.5	42.4%	3.60
Cultivated Lands	11.3	8.8	2.5	4.4	13.2	1.8	16.2%	1.51
Pasture	63.0	28.1	34.9	6.7	34.8	(28.2)	-44.7%	-5.76
Urban Development	13.1	8.6	4.5	10.7	19.2	6.1	46.7%	3.91
Non Forest	5.7	3.0	2.7	4.5	7.5	1.8	31.0%	2.74
Total	136.8	85.3	51.5	51.5	136.8	-	-	-

Note. *Square kilometers values extracted from ArcGIS Summarize of Land Cover shapefile polygons.

**Non Forest include Wetland, Barren lands and Water bodies are consolidated into Non Forest class.

Source data from the Landsat TM+ satellite images, US Department of Agriculture (USDA), and US Geological Survey (USGS).

Land Cover Transition Matrix Analysis

Land Cover Transition Matrix gives the ability to quantify, identify and compare land cover change rates and provide insights on how land changes depend on agricultural activities and urban development JBNERR, and how this compared with Puerto Rico. The use of Landsat images for assessing human imprints on the land indicative, such as population settlements patterns; land clearing for the cultivation of crops, and a host of other land transformations that have necessary population-environment signatures and cause and consequence implications for examining land use and land cover dynamics (Walsh, Rindfuss, Prasartkul, Entwisle, & Chamratrithirong, 2005). The Transition Matrix is the table where the rows signify the land cover status in time one, while the columns of the table represent the land cover status in the latest time or time two. We can also refer to the transferring-out situation of land cover change in the rows in time one and the transferring-in in the final state or time two (Liping et al., 2018).

Transition Matrix 1977 - 1991

Table 9 is the matrix for 1977 – 1991, shows cultivated land presented the largest unchanged area of 22.6 km^2 compared to the rest of land cover classes. However, cultivated land transferred 17.4 km^2 into pasture land, being the most significant land transfer related to other land classes. Forest ranked second with the highest unchanged land area, 22.6 km^2. The forest transfers out are 25.4 km^2 into the pasture, being the most critical forest land transfer related to other land classes. In sum, pasture had the most significant expansion from the forest and cultivated lands. An explanation to our findings is that almost the entire coastal plain of Jobos Bay was under sugarcane cultivation until the sugarcane market's demise during the 1960s (Whitall et al., 2011; Zitello et al., 2008). These land change trends were expected because, from Spanish Colonial times up to the

1970s, the Jobos Bay watershed was primarily used for agricultural production (Laboy et al., 2008), and after 1991 sugarcane lands were abandoned. Besides, close to the JBNERR watershed, the Central Aguirre sugar mill was located. The sugarcane fields extended throughout the South Coastal Plain with other plantations, coconut plantations bordering the shoreline (Laboy et al., 2008). Similarly to these results, in Puerto Rico, the agricultural lands decrease 64% having the most considerable land cover change to pasture (~ 480 km^2), forest (~ 330 km^2), and urban/developed lands (~ 73 km^2) on the island between 1977 and 1991 (Helmer, 2004).

Table 9

Transition matrix for 1977 - 1991 (km^2).

		1991					Total area 1977
LULC Class		**Forest**	**Cultivated Lands**	**Pasture**	**Urban Develop**	**Non Forest**	
1977	**Forest**	22.6	1.0	25.4	1.5	1.4	52.0
	Cultivated Lands	1.4	22.5	17.4	1.6	0.4	43.3
	Pasture	2.1	1.4	17.9	2.6	0.4	24.3
	Urban Development	0.5	0.5	2.6	4.8	0.4	8.9
	Non Forest	3.4	0.1	1.5	0.6	2.6	8.3
	Total area 1991	29.9	25.5	64.9	11.1	5.3	136.8

Note. Matrix cell values derived from ArcGIS Geometry calculations for 1977 and 1991 Land Cover shapefiles at 30-meters cell size.
*Square kilometers values extracted from ArcGIS Summarize of Land Cover shapefile polygons.
**Non Forest include Barren lands and Water bodies are consolidated into Non Forest class.
Source data from the Landsat TM+ satellite images, US Department of Agriculture (USDA), and US Geological Survey (USGS).

Transition Matrix 1991 - 2000

During the period from 1991 to 2000 (Table 10), cultivated lands continue to decline, and the significant changes were 11.6 km^2 was converted to pasture, 2.1 km^2 were transferred out to the forest, and 1.5km^2 became urban areas. Forest land increase

mostly by transferring in 15.9 km^2 from pasture and 2.1 km^2 from cultivated lands. The urban areas slightly expanded 2.6 km^2 from previous pasture lands. At the same time, pasture lands transferred in 11.6km^2 from cultivated lands. Even in Puerto Rico, land cover changes from 1991 to 2000 were mostly featured with urban expansion and loss of sugarcane, pineapple, and other lowland agriculture to pasture (Kennaway & Helmer, 2007). Likewise, in the Jobos watershed, 43.1 km^2 of pasture remains unchanged and is the land class with the highest area of unchanged land during this period. Also, 23.9km^2 of unchanged forest and 10.2km^2 of cultivated land remain unchanged. Our findings are similar to Puerto Rico for 1991 and 2000; herbaceous agriculture transitioned to pasture, hay, or inactive agriculture, pasture reverted to the forest or underwent land development (Helmer, 2004; Kennaway & Helmer, 2007).

Table 10

Transition matrix for 1991 - 2000 (km^2).

LULC Class		2000					Total area 1991
		Forest	**Cultivated Lands**	**Pasture**	**Urban Develop**	**Non Forest**	
1991	**Forest**	23.9	0.1	4.0	0.5	1.6	30.0
	Cultivated Lands	2.1	10.2	11.6	1.5	0.1	25.5
	Pasture	15.9	0.9	44.1	2.7	1.0	64.6
	Urban Development	0.6	0.1	2.6	7.6	0.4	11.3
	Non Forest	1.1	0.0	0.7	0.8	2.6	5.3
	Total area 2000	43.6	11.3	62.9	13.2	5.7	136.8

Note. Matrix cell values derived from ArcGIS Geometry calculations for 1991 and 2000 Land Cover shapefiles at 30-meters cell size.
*Square kilometers values extracted from ArcGIS Summarize of Land Cover shapefile polygons.
** Non Forest include Barren lands and Water bodies are consolidated into Non Forest class.
Source data from the Landsat TM+ satellite images, US Department of Agriculture (USDA) and US Geological Survey (USGS).

Transition Matrix 2000 - 2010

From 2000 to 2010, the most significant change was found in a forest, increasing from transferring 20.5 km^2 from pasture, and it also had the largest unchanged territorial extension (Table 11). The cultivated lands transferred out 1.0 km^2 into a pasture, 0.6 km^2 into Forest, and in 0.9 km^2 into urban areas. Cultivated lands slightly increased from 11.3 km^2 in 2000 to 13.2 km^2 in 2010 as 4.2 km^2 was transferred from pasture. Pasture ranked second with 28.1 km^2 unchanged land area, and cultivated land ranked third with 8.8km^2 that remained. It is essential to highlight that, according to Whitall et al. (2008), pasturage is also considered a principal agricultural use in the Jobos Bay watershed. Forest also had 36.8 km^2 remaining unchanged. Consequently, the urban areas increased from 13.3 km^2 in 2000 to 19.1 km^2 and mainly transferred in 8.2 km^2 from pasture. In JBNERR, during these years, more than 500 housing units, the golf course, hotel, Villas Complex, and the AES coal energy generating plant have been constructed as part of the urban and economic development (Laboy et al., 2008). As a result, in JBNERR, with the end of the sugarcane era in 1994 (Whitall et al., 2011), the remaining vestiges of sugarcane lands are steadily being supplanted by fruit and vegetable cultivation (Laboy et al., 2008) in minor land area extension during this period.

Table 11

Transition matrix for 2000 - 2010 (km^2).

		2010					Total
		Forest	**Cultivated Lands**	**Pasture**	**Urban Develop**	**Non Forest**	area
LULC Class							2000
2000	**Forest**	36.8	0.1	3.2	0.9	2.6	43.7
	Cultivated Lands	0.6	8.8	1.0	0.9	0.0	11.3
	Pasture	20.5	4.2	28.1	8.2	1.6	62.5
	Urban Development	2.1	0.1	2.3	8.6	0.3	13.3
	Non Forest	1.7	0.0	0.4	0.6	3.0	5.7
	Total area 2010	61.8	13.2	34.9	19.1	7.5	136.5

Note. Matrix cell values derived from ArcGIS Geometry calculations for 2000 and 2007 Land Cover shapefiles at 30-meters cell size.
*Square kilometers values extracted from ArcGIS Summarize of Land Cover shapefile polygons.
**Non Forest including Barren lands and Water bodies are consolidated into Non Forest class.
Source data from the Landsat TM+ satellite images, US Department of Agriculture (USDA), and US Geological Survey (USGS).

Overall, our results discerned that those forests experienced great recovery, and cultivated lands mainly shifted to pasture because of the economic shift from agriculture. It should be highlighted that even when forest decreased from 1977 to 1991, the magnitude of that decreased might be overestimate by the classification system of 1977. However, forest was increasing during the last 20 years of our period, from 1991 to 2010. At the same time, urban expansion increased in the Jobos watershed. According to Wang, Yu, and Gao (2017), urban areas continued to expand by converting herbaceous cover, even when both land cover classes dominate regions of lower slopes, such as coastal areas. Forests regenerating largely through natural processes after total abandonment of alternative land use (plantations, agriculture, pasture, etc.) on formerly forested lands (Chokkalingam & De Jong, 2001). Depending on the nature of alternate land use prior to abandonment, numerous subtypes can be further distinguished, e.g., post-agriculture, post-ranching, etc. (Chokkalingam & De Jong, 2001). These results explained that forest

recovery is the biggest asset for JBW since land sparing drives the abandonment of low-yield pastures that enhance the recovery of secondary forests (F. A. Edwards et al., 2021).

The most agricultural transformation occurred between 1977 and 1991 and between 1991 and 2000 in our study area. In JBW, pasture land uses mostly abandoned sugar cane fields and supports man-modified vegetation characterized by a complete grass cover and sparsely distributed tall trees with flattened spreading crowns (Zitello et al., 2008). This land transformation trend compared to the Caribbean island of Puerto Rico, where the forest, urban/built-up, and pasture lands have replaced most formerly cultivated lands (Kennaway & Helmer, 2007). In particular, a previous study found a correlation between forest cover and the agricultural cover of -0.50, indicating the reforestation was mostly from pasture and abandoned agriculture (Gao & Yu, 2017).

In addition, the Caribbean island of Puerto Rico was one of the few tropical sites in the world where reforestation is occurring at a higher rate than deforestation after 1940, and by 1980 forests had recovered because cropland and pasture were abandoned on eroded hillsides in the mountainous regions (Birdsey & Weaver, 1987). According to Dietz (1986), the economic changes after World War II dramatically decreased the pressure of human activities on local forests during the 1940s. The governments of Puerto Rico and the United States promoted a major shift in the island's economic base from agriculture to industry (Dietz, 1986). This economic shift is considered a land change driver. Specifically, that led to the abandonment of agricultural lands across the island and the extensive recovery of secondary forests (Birdsey & Weaver, 1987). However, previous studies in tropical (Buschbacher, 1986) suggest that forest recovery will be much slower in abandoned pastures by economic causes when compared with

regeneration following natural disturbances (e.g., treefalls and hurricanes). Some of the factors that may contribute to the prolonged recovery of pastures are lack of forest tree propagules because of the inhibition of tree establishment, high levels of seed and seedling predation, degraded soils or competition with established grasses and herbaceous species (Aide et al., 1995; Aide & Cavelier, 1994). Reviews of forest recovery following slash and burn agriculture or shifting agriculture result as secondary forest (Brown & Lugo, 1990). In fact, secondary forests are fast growing ecosystems whose species life cycles coincide with those of human land uses (Brown & Lugo, 1990).

Discussion

The municipalities where the JBW is located is considered an important site for agriculture in Puerto Rico (Gould et al., 2017). Even the historic prevalence of agriculture in the JBW, existing land cover indicates an ecosystem in a natural state (Whitall et al., 2011). As of 1995, most of the land area falling within the Jobos Bay Special Planning Area (SPA) was still devoted to agriculture (Laboy et al., 2008). In that matter, agriculture and urban growth along the coast invade estuarine habitat and increase the direct discharge of untreated wastewater from local communities with no water treatment facilities (Laboy et al., 2008). From our knowledge, the most recent study presents that during 2002 and 2012, JBNERR watershed shows the following land-use changes: agriculture decreased by 17.3%, forested land increased by 227.1%, grassland/scrub-shrub increased by 12.9%, urban residential increased by 15.3% (low density), 16.3% (medium density), and 6.5% (high density) (PRWRERI, 2013).

In contrast, our land changes results from 2000 to 2010 show the not following land changes: agriculture increased by 16.2%, forest increased by 42.4%,

pasture/grassland decreased by 8.5%, total urban development increased by 5.5%. Our results are different from the study of PRWRERI (2013). The difference might be explained because they used IKONOS images and digital aerial photography from 2002 and 2012 (PRWRERI, 2013). The classification scheme doesn't meet the need of the NERRS, where the main focus is the detailed inventory of coastal habitat and landscape features (PRWRERI, 2013). However, both studies present an increase in forested lands and an increased in urban development in ten years. Even when our results reinforce these observations from previous studies in JBNERR, we decided to compare our findings trends with Guánica Bay watershed (GBW), San Juan Bay watershed (SJBW), and the general land changes trends in Puerto Rico similar time (Table 12).

Guánica Bay is a major estuary on the southwest coast of Puerto Rico (Whitall et al., 2013) and receives water directly only by the Rio Loco (Viqueira, 2018). The historical agricultural land use (sugarcane farming) has given way to several land uses, including coffee farming in the mountains, small urban areas, and forest (Whitall et al., 2013). Like JBW, the Guánica Bay watershed (GBW) experienced human alteration of its hydrology via irrigation and drainage, causing concerns related to land-based sources of pollution (Whitall et al., 2013). In 2004 the current GBW land use was 48% forested, 43% agriculture, and 9% urban, totaling approximately 57,000 acres (230.7 km^2) (Center for Watershed Protection, 2008). In 2000, the LULC in JBW was different from GBW because the forest was 31.9%, agriculture cover was 8.3%, while urban areas were very similar with 9.6% coverage within 137 km^2. According to the literature, even when JBW still an important agriculture site, sugarcane fields were abandoned and transitioned to pasture after 1993. These land changes enhance anthropogenic threats to the bay (Apeti et

al., 2012; Estudios Técnicos Inc., 2017; Laboy-Nieves, 2009; Laboy et al., 2008; Whitall et al., 2011). Thus, the Management Plan for the Jobos Bay National Estuarine Research Reserve, 2010 to 2015, pursues to strengthen the protection and management of the JBNERR to advance estuarine conservation, research, and education opportunities (DNER, 2010). Likewise, the Implementation of the GBW Management Plan seeks to outline a comprehensive set of actions and an overall management strategy for improving and protecting the watershed from nonpoint sources of pollution derived from land-use alterations and residential, commercial, and agricultural uses (Viqueira, 2018). In sum, both sites are considered well-suited to mechanized agriculture with under 10 percent slope, and also to non-mechanized agriculture on moderate slopes between 2.02 – 4.05 km^2 (Gould et al., 2017). Besides, the municipalities where the JBW and GBW are located are considered as Prime farmland if irrigated by the Natural Resource Conservation Service (NRCS) (Gould et al., 2017). A Prime farmland, as defined by the US Department of Agriculture, is a land that has the best combination of physical and chemical characteristics for producing food, feed, forage, fiber, and oilseed crops and is available for these uses (USDA-NRCS, n.d.). It could be cultivated land, pastureland, forestland, or another land, but it is not urban or built-up land or water areas (USDA-NRCS, n.d.). In this sense, some areas have been losing some prime farmland to industrial and urban uses, like the recent land-use trend (USDA-NRCS, n.d.).

The San Juan Bay Estuary is the biggest on the island, located in the north of Puerto Rico. The San Juan Bay watershed (SJBW) encompassed parts of eight municipalities: San Juan, Bayamón, Cataño, Toa Baja, Guaynabo, Carolina, Loíza, and Trujillo Alto, making it the most populated estuary of Puerto Rico (Govender &

Thomlinson, 2010). The study of Govender and Thomlinson (2010) compared land changes between the SJBW and JBW from 1936 to 2002. They found that from 1936, 1971/1977, and 2002 for both studies sites drastic changes to LULC where 100 % loss of agriculture and 182 % increase in urban development and 77 % loss in agriculture and 650 % increase in urban development for San Juan Bay Estuary and Jobos Bay Estuary, respectively (Govender & Thomlinson, 2010). In another study from 2011, the average ground cover within SJBW, excluding larger bodies of water considered census waters, 10.6 percent of the ground was covered in duff/mulch, 20.7 percent in herbaceous plants (excluding grass), 15.9 percent in grass (both maintained and unmaintained), 8.2 percent in water, 17.0 percent with buildings, and 27.6 percent with impervious (for example, cement or tar) and other surfaces (Brandeis et al., 2014), cultivated lands were not detected or not studied. In 2013, the SJBW has fifty-five percent of the watershed covered by urban areas or gray infrastructure, such as roads, residential units, and commercial buildings (51.5% high-density urban areas and 3.6% low-density urban areas), 20% are green areas (10.7% woods and 9.4% grass and pasture), and 23.2% are wetlands (Gould et al., 2008; Méndez-Lázaro et al., 2018), any cultivated lands were not detected or not studied. Comparing the different studies' land changes results for SJBW to ours results in JBW, the land changes trends are similar from 1977 to 2000 where agriculture decreased as observed by Govender and Thomlinson (2010) 1936 to 2002. While in SJBW, urban areas are greater than 50% according to the land-use history between 1999 and 2003 (Gould et al., 2008; Méndez-Lázaro et al., 2018), which is greater than urban cover in JBW, 9.6% in 2000, and 14.0% in 2010. Consequently, the end of the agriculture era in the SJBW and the changes made to irrigation techniques in

the cultivated lands in JBW resulted in changes to the hydrological conditions within both estuaries (Yogani & Thomlinson, 2010). Changes in irrigations systems for cultivated lands might have a considerable impact increasing surface runoff, which has significant on- and off-site impacts (e.g., depletion of soil moisture and increased soil erosion and sediment de- position in downstream areas) (Berihun et al., 2019). Thus, population growth associated with changing farming practices (e.g., irrigation systems) were the major drivers for LULC changes (Berihun et al., 2019), as is the case of JBW.

Our results highlight is more aligned to urban sprawl development, which leads the urban development in Puerto Rico, contrary to the case of SJBW that seems to densify existent urban areas. Uncontrolled development has led to a high degree of sprawl in 40% of Puerto Rico, with cities and towns poorly populated and surrounded by large sprawl areas (Martinuzzi et al., 2007). A 64% decrease in agricultural lands of about 1,190 km^2 is the largest land-cover change on the Puerto Rico island between 1977-78 and 1991-92 (Helmer, 2004). Analyses showed that in 1977, 11.3% of Puerto Rico was classified as urban, but after 17 years (1994), urban areas had increased by 27.4%, and urban growth on soils suitable for agriculture had increased by 41.6% (T. Del Mar López et al., 2001).

Other agricultural lands change to pasture ~ 480 km^2, forest ~ 330 km^2, and urban/developed lands ~ 73 km^2 from 1977 to 1991 (Helmer, 2004). Although the pasture/grass area increases overall as agricultural lands change to pasture, about 680 km^2 revert to the forest from 1977 to 1991 (Helmer, 2004). The largest extents of land development occur on pasture/grass lands over 150 km^2, forested land ~95 $km^{2,}$ and agricultural lands ~73 km^2 from 1977 to 1991 (Helmer, 2004). Like our results, the

biggest land change in JBNERR was reducing cultivated land coverage from 1977 to 2000, decreasing 73.79% (20.3km^2).

Other studies reported 953.42 km^2 of developed lands in Puerto Rico for 2000 to 2003, equivalent to 11% of the island (Gould et al., 2008; Martinuzzi et al., 2007). In 2003, 53% of Puerto Rico was covered by predominantly woody vegetation, 35% is grassland or herbaceous agriculture, 11% is developed land, and water and barrens each cover about 1% (Gould et al., 2008). In JBW, in 2000, developed lands cover 9.6%, and it is mainly covered by pasture in 46%, and forest 32% in 2000. From 2000 to 2010 in Puerto Rico, the next ten years span, herbaceous agriculture/pasture was mainly changed into woodland, forests, and urban land (Wang et al., 2017). Woodland was mostly transformed into forest and herbaceous agriculture/pasture (Wang et al., 2017). Our results highlight that the most significant change was found in the growth forest because the pasture changed around 21 km^2 into the forest. It also had the largest unchanged territorial extension. At the same time, urban areas increased 6 km^2 and mostly have transferred in 8.2 km^2 from pasture from 2000 to 2010. Similarly, in Puerto Rico, the urban land also increases 26% in total area (Wang et al., 2017).

Table 12

Primary Literature on LULCC in Guánica Bay watershed, San Juan Bay Estuary, and in Puerto Rico Reviewed.

Study	Findings	Study Period	Site
Center for Watershed Protection, (2008)	The current land use is 48% forested, 43% agriculture, and 9% urban, totaling approximately 57,000 acres as CWP delineated the watershed.	2004	Guánica Bay watershed
D. Whitall et al., (2013)	Historically, sugar cane, coffee, tobacco, and sustenance crops were grown in Lajas Valley. Agricultural production has declined since the 1950s due to a shift in government policy that moves towards the small industry.	2004	Guánica Bay watershed
Viqueira (2018)	Protect the Guánica Bay watershed from nonpoint sources of pollution derived from land-use alterations, and residential, commercial, and agricultural uses	2010	Guánica Bay Watershed
W. Gould et al., (2008) Méndez-Lázaro et al., (2018)	The watershed has 55% as urban areas or gray infrastructure, 11% woods, 9.4% grass and pasture, and 23% are wetlands, according to the Landsat 8 images for 2013.	2013	San Juan Bay Estuary
Brandeis et al. (2014)	Overall, there seemed to be a pattern of increasing tree cover from 2001 to 2011 in the developed land uses, particularly in vacant land. Despite being heavily urbanized and densely populated, the watershed maintains a relatively large, contiguous mangrove forest centered on the Piñones Commonwealth Forest that provides valuable ecosystem services to the adjoining city.	2001 - 2011	San Juan Bay Estuary
Govender & Thomlinson, (2010)	From 1936 to 2002, in both study areas, agriculture significantly decreases, especially from 1977 to 2002, while urban development increased. Still, forest cover increased only at JBNERR	1936, 1971/1977, and 2002	San Juan Bay Estuary, JBNERR

Study	Findings	Study Period	Site
	according to the aerial photos from 1936 and 1971, and IKONOS image for 2002.		
PRWRERI, (2013)	Due to the rapid changes in the area is recommended to keep updating the detailed land use/habitat inventory of the watershed regularly, especially in the lower part of the watershed (south of Highway 53).	2002 - 2012	JBNERR
W. Gould et al., (2008)	Results show that 53% of Puerto Rico is covered by predominantly woody vegetation, 35% is grassland or herbaceous agriculture, 11% is developed land, and water and barrens each cover about 1% according to the 2003 land cover map of Puerto Rico (Gould et al., 2008).	2003	Puerto Rico
E. H. Helmer, (2004)	A 64% decrease in agricultural lands of about 119,000 hectares is the largest land-cover change on the island between 1977-78 and 1991-92.	1977/78 – 1991/92	Puerto Rico
Wang et al. (2017)	Herbaceous agriculture/pasture was mainly changed into woodland, forests, and urban land. Woodland was mainly changed into the forest and herbaceous agriculture/pasture. The urban land also obtained an increase of 26% in total area.	2000 - 2010	Puerto Rico

On the other hand, despite our analysis not strictly designed to identify the land change drivers in JBW, several aspects like economic development and land use policy in Puerto Rico promote land changes or new developments. Tax-related benefits, warm weather conditions throughout the year, and tropical beaches are some of the factors that make Puerto Rico an ideal retirement destination for US citizens (Castro-Prieto et al., 2017). Programs like "Impulso a la Vivienda" Act 152, the American Recovery and Reinvestment Act of 2009, and the USDA Rural Housing Service, and the identification of public lands for affordable housing development to low and moderate-income

households are a priority in the Puerto Rico State Housing Plan for fiscal years 2014-2018 (Castro-Prieto et al., 2017; Estudios Tecnicos Inc, 2014). Coastal areas in semi-urban or semi-rural settings may be surrounded by: developments of (main and) second homes and Tourist facilities, such as hotels or camping areas (Estudios Técnicos Inc., 2014). A limited amount of temporary or permanent housing; plots located in front of the coast subdivided into rural areas; or farms used for agricultural production (Estudios Técnicos Inc., 2014).

On its part, the Puerto Rico Planning Board has regulations codes known as Reglamento Conjunto for the Evaluation and Issuance of Permits Related to the Development, Land Use and Business Operation (Junta de Planificación de Puerto Rico, 2019, 2020). The Reglamento Conjunto is used to ensure that new developments are made according to current building codes and construction permits (Junta de Planificación de Puerto Rico, 2020). According to the Plan Conjunto, established that a Developable Land or Usable Land for Development is:

> *Land that is available for development, excluding terrain that is subject to easements, including rights of way, land owned by public agencies, land that is subject to easements of conservation or other restrictive agreements that prohibit development, floodplains, lands that are under the elevation of the base flood and lands with slopes exceeding twenty-five percent (25%).*

In Puerto Rico, the coastal areas, as JBNERR, are more vulnerable to LULC changes. The coastal management issues and goals related to land use impacts such as sedimentation from urban development and groundwater withdrawal to support agriculture and communities are connected to habitat loss and degradation in the study area (Estudios Técnicos Inc., 2017).

Conclusion

The land change trends in the JBNERR watershed showed forest recovery and cultivated land conversion despite the significant importance as an agricultural watershed and as a natural reserve. The forest growth occurred as secondary forest from previous pasture land in the study area. According to previous studies, secondary forest cover has increased in many tropical regions due to socioeconomic changes and abandonment of agricultural land and pastures (Flynn et al., 2010; Hecht & Saatchi, 2007; Rudel et al., 2000). In the Jobos Bay watershed, the cultivated lands mostly decreased in the first two periods, 1977 – 1991 and 1991 – 2000, while urban areas were increasing as part of an economic shift in Puerto Rico. However, many factors are involved in land change processes. The explanations rely not only on socioeconomic activities but also on the environmental factors that play an important role, especially in forest recovery.

Even when this study does not analyze how the land change trends and major environmental events like hurricane disturbance interact to determine the structure and composition of forests, it is recognized as part of the global driver of land changes. Future work is recommended to explore how hurricanes and land-use history impact forest recovery and the land in transitions due to the abandonment of agricultural land and pastures. The most extensive form of a major disturbance in the forests is JBNERR. In Puerto Rico, from 1991 to 2000, the island faced the following hurricanes: Hurricane Marilyn in 1995, Hurricane Hortense in 1996, and Hurricane Georges in 1998 (Metro de Puerto Rico, 2017). From 2000 to 2010, Hurricanes Frances in 2004, and Earl in 2010. After 2010, the major hurricanes were Hurricane Irma and Hurricane María, both in 2017. However, the secondary forests increase even if trees are severely damaged, as occurs during storms or logging, because many species can resprout (Chazdon, 2003).

Equally, studies on the effects of land-use history and hurricane disturbance on forest structure, composition, and recovery require long- term data sets, which span a broad range of land-use histories, since the space-for-time substitution do not necessarily predict the rate of change in forest dynamics (Chazdon et al., 2007; Flynn et al., 2010; E. A. Johnson & Miyanishi, 2008).

Lastly, even the great extension of vegetated lands may lead to the inaccurate conclusion that the JBW is a relatively pristine system (Whitall et al., 2011). Recognizing that the current land change models are hampered by limited knowledge of the historical precedence for events (Runfola & Pontius, 2013). This research provides an insight into the understanding of urban sprawl and cultivated lands conversion in JBNERR. The socioeconomic causes to land changes Puerto Rico is a consequence of the political and economic decisions have determined throughout the history of Puerto Rican land use for agriculture, livestock and urban sprawl (Salazar-Ortiz & Cuevas, 2017). It is hypothesized that these changes affected the hydrology of the area, resulting in increased salinity, providing the right niche for the development of current mangrove (Salazar-Ortiz & Cuevas, 2017). For this reason, the results obtained from this study have practical and useful relevance for experts and practitioners who are responsible for forest, agriculture, and water management in JBNERR. The methods applied in the study can be adapted and replicated because this will enable them to identify areas susceptible to urban development and agriculture activities. Likewise, our findings can support the prediction, assessment, tracking of land changes related to the conservation policy. Conservation opportunities exist where agriculture or pasture land has reverted to the forest in various successional stages (Kennaway & Helmer, 2007).

Chapter Three. Soil Erodibility, Rainfall Erosivity, and Land-Use effects in the Tropical Estuary of Jobos Bay National Estuarine Research Reserve (JBNERR), Puerto Rico during 1977-2010.

Abstract

Jobos Bay National Estuarine Research Reserve (JBNERR), located on the southern coast of Puerto Rico, includes extensive drylands in the uplands and semi-enclosed coastal lowlands isolated from the ocean by barrier reefs and mangrove growth. However, increasing land changes (i.e., urbanization and agricultural practices) in the watershed of JBNERR has exacerbated the anthropogenic stress on local coastal ecosystems (Apeti et al., 2012; Estudios Técnicos Inc., 2017; Laboy-Nieves, 2009; Laboy et al., 2008; Whitall et al., 2011). Sedimentation from terrestrial soil erosion not only degrades ecosystem health, but also affects coastal water quality. Yet accurate estimation of soil erosion rates for JBNERR remains a knowledge gap. This study illustrated spatiotemporal changes of soil erosion rates based on the Revised Universal Soil Loss Equation (RUSLE). The annual average soil loss was estimated to be 9.8 ton/ha/y in 1977, increasing to 16.0 ton/ha/y in 1991, 11.5 ton/ha/y in 2000, and decreasing to 8.7 ton/ha/y in 2010. The dramatic increase from 1977 to 1991 was caused by a noticeable increase in grazing in the upper and steeper areas. The spatiotemporal distribution of soil erosion exposure showed that from 1977 to 2010, more than 40% of the watershed had slight soil loss, around 10% was slight to moderate, more than 13% was moderate, around 5% was moderate and around 11% was very highly exposed. The highest soil loss areas correlate with cover management and topographic factors. The potential soil erosion risk and severity increase from the mid-upper Northeast to the lowlands reaches of the Jobos Bay Watershed. As evidence from 1977 to 2010, hot spots analysis related to soil loss confirmed that pasture/grass in steep areas are more vulnerable to soil loss, and cultivated land placed very close to the coast is also vulnerable to soil erosion. This analysis revealed that the assessment of soil erosion provides an insight into the

understanding of economic shift and cultivated land conversion in JBNERR, which can support the prediction and tracking of cultivated land changes related to the conservation policy.

Introduction

Soil erosion is a major environmental concern globally, particularly in tropical and subtropical regions (De Mello et al., 2015). Soil erosion arises from agricultural intensification, land degradation, and other anthropogenic activities (Ganasri & Ramesh, 2016). It is considered the second most important environmental problem after population growth (Jahun et al., 2015). Soil erosion is how topsoil on the soil surface is carried away from the land by water or wind and transported to other surfaces (Jahun et al., 2015). Erosion can be caused by wind (wind erosion), rainfall (rainfall erosion), or runoff (runoff erosion) (Aksoy & Kavvas, 2005). These processes are accentuated and driven by soil disturbance (by tillage, vehicular traffic), lack of ground cover (bare fallow, residue removal, or burning), and harsh climate (high rainfall intensity and wind velocity) (Saha, 2003). The effect of soil processes is modified by the biophysical environment comprising soil, climate, terrain, and ground cover, through interaction between them, and influenced by economic, social, and political causes (Ganasri & Ramesh, 2016; Lal, 2001). The sum of these factors and causes result in land degradation. Then the biophysical factors are soil erodibility, climate (e.g., rainfall erosivity), topographic factor (terrain properties), and the physical factors are land cover and land use (e.g., cropland practices and conservation support against soil erosion).

The factors that make a soil susceptible to erosion and the causes of soil erosion make the soil have higher or lower erosion rates. The susceptibility of soil to erosion and

the magnitude of soil erosion resulting in soil degradation. Average soil erosion rates under natural, non-cropped conditions have been less than 2 Mg ha^{-1} yr^{-1} (Nearing et al., 2017). On-site rates of erosion of lands under cultivation over large cropland areas, such as in the United States, have been documented as 6 Mg ha^{-1} yr^{-1} or more (Nearing et al., 2017). A large proportion of soil erosion in the US occurs on the cropland, and the magnitude of sheet and rill erosion on US cropland where the sheet and rill erosion were 1.55 billion Mg/year in 1982, 1.36 billion Mg/year in 1987, and 1.09 billion Mg/year in 1992 (Lal, 1998). Runoff erosion can happen in non-concentrated flow (sheet erosion), in rills (rill erosion), or gullies (gully erosion) (Aksoy & Kavvas, 2005).

On the other hand, relatively small changes in the type of land cover could have major effects on rates of soil erosion, for example, if only the 5% of the watershed with the highest erosion rates (bare soil, agriculture on steep slopes) is transformed into closed-canopy forests, erosion in the watershed will decrease by 20% (Grau et al., 2003). Detailed analysis revealed several general features, including positive relationships of erosion rate with slope and annual precipitation and a significant effect of land use. Agricultural lands yield the highest erosion rates, and forest and shrublands yield the lowest (García-Ruiz et al., 2015). It was concluded that erosion rates are controlled by rainfall intensity, soil erodibility, slope, land cover, and management practices (Grau et al., 2003). Then, the Revised Universal Loss Equation (RUSLE) is the best available practical erosion prediction model that can be easily applied at the local or regional level (Ganasri & Ramesh, 2016). The disadvantage of RUSLE is that it does not have the capability for routing sediment through channels; hence its application is limited to small areas (Ganasri & Ramesh, 2016).

Therefore, the need for simple and localized methods to evaluate the influences of land changes and climate on soil loss, this paper analyzes the spatial and temporal distribution of rainfall erosivity, land use/land cover (LULC) impact on soil loss by RUSLE in the watershed of Jobos Bay National Estuarine Research Reserve (JBNERR). Jobos Bay Watershed (JBW) has been facing increased anthropogenic stress such as inappropriate land use management that may strongly impact the terrestrial aquatic ecosystems in its watershed. Even after being designated a National Reserve, JBNERR is still threatened by coastal land-use changes such as urban development, industry, and agricultural activities in the watershed. However, little information is available on how the LULC changes were distributed in JBNERR to detect areas that are more prone to erode despite anthropogenic threats and stressors. Furthermore, the performance of available erodibility factors by investigating the role of rainfall erosivity (R), topographic factor (LS), and soil erodibility (K) on soil erosion in JBNERR from 1977 to 2015 will be assessed.

Methodology

The erosion rates' objective using the RUSLE will be analyzed to identify and describe how erosion rates relate to land changes from 1977 to 2010. The hypothesis regarding this question will be tested by comparing the integrated RUSLE result with any individual factor.

Study area

The JBW covers 137.3 km² (34,000-acres) of the southern coastal plain (Whitall et al., 2011). JBNERR is the second widest estuary in Puerto Rico, only surpassed by the San Juan Bay estuary, and it was designated a National Estuarine Research Reserve by NOAA in the 1980s. The watershed belongs to the Rio Coamo watershed and is divided

into four subwatersheds: Rio Nigua, Rio Seco, Quebrada Aguas Verdes, Rio Seco West, and East (Figure 22). However, Rio Seco is the only river system that discharges into the bay. In addition, the Canal de Patillas (Patillas'channel) and Canal de Guamaní (Guamaní's channel) are the primary irrigation system for agriculture in this area.

Figure 22

JBNERR watershed delimitation.

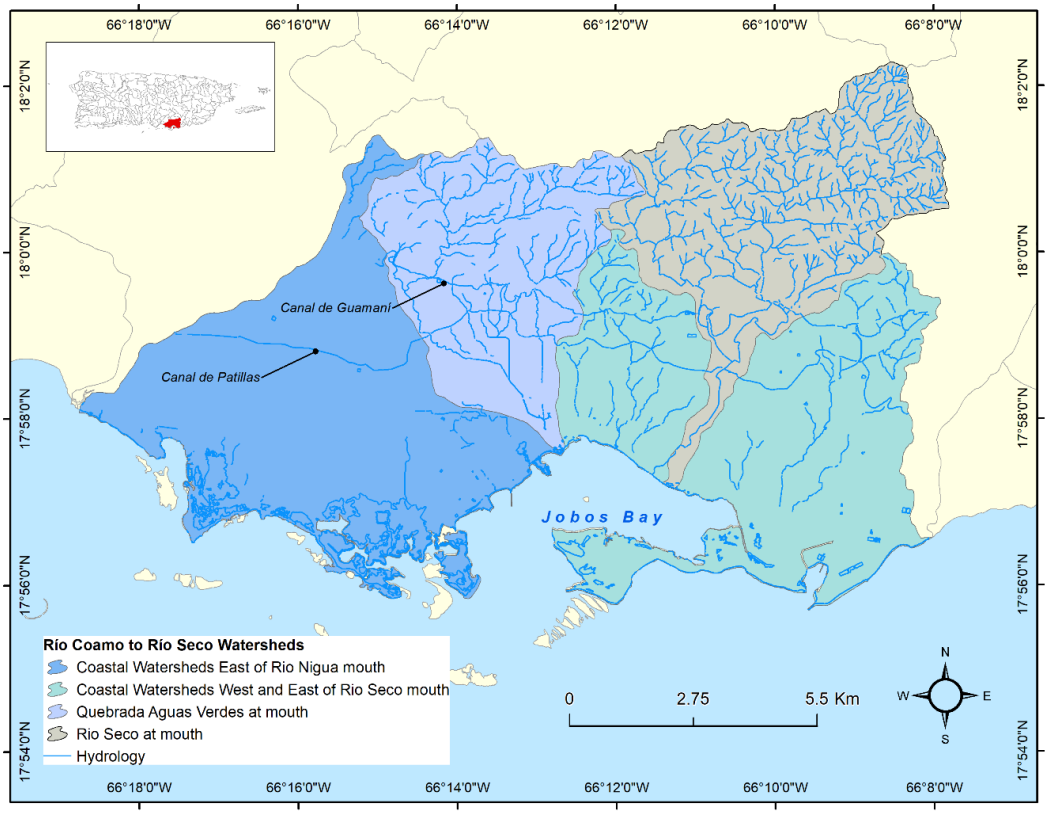

RUSLE

In 1997, the RUSLE updated the information on data required after the 1978 release, incorporated several process-based erosion models, and remains to be a regression equation (Renard et al., 1997). The major modification is the R factor, which includes rainfall and runoff erosivity (snowmelt when applying). The general method to apply the RUSLE estimates each factor in the model based on the literature. Previous

researchers have developed several techniques for assessing these factors, ranging from the use of climate data, soil and geological maps, remotely sensed satellite images, empirical formulas, and digital elevation model (DEM) obtained from various sources (Jahun et al., 2015). The RUSLE model and its factors are described in Equation 7.

Equation 7. Revised Universal Soil Loss Equation (RUSLE)

$$\boldsymbol{A = R * K * L * S * C * P}$$

Where;

A = In tons per acre per year but, other units can be selected.

R = Rainfall and Runoff factor. Is the number of rainfall erosion index units plus a factor for runoff from applied water where runoff is significant.

K = Soil erodibility factor. Is the soil loss rate per erosion index for a specific soil as measured on a unit plot, defined as 72.6 ft. length of uniform 9% slope continuously in clean-tilled fallow.

L = Slope length factor. Is the ratio for soil loss from the field slope to that form 72.6ft length, under identical conditions.

S = Steepness factor. Is the ratio of soil loss from the field slope gradient to that form a 9% slope, under otherwise identical conditions.

C = Cover and management factor. Is the ratio of soil loss from an area with specified cover and management to that from an identical area in continuous tilled fallow.

P = Support Practice factor. Is the ratio of soil loss with a support practice like contouring, strip cropping, or terracing to that with straight-row farming up and down the slope.

The average annual soil loss rate generated by the RUSLE was classified into six (7) soil erosion risk categories: slight, slight to moderate, moderate, moderate to high, high, and very high, (Aouichaty et al., 2021; Carlos Rogério de Mello et al., 2016a; de Oliveira et al., 2014; Mohammed et al., 2020).

Rainfall erosivity factor (R)

After calculating the rainfall erosivity factor, the rainfall data should be prepared by analyzing the missing values according to the data covered in each station (Table 13). Missing values occur when no data value is collected for a variable. Several facts can cause missing values. For example, the data gathering is incorrectly done, data entry mistakes, and instrument failures. The missing data understanding is crucial to decide how to work with imputation or deletion effectively.

Generally, working missing values through imputation is a well-known problem but somewhat difficult to approach. However, the R programming language is dedicated to statistical computing, and R packages broadly cover the imputation methods. In R a comparison of different methods for univariate time series imputation found that zoo and forecast packages were the most effective methods for dealing with missing data (Moritz et al., 2015). The function calculates the mean, median, or mode over all the non-NA values and replaces all NAs with this value (Moritz & Bartz-Beielstein, 2017). A disadvantage of mean imputation is that it reduces variance in the dataset. Even when the code na_mean is considered a simple imputation, in this case, the mean is the best

performing method because the southeast of Puerto Rico does not present a strong seasonality. Otherwise, for time series with strong seasonality, na_kalman and na_seadec, na_seasplit performs best (Moritz & Bartz-Beielstein, 2017). This chapter replaced missing values with overall mean values (Multiannual mean).

Rainfall erosivity factor predictions have been useful for land use planning in agricultural areas related to soil erosion risk assessment, crucial at the regional scale (De Mello et al., 2015). This factor reflects the effect of rainfall intensity on soil erosion and requires detailed, continuous precipitation data for its calculation (Wischmeier & Smith, 1978). The intensity and kinetic energy of the rainfall events characterize the rainfall erosivity (De Mello et al., 2016a). The kinetic energy of a given amount of rain depends on the sizes and terminal velocities of the raindrops, which are related to rainfall intensity (Wischmer & Smith, 1978). However, the estimation of the R factor poses a challenge in data-poor areas or in situations where climate stations are extremely sparse (Jahun et al., 2015). Therefore, the modified R Factor was calculated using the formula developed by Arnoldus (1980) but following the principle of Wischmeier & Smith (1978). The data used were the average monthly (p) and the average annual precipitation (P) (Renard & Freimund, 1994). The equation for rainfall factor (R) in metric units MJ*mm/ha*h is:

Equation 8. Modified R Factor

$$R = 1.735 * 10^{\left(1.5*\log\left(\sum p^2/_P\right)-0.8188\right)}$$

Where p is the average monthly precipitation, and P is the average annual precipitation.

For study areas where the stations are sparse, or the data is not available to calculate the EI_{30}, then the Modified Fournier Index can be used (Equation 9). This index provides a rapid way of approximating the rainfall factor value; although a minimum number of stations still need to be processed more elaborately, the precision seems adequate (Arnoldus, 1980). Previous studies considering the rainfall data availability limitations used the Arnoldous (1980) modified equation that includes this index to calculate the rainfall erosivity factor (Ghosal & Das Bhattacharya, 2020; Ozsahin et al., 2018; Prasannakumar et al., 2012, Renard & Freimund, 1994, Sharma et al., 2011; Vijith et al., 2017). In Puerto Rico this rainfall erosivity approach was used for Río Grande de Añasco watershed (Anaya & Colon, 2014 and Rojas-González, 2008), and Guadiana watershed (Del Mar López, Aide, & Scatena, 1998).

Equation 9. Modified Fournier Index

$$\text{Modified Fournier Index (mm units)} = \log {\sum_1^{12} p^2}/{P}$$

This index was applied to calculate Factor R for the three stations in JBNERR. The Aguirre station is the only station within the watershed, and the two other stations are located near the watershed (Table 13). Therefore, the annual and monthly precipitation were recovered from these three stations in the study area for the 1970 – 2015 period for 46 years of rainfall data. In addition, before estimating the Factor R, it was important to establish the rainfall time intervals to evaluate the effect of the record length on the Factor R estimation.

Table 13

Description of the rainfall stations.

Station	Latitude	Longitude	Elevation (m)	Status	Data cover
Aguirre	17.9555	-66.2222	7.6	Active	89%
Guayama 2 E	17.9783	-66.0874	21.9	Active	94%
Jájome Alto	18.0716	-66.1427	719.3	Active	99%

The rainfall time intervals were established in our study related to the LULC images used in Factor C (Table 14). These LULC images correspond to 1977, 1991, 2000, and 2010. Thus, the rainfall period was selected close to each image year. According to Hernando & Romana (2016), their results confirmed that record length increased both precision and accuracy of the estimates when time intervals up to ten years or five years were considered, but slight improvement was obtained beyond that. A record length of 10 years seemed adequate to estimate the R-factor globally (Hernando & Romana, 2016). The rainfall time intervals range between 7 and 15 years and should be adequate to estimate the Factor R with the Modified Fournier Index. This index outperformed other Factor R estimators (Hernando & Romana, 2016).

Table 14

Description of rainfall stations time selected in this study.

LULC data	Rainfall period covered	Rainfall time interval
1977	1970 - 1984	15 years
1991	1985 - 1999	15 years
2000	2000 - 2009	10 years
2010	2010 - 2015	6 years

However, soil losses are frequently due to a few severe storms characterized by high intensity and large total rainfall amount (Ferro et al., 1999). Even when global soil

erosion modeling results suggest that water erosion is a common phenomenon under all climatic conditions across all observed continents (Borrelli et al., 2020). However, the distribution of the spatial soil erosion patterns suggests that soil erosion seems to threaten areas of large continents. The distribution of the spatial soil erosion patterns suggests that soil erosion seems to threaten areas of large- scale reclamation such as major agricultural sectors, especially if it patterns suggests that soil erosion seems to threaten areas of large scale reclamation such as major agricultural sectors, especially if it occurs in conjunction with concentrated intense rainfall events (Borrelli et al., 2020). Wischmeier and Smith (1978) omitted rains of less than 12.7 mm (0.5 in) of total rainfall in erosion index computations unless as much as 6.4 mm (0.25 in) of rain fell in 15 minutes (Xie et al., 2002). Likewise, less than 12 mm (0.5 inches) rain showers are omitted as insignificant unless they include a 15-minute intensity of at least 25 mm/h (Wischmeier & Smith, 1978). The threshold value of the rainfall amount recommended here is very similar to the value of 12.7 mm used by Wischmeier and Smith (1958). The threshold value of 12.7 mm total rainfall suggested by Wischmeier and Smith (1978) is often used in making isoerodent maps in many countries (Elsenbeer et al., 1993; Kenneth G Renard & Freimund, 1994; Yu & Rosewell, 1996). However, the criterion of 63.5 and 25 mm/h maximum intensity has also been used as a threshold by other researchers (Ferro et al., 1991; Xie et al., 2002).

Nonetheless, several authors have suggested using the 90th or 95th percentile as extreme rainfall indexes (Haylock & Nicholls, 2000; Salinger & Griffiths, 2001; Vallebona et al., 2015). According to (Suppiah & Hennessy, 1998), heavy rainfall is defined as the 90th and 95th percentiles of daily rainfall in each half-year. Because of

90th percentile would be focusing on the top five to ten annual events, which contributed around 30–40% of the total rainfall (Haylock & Nicholls, 2000). Hence, we worked with only daily rainfall since the information about the short-time downpour is unknown. We examined the days with large rainfall choosing the 90th percentiles of the daily rainfall dataset as a threshold exceeded or equaled by the top 10% of events suggested by previous studies to tackle the short time rainfall exceeding that threshold in those days. The percentiles were computed using non-missing daily rainfall (mm) (Salinger & Griffiths, 2001). The percentile 90^{th} to our stations was 5.3mm in Aguirre, 8.6 mm in Guayama 2E, and 13.7 mm in Jajome Alto for 1970 – 2015 (Figure 23). Once the rainfall threshold was set, the rainfall erosivity factor was calculated for each station and period.

Figure 23

Percentile 90 for precipitation for Aguirre, Guayama, and Jajome Alto stations JBW during 1970 - 2015.

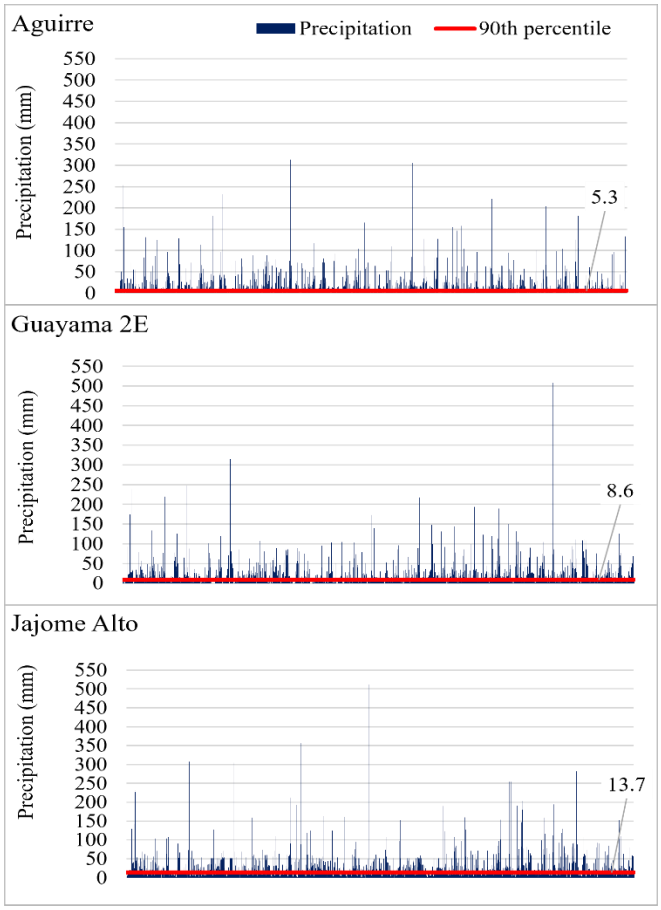

Another process was applied to mapping this factor for JBW. In June 2014, the Department of Commerce (DOC), National Oceanic and Atmospheric Administration (NOAA), National Ocean Service (NOS), Office for Coastal Management (OCM) published the R Factor for the United States watersheds, including Puerto Rico, as part of its territories. The R factor was derived from isoerodent maps in the Runoff Estimates for Small Rural Watersheds for around the fifty states (Fletcher et al., 1977) and was updated

on April 2, 2021. The isoerodent plotted on a map of the Island of Puerto Rico were digitized, then values between these (isoerodent) lines were obtained by linear interpolation (Fletcher et al., 1977). The final R-Factor data are in raster GeoTiff format at 30-meter resolution in UTM, Zone 20, GRS80, NAD83 (DOC, NOAA, NOS, 2020). The range of dates used was 30 minutes of rainfall from 1965 to 1975. The R Values are the Mean Annual Rainfall Kinetic Energy Times the 30-Minute Rainfall Intensity Divided by 100 following the method proposed by the Agricu1tura1 Research Service (Fletcher et al., 1977). A conversion unit is needed in NOAA, their Factor R was converted into the MJ*mm/ha*h*y. Multiplying by 17.02 as the report suggested by Foster et al. (1981).

Equation 10. Annual erosivity conversion factor equation

$$Annual\ erosivity, R = \frac{hundreds\ of\ foot * tonf * inch}{acre * hour * year}\ x\ 17.02$$

$$= \frac{megajoule * millimeter}{hectare * hour * year} = \frac{MJ * mm}{ha * h * y}$$

The interpolation process Inverse Distance Weighting (IDW) was needed to use remote rainfall stations and rainfall data and apply the Spatial Analyst Tools in GIS. The IDW interpolation assumes that the climatic value at an unsampled point is a distance-weighting average of the climatic values at nearby sampling points (Angulo-Martínez et al., 2009). In other words, for this method, the influence of a known data point is inversely related to the distance from the unknown location that is being estimated because the nearby values contribute more to the interpolated values than distant observations (Hernández et al., 2016). Therefore, in terms of how well the Factor R was predicted, the IDW method gives the best spatially Factor R prediction, followed by the kriging method

(Abdulkareem et al., 2019; Angulo-Martínez et al., 2009; Ozsahin et al., 2018; Prasannakumar et al., 2012).

After applying the IDW process, a ratio was multiplied to this R-factor as a correction factor between our and the NOAA results. Using the same rainfall period 1965 to 1975, the ratio was developed as:

Equation 11. Annual erosivity correction factor

$$\text{Ratio} = \frac{\bar{x}_{R_{NOAA}}}{\bar{x}_{R_{our\ result}}}$$

For this study, the resulting ratio was 41.66 MJ*mm/ha*h*y. This ratio was multiplied to get an approximate R-Factor estimate in the latest period's 1977 - 2015. This ratio was determined after regressing the R-Factor by NOAA to our R-Factor. The coefficient of multiple correlations (R^2) was 0.9986, and the adjusted R^2 was 0.9971 for the rainfall period 1965 – 1975, given the regression equation of $y = 0.9619x - 6525.6$. This indicates that our model explains 99% of the variation within the data when regressed to R-Factor from NOAA. Therefore, the conversion factor should be appropriate to estimate the annual rainfall erosivity factor.

Soil Erodibility Factor (K)

Some soils erode more readily than others, even when other factors are the same (Wischmer & Smith, 1978). Soil erodibility is the susceptibility of soil to an agent of erosion determined by inherent soil properties, e.g., texture, structure, soil organic matter content, clay minerals, exchangeable cations, and water retention and transmission properties (Saha, 2003). The soil composition and distribution of its properties impact how the sediment will be transported. Water infiltration determines the runoff rate given

a particular rainfall intensity (Ganasri & Ramesh, 2016; Wischmeier & Smith, 1978). The soil properties considered are the particle size (% clay, % sand, % silt), percent organic matter, soil structure (granular, coarse, or blocky), and soil permeability (Ganasri & Ramesh, 2016; Wischmeier & Smith, 1978). For example, the properties related to soil erosion, when the percent of very fine sand and silt particles is greater than 70%, the soil permeability is slow to moderate because of the fine granular and more compact soil structure (Figure 24). Many agricultural soils have fine granular topsoil and moderate permeability (Wischmeier & Smith, 1978).

However, the K factor is difficult to assess. For example, soil with a high natural erodibility factor may show little evidence of actual erosion under gentle rainfall when it occurs on short and gentle slopes or when the best possible management is practiced (Wischmer & Smith, 1978).

Figure 24

Soil erodibility nomograph.

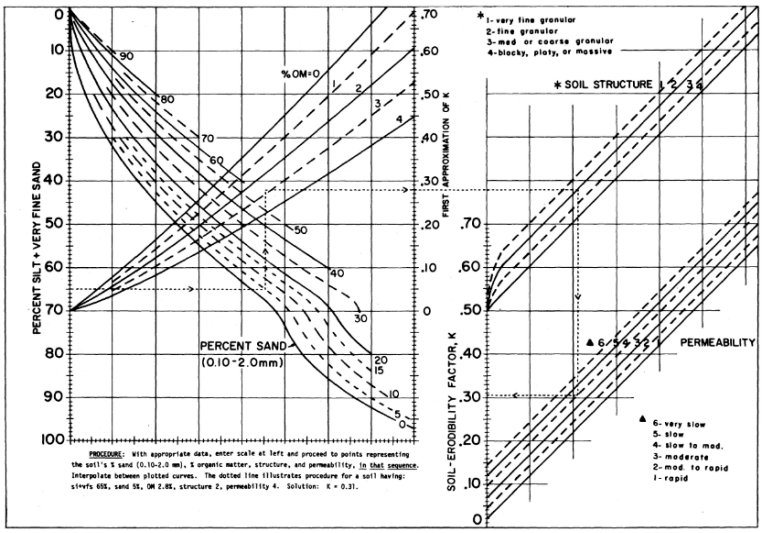

Note. The nomograph determines the erodibility of soils (K).
Source: Wischmeier, W. H., & Smith, D. D. (1978). Predicting rainfall erosion losses: a guide to conservation planning. US Department of Agriculture Handbook No. 537.

Before calculating the Factor K, the soil data for Jobos watershed at the USDA National Resources Conservation Service (NRCS) – Web Soil Survey website were examined. The spatial soil data and its report were downloaded from the Soil Survey Staff, Natural Resources Conservation Service (2019). The K Factor by the Soil Erodibility Nomograph was estimated through the following experimental equation developed by Wischmeier & Smith (1978). The equation follows:

Equation 12. Soil Erodibility Nomograph Equation

$$100K = 2.1M^{1.14} * 10^{-4}(12 - OM) + 3.25(S - 2) + 2.5(P - 3)$$

Equation 13. K Factor Equation

$$K = \frac{2.1M^{1.14} * 10^{-4}(12 - OM) + 3.25(S - 2) + 2.5(P - 3)}{100}$$

Where:

M = (% silt + %fine sand) × (100 − %clay)

OM = % of organic matter

S = soil structure code which (1) is very fine granular, (2) is fine granular, (3) is med or coarse granular, and (4) is blocky, platy, or massive.

P = permeability code in which (1) is rapid (> 150 mm/hr.), (2) is moderate to rapid (50-150 mm/hr.), (3) is moderate (15-50 mm/hr.), (4) is slow to moderate (5-15 mm/hr.), (5) is slow (1-5 mm/hr.), and (6) very slow (< 1 mm/hr.). The profile permeability classes are based on the profile's lowest saturated hydraulic conductivity (ksat).

Soil Types in JBNERR

The soil type data availability is assembled from other sources, such as research information, production records, and field experiences (USDA-NRCS, 2019). For example, data on crop yields under defined levels of management are assembled from farm records and field or plot experiments on the same kinds of soil (USDA-NRCS, 2019). For JBW, the soil type data were collected, organized, and available online by the Natural Resources Conservation Services of the United States Department of Agriculture (USDA – NRCS).

In JBW, the top five soil types are DrF-Descalabrado-Rock, Tidal Swamp, Descalabrado and Guayama Soils, Poncena clay, Paso Seco clay. The soil DrF—Descalabrado-Rock land complex at 40 to 60 percent slopes has a major extension with 11% coverage of the study area (Table 15). Tidal Swamp (Ts) and Descalabrado and Guayama (DgF2) soils at 20 to 60 percent slopes have 7.5% and 7.0% of JBNERR area extension. Meanwhile, Poncena clay (Po) and Paso Seco clay (PIB) at 0 to 5 percent slopes have both 6.5% extension area. Other soil types have significant extension area: 6.3% Guamani silty clay loam (Gm), 6.4% Fraternidad clay, 0 to 2 percent slopes (FrA) and 3.6% Cartagena clay (Ce).

Table 15

Soil type description in JBNERR.

Soil Unit Symbol	Soil Unit Name	Surface Texture	AOI Km^2	Percent of AOI
Ad	Aguadilla loamy sand	Loamy sand	0.66	0.5%
AmB	Amelia gravelly clay loam, 2 to 5 percent slopes	Gravelly clay loam	4.55	3.3%
AmC2	Amelia gravelly clay loam, 5 to 12 percent slopes, eroded	Gravelly clay loam	3.80	2.8%
An	Arenales sandy loam	Sandy loam	1.36	1.0%
Ar	Arenales sandy loam, gravelly substratum	Sandy loam	0.22	0.2%
CbF	Caguabo clay loam, 20 to 60 percent slopes	Clay loam	0.27	0.2%
Ce	Cartagena clay	Clay	4.95	3.6%
Cf	Catano loamy sand, 0 to 2 percent slopes	Loamy sand	0.16	0.1%
ClB	Coamo clay loam, 2 to 5 percent slopes	Clay loam	2.60	1.9%
Cm	Coastal beaches	Sand	0.24	0.2%
Cn	Cobbly alluvial land	-	0.88	0.6%
DcE2	Daguao clay, 20 to 40 percent slopes, eroded	Clay	0.14	0.1%
DeE2	Descalabrado clay loam, 5 to 12 percent slopes, eroded	Clay loam	0.93	0.7%
DeE2	Descalabrado clay loam, 20 to 40 percent slopes, eroded	Clay loam	4.17	3.0%
DgF2	Descalabrado and Guayama soils, 20 to 60 percent slopes, eroded	Clay loam	9.64	7.0%
DrF	Descalabrado-Rock land complex, 40 to 60 percent slopes	Clay loam	15.03	11.0%
FrA	Fraternidad clay, 0 to 2 percent slopes	Clay	8.79	6.4%
FrB	Fraternidad clay, 2 to 5 percent slopes	Clay	0.72	0.5%

Soil Unit Symbol	Soil Unit Name	Surface Texture	AOI Km^2	Percent of AOI
Gm	Guamani silty clay loam	Silty clay loam	8.57	6.3%
JaB	Jacana clay, 2 to 5 percent slopes	Clay	1.15	0.8%
JaC2	Jacana clay, 5 to 12 percent slopes, eroded	Clay	2.99	2.2%
MrB	Meros sand, 1 to 6 percent slopes	Sand	1.38	1.0%
NaF	Naranjito silty clay loam, 40 to 60 percent slopes	Silty clay loam	0.02	0.0%
NOTCOM	No Digital Data Available	-	2.27	1.7%
NOTPUB	Not Public Information	-	0.03	0.0%
PlB	Paso Seco clay, 0 to 5 percent slopes	Clay	8.91	6.5%
Po	Poncena clay	Clay	8.93	6.5%
PrC2	Pozo Blanco clay loam, 5 to 12 percent slopes, eroded	Clay loam	1.01	0.7%
Rs	Rock land	Unweathered bedrock	8.78	6.4%
Sm	Saltwater marsh	Variable	0.00	0.0%
Tf	Tidal flats	Variable	4.10	3.0%
Ts	Tidal swamp	Variable	10.23	7.5%
Vc	Vayas silty clay frequently flooded	Silty clay	3.65	2.7%
Vs	Vives silty clay loam, high bottom	Silty clay loam	7.72	5.6%
VvB	Vives clay, 2 to 7 percent slopes	Clay	7.06	5.2%
W	Water	-	0.46	0.3%
Total			136.83	100.0%

Note. AOI is the Area of Interest.

For JBW, the soils containing less than 70 percent silt and very fine sand, according to the nomograph (Figure 24), were considered to estimate the erodibility. The study area showed in terms of the soil type composition, DrF and DgF2 have the same composition, 30.2% sand, 32.3% silt, 37.5% clay and, 4% organic matter (Figure 25 and

Table 16). Po soil has 23.3% sand, 29.2% silt, 47.5% clay and, 7.5% organic matter. PIB and FrA soils have the same profile, 17.1% sand, 27.9% silt, 55% clay and, 3% organic matter. Overall, Po has the biggest organic matter content. Gm soil has 20.0 % sand, 49% silt, 31% clay and, 3% organic matter. Ce soil has 23.3% sand, 29.2% silt 47.5% clay and, 3.5% organic matter. According to Djuwansah and Mulyono (2018), the high erodibility level from one place to another is due to the condition of the soil texture with a small percentage of clay. In addition, particles such as silt and very fine sand are resistant to erosion because of soil cohesion, and soil sensitive to erosion has the lowest percentage of clay aggregates (Djuwansah & Mulyono, 2018). Another aspect to consider is soil organic matter, where the soil organic matter and clay contents are recognized as the principal factors that influence soil erodibility (B. Wang, Zheng, & Römkens, 2013). The soil organic matter had an important impact on soil erodibility because the region with the highest amount of Soil Organic Matter (SOM) was roughly provided with the lowest K-value, high mean SOM indicated relatively low soil erodibility values (less than 0.0300) as presented in Wang et al., (2016).

Figure 25

Soil Type in JBNERR watershed.

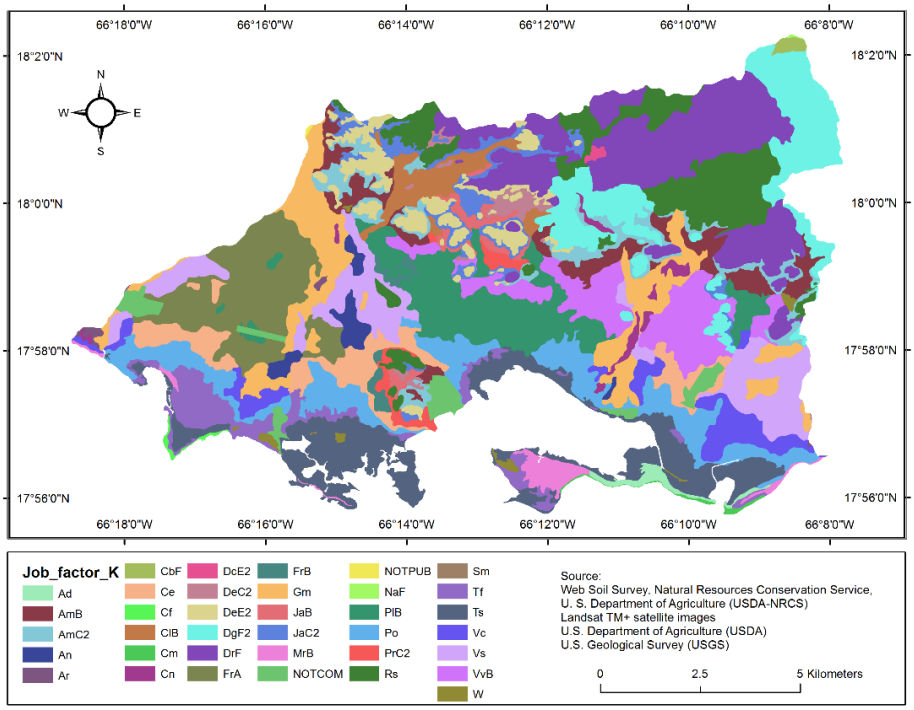

Soil type description is of relevance to help explain how the erodibility factor behaves and the land cover classes in the study area. The erodibility factor decreased as the geometric mean particle diameter (dg) increased due to the dominance of coarse-textured material, reflecting higher infiltration rates (sandy soils) or as dg decreased, reflecting the structural stability of soils due to higher clay content and clay-associated organic and inorganic binding agents as well as greater infiltration rates (B. Wang, Zheng, & Römkens, 2013). In sum, Wang et al. (2013) found that soil organic matter and clay contents are the key factors that influence soil erodibility.

Table 16

Physic properties of soil types in JBNERR.

Soil unit symbol	Soil unit name	% Sand (0.05-2.00 mm)	% Silt (0.002-0.05 mm)	% Clay (< 0.002 mm)	% Org (< 0.002 mm)	Rating Soil Structure (0-12 inches)	Ksat Rating code (µm/sec)
Ad	Aguadilla loamy sand	83.5	9	7.5	2	1.00	2.00
AmB	Amelia gravelly clay loam, 2 to 5 percent slopes	30.2	32.3	37.5	4	1.00	3.00
AmC2	Amelia gravelly clay loam, 5 to 12 percent slopes, eroded	30.2	32.3	37.5	4	1.00	3.00
An	Arenales sandy loam	66	31	3	2	1.00	2.00
Ar	Arenales sandy loam, gravelly substratum	66	31	3	2	1.00	2.00
CbF	Caguabo clay loam, 20 to 60 percent slopes	35	34	31	2	1.00	3.00
Ce	Cartagena clay	23.3	29.2	47.5	3.5	1.00	4.00
Cf	Catano loamy sand, 0 to 2 percent slopes	83	9	8	2	1.00	2.00
ClB	Coamo clay loam, 2 to 5 percent slopes	42	30	28	4.5	1.00	3.00
Cm	Coastal beaches	97.9	1.6	0.5	0.05	1.00	2.00
Cn	Cobbly alluvial land						
DcE2	Daguao clay, 20 to 40	17.1	27.9	55	2	1.00	4.00

Soil unit symbol	Soil unit name	% Sand (0.05-2.00 mm)	% Silt (0.002-0.05 mm)	% Clay (< 0.002 mm)	% Org (< 0.002 mm)	Rating Soil Structure (0-12 inches)	Ksat Rating code (µm/sec)
	percent slopes, eroded						
DeC2	Descalabrado clay loam, 5 to 12 percent slopes, eroded	30.2	32.3	37.5	4	1.00	3.00
DeE2	Descalabrado clay loam, 20 to 40 percent slopes, eroded	30.2	32.3	37.5	4	1.00	3.00
DgF2	Descalabrado and Guayama soils, 20 to 60 percent slopes, eroded	30.7	32.8	37.5	4	1.00	3.00
DrF	Descalabrado-Rock land complex, 40 to 60 percent slopes	30.2	32.3	37.5	4	1.00	3.00
FrA	Fraternidad clay, 0 to 2 percent slopes	17.1	27.9	55	3		4.00
FrB	Fraternidad clay, 2 to 5 percent slopes	17.1	27.9	55	3	1.00	4.00
Gm	Guamani silty clay loam	20	49	31	3	1.00	3.00
JaB	Jacana clay, 2 to 5 percent slopes	23.3	29.2	47.5	4	1.00	3.00
JaC2	Jacana clay, 5 to 12 percent slopes, eroded	23.3	29.2	47.5	4	1.00	3.00
MrB	Meros sand, 1 to 6 percent slopes	96.5	1.5	2	0.75	1.00	2.00

Soil unit symbol	Soil unit name	% Sand (0.05-2.00 mm)	% Silt (0.002-0.05 mm)	% Clay (< 0.002 mm)	% Org (< 0.002 mm)	Rating Soil Structure (0-12 inches)	Ksat Rating code (µm/sec)
NaF	Naranjito silty clay loam, 40 to 60 percent slopes	18.7	45.3	35	2.5	1.00	3.00
NOTCOM	No Digital Data Available						
NOTPUB	Not Public Information						
PlB	Paso Seco clay, 0 to 5 percent slopes	17.1	27.9	55	3	1.00	4.00
Po	Poncena clay	23.3	29.2	47.5	7.5	1.00	4.00
PrC2	Pozo Blanco clay loam, 5 to 12 percent slopes, eroded	35.3	33.2	31.5	7.5	1.00	3.00
Rs	Rock land						2.00
Sm	Salt water marsh				4.5		
Tf	Tidal flats				4.5		
Ts	Tidal swamp						
Vc	Vayas silty clay, frequently flooded	5.5	47	47.5	3	1.00	4.00
Vs	Vives silty clay loam, high bottom	7.6	54.9	37.5	3	1.00	3.00
VvB	Vives clay, 2 to 7 percent slopes	28.1	29.4	42.5	3	1.00	4.00
W	Water						

Source: Soil Survey Staff, Natural Resources Conservation Service, United States Department of Agriculture. Web Soil Survey. Available online at the following link: https://websoilsurvey.sc.egov.usda.gov/.

Topographic Factor (LS)

The topographical factors are slope length (L) and slope steepness (S). The slope length is defined as the distance from the source of runoff to the point where deposition

begins, or runoff enters a well-defined channel that may be part of a drainage network or a constructed channel (Wischmeier & Smith, 1978). Combined with the slope steepness factor (S), the LS factor attempts to quantify the effect of topographical characteristics on soil loss (Renschler et al., 1999). However, slope steepness has a greater impact on soil loss than slope length (Ganasri & Ramesh, 2016). Slope gradients ranging from about 1% to 25% slope steepness are included in determining the relationship between slope and soil loss (Ganasri & Ramesh, 2016; Laflen & Flanagan, 2013; Wischmer, & Smith, 1978). The impact of slope and aspect would play a major role in runoff mechanism; the more the slope, the more the runoff, and thus infiltration reduces (Ganasri & Ramesh, 2016). Runoff, including surface and subsurface draining flows, is generated when daily rainfall exceeds the field capacity of a calculated average penetrable soil depth, redistributed to and possibly reabsorbed in downslope (Gao et al., 2007).

Generalized LS factor values for simple slopes can be used with the RUSLE, the RUSLE computer program calculates more location-specific values, including values for complex (nonuniform) slopes (Weil & Brady, 2017). To generate Factor L and Factor S for JBW, the Digital Elevation Model (DEM) with five (5) meters of spatial resolution will be used. CZO Dataset develops the DEM to the Coastal Zone of Puerto Rico, LiDAR (2016) USACE NCMP Topobathy Lidar used as a base to estimate Factor LS and to create the Slope map for JBNERR (NOAA Office for Coastal Management (NOAA/OCM), 2009, 2017). Factor L and the Slope map will be created using the following equations developed by Desmet and Govers (1996).

Equation 14. Slope Length factor Equation

$$L_{i,j} = \frac{\left[A_{i,j} + D^2\right]^{(m+1)} - {A_{i,j}}^{m+1}}{x^m D^{m+2} (22.13)^m}$$

Where:

Equation 15. Length exponent of the LS-factor

$$m = \frac{F}{1+F}$$

Equation 16. Parameter F in Factor L

$$F = \frac{\sin\beta / 0.0896}{3(\sin\beta)^{0.8} + 0.56}$$

β = slope in degrees with the coordinates *(i, j).* The expression should be in radians. The degrees must be multiplied by 0.01745 to convert to radians.

A = is the flow accumulation at the pixel level.

D = is the grid cell size (*m*).

X = shape coefficient (x = 1 for pixel systems).

In sum, to calculate these factors, it is important to convert the slope from grades to radians because the radians are a unit of the angle where 1^o = 0.01745 radians. The *Sin function* indicates the slope angle where slope steepness is up to 21%. Then the Flow Direction and the Flow Accumulation calculations are needed to calculate Factor L because this involves the points where deposition occurs.

Flow Direction and Flow Accumulation

Flow Direction returned a raster with values from 1 through 255. Most of the cells have the standard values of 1, 2, 4, 8, 16, etc.; however, there is at least one entry for every other number from 1 to 255 (Esri, 2019b; Esri Community, 2012). Flow accumulation operation performs a cumulative count of the number of pixels that naturally drain into outlets. That can be used to find the drainage pattern (Esri, 2019). In GIS, the Flow Accumulation raster and the Flow Direction raster will be created thru Spatial Analyst Tool with Hydrology functions regarding Flow Direction or Flow Accumulation rasters are shown in Figure 26 and Figure 27:

Figure 26

Flow Direction in JBW.

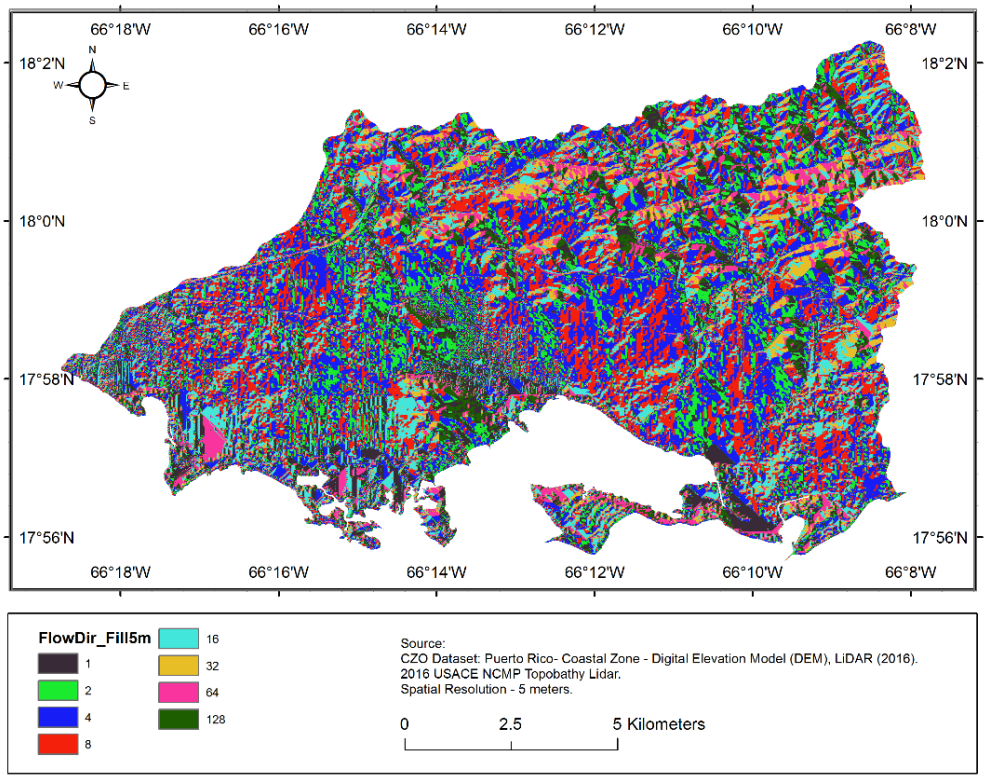

Figure 27

Flow Accumulation in JBW.

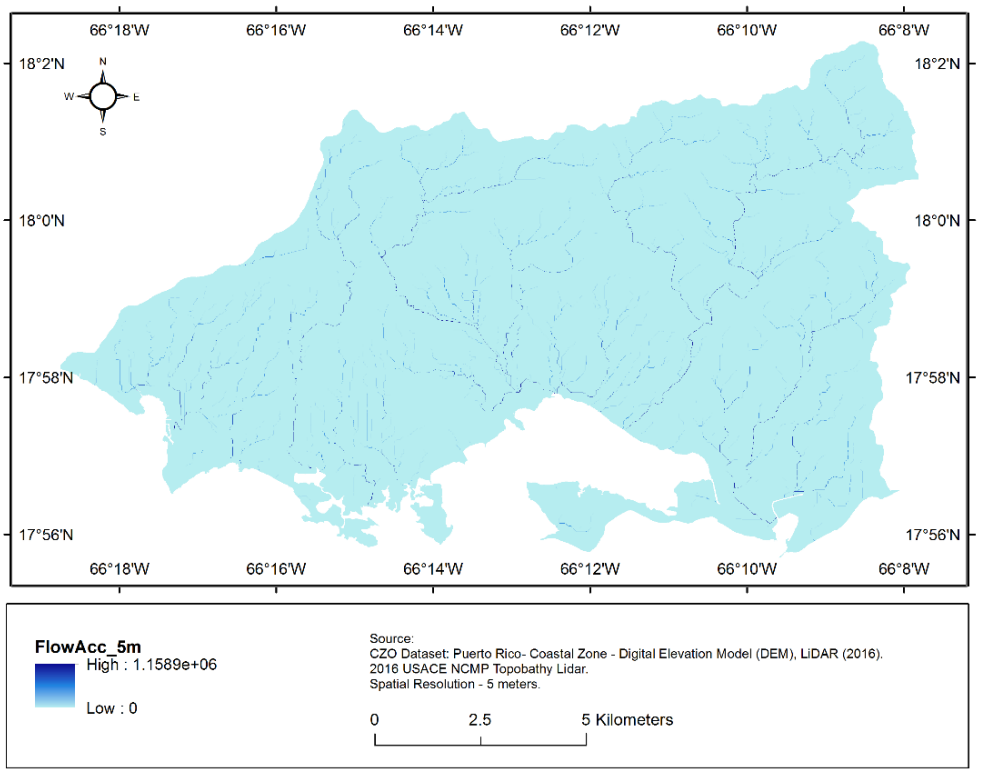

McCool et al. (1987) derived two relationships for moderate slopes (s <9%) and steeper slopes (s ≥ 9%), which is represented by the factor S in the RUSLE equation:

Equation 17. Steepness Factor

$$When\ \tan\beta_{i,j} < 0.09\ \ THEN\ \ S = 10.8\sin\beta_{i,j} + 0.03$$

$$When\ \tan\beta_{i,j} \geq 0.09\ \ THEN\ \ S = 16.8\sin\beta_{i,j} - 0.5$$

Modified LS Factor

The modified equation for computation of the LS factor in finite difference form in a grid cell representing a hillslope segment was derived by Desmet and Govers (1996).

LS factor was calculated by considering the flow accumulation and slope in degrees as an input (Ganasri & Ramesh, 2016). Therefore, the topographic factor is computed using the equation of Moore and Burch, and this technique requires flow accumulation and slope steepness (Jahun, Ibrahim, Dlamini, and Musa, 2015):

Equation 18. Topographical factor

$$LS = \left(Flow\ Accumulation * \frac{cell\ size}{22.13}\right)^{0.4} * \left(\frac{\sin slope}{0.0896}\right)^{1.3}$$

Where:

LS = Topographical factor or slope length and steepness factor.

Cover management factor (C)

The cover management factor (C) corresponds to soil loss under specific cropping conditions related to that occurring in bare soil (Wischmeier & Smith, 1978). The C values can vary from 0 for very well-protected soils to 1.5 for finely tilled, ridged surfaces that produce much runoff, leaving it susceptible to rill erosion (Simms et al., 2003). This ratio C will approach 1.0 where there is little soil cover (e.g., a bare seedbed in the spring or freshly grated bare soil on a construction site) (Weil & Brady, 2017). It will be low (e.g., < 0.10) where large amounts of plant residues are left on the land or in areas of dense perennial vegetation (Weil & Brady, 2017). However, the C factor values do not accurately represent vegetation variation, particularly in large areas, resulting in mistaken soil loss estimates (Asis & Omasa, 2007). Conditions where soil loss varies little with slope length, tend to have relatively low C-factor values: less than 0.15, if not where soil loss varies greatly with slope length typically have high C-factor values

(Renard, Foster, Weesies, McCool, 1996), which is the case of JBW. Factors C and P are dimensionless.

The C factor was estimated assuming that abundant vegetation cover results in less soil loss and the corresponding higher losses result from less vegetation cover (Jahun et al., 2015). Therefore, since C factor values are not available for the croplands at JBW. However, according with the literature the C values factors utilized by Bonilla et al., 2010; Del Mar López et al., 1998; M. & Jamal, 1999; Medeiros et al., 2016; Morgan, 2005; Ozsoy & Aksoy, 2015; Ramos-Scharrón et al., 2015a were used. Since, the mentioned literature presents different C values for forest, sugarcane crop, plantains crops, and pasture land applied in similar conditions as JBW. The values were averaged by each LULC class seeking a confident value for JBW. This recommendations was made by Morgan, (2005) and de Carvalho et al., (2014) when C factor values where determined for the crop rotations and management practices found in the USA, for other countries, a detailed information for calculating the C factor in this way does not always exist and it may be more appropriate to use average annual values. Related to urban development the C value used by Del Mar López et al., (1998) was selected because that study was done for a watershed in Puerto Rico with similar conditions as JBW. The same reasoning was applying choosing the C values for bare land and non-forest classes. First, the C factor was assigned to different land-use patterns using the values given in Table 17.

Table 17

RUSLE's Cover factor (C) values were used to evaluate the potential impacts of land-use change in surface runoff and erosion.

LULC class	*Description	Cover factor range	Information Source	Cover factor value for JBW
Forest	Woods	0.0001	Ramos-Scharrón et al., (2015)	0.0027
		0.0001	Medeiros et al., (2016)	
		0.01	Beskow et al., (2009)	
		0.002 - 0.3	Ozsoy & Aksoy, (2015)	
		0.001	Morgan, (2005)	
		0.003	Ochoa et al., (2016)	
Cropland	Mainly **Sugarcane** in 1977 and 1991.	0.35 - 0.55	Ramos-Scharrón et al., (2015)	0.2921
		0.056	Armour et al., (2009)	
		0.3066	Medeiros et al., (2016)	
		0.13 – 0.40	Morgan, (2005)	
		0.252	Ochoa et al., (2016)	
	Mainly **Plantain** crop in 2000 and 2010.	0.05	Del Mar López et al., (1998)	0.1642
		0.056	Armour et al., (2009)	
		0.346	Almas and Jamal, 1999	
		0.1318	Medeiros et al., (2016)	
		0.1 to 0.5	Ozsoy & Aksoy, (2015)	
		0.05–0.10	Morgan, (2005)	
Pasture/Grass	Pasture, hay, or inactive agriculture (e.g., abandoned sugarcane).	0.032	Del Mar López et al, 1998	0.1304
		0.016	Armour et al., (2009)	
		0.061	Medeiros et al., (2016)	
		0.09	Ozsoy et al. 2012	
		0.003–0.45	Ramos-Scharrón et al., (2015)	
		0.10 - 0.36	Ozsoy & Aksoy, (2015)	
		0.062	Ochoa et al., (2016)	
Urban	Built up area	0.02	Del Mar López et al., (1998) (*Less dense urban - Scattered buildings within areas of pasture or forest)	0.02
Non-Forest	Emergent wetlands,	0	Bonilla et al., (2010); Ganasri & Ramesh, (2016)	0

LULC class	*Description	Cover factor range	Information Source	Cover factor value for JBW
	coastal sand, and rocks, water permanent.			
Bare land	Areas with no vegetation	1	Morgan, (2005); Wischmeier & Smith, (1978)	1

Note. *For more details about LULC classes description consult the Kennaway & Helmer, (2007)

However, Bare land was considered as Non-Forest land according to the Kennaway & Helmer (2007) classification land methods. Hence, bare land is viewed as an erosion reference because erosion was greatest in areas of bare soil (Almagro et al., 2019; Aouichaty et al., 2021; Del Mar López et al., 1998; Wischmeier & Smith, 1978). Therefore, bare land was left as another land cover class for this chapter. In general bare soil or barren land is described as transitional areas for construction, land fill, gravel pit or barren natural land including exposed sediments, rocks, river banks, gravel, etc. (Ramos-Scharrón et al., 2015).

Conservation support practice factor (P)

The conservation practice support factor (P) represents how surface conditions such as contouring, tillage marks, or terracing influence erosion–deposition processes when surface runoff occurs (Renschler et al., 1999). Broadly applied soil conservation practices, particularly conservation tillage and no-till cropping, have effectively reduced erosion rates (Nearing et al., 2017). However, agricultural policies or economic incentives generally induce land-use changes or even agricultural crop rotation changes, resulting in different erosional behavior of cultivated soil (Renschler et al., 1999).

Therefore, factor P does not consider improved tillage practices such as no-till and other conservation tillage systems, sod-based crop rotations, fertility treatments, and crop-residue management. Instead, such erosion-control practices are considered in the C factor (Renard, Foster, Weesies, McCool, 1996). The estimation of this factor is conditioned by Contouring, Slope-Length, Contour Listing, Controlled-Row Grade Ridge Planting, Contoured-Residue Strips, Contour Stripcropping, or Terracing. However, when terraces are not maintained and overtopping is frequent, P = 1 and the slope length is the field slope length (Wischmeier & Smith, 1978). For areas with no support practice, the P factor is set to 1.0 (Simms et al., 2003).

Hot Spot Analysis

Lastly, an erosion rates differences between 1977 - 1991, 1991 - 2000, 2000 – 2010, and 1977 - 2010 hotspot analysis was performed using Getis-Ord-Gi statistic. This analysis seeks to determine the distribution soil loss occurrence based on historical hotspot data during a 46-year period. The Getis-Ord-Gi statistics is available as a spatial analysis tool in ArcGIS software. The input data was converted into point feature hotspot data based on the difference between periods described above. The tool then determines statistically significant spatial clusters of high values (known as hotspots), low values (called coldspots) and non- significant areas (Mora et al., 2019, Table 18). The G statistic can vary between 0.0 and 1.0 (Abdulhafedh, 2017). The statistical significance of the local autocorrelation between each point and its neighbors is assessed by the z-score test and the p-value (Abdulhafedh, 2017). Furthermore, the hotspot and coldspot areas are classified into 90%, 95% and 99% probability occurrence areas (Prasetyo et al., 2016).

The Getis-Ord Gi statistic measures the intensity of clustering of high or low values in a bin relative to its neighboring bins in the data (Getis & Ord, 1992). When a bin's sum was different than expected, and that difference was too large to be the result of random chance, a statistically significant Z-scores (standard deviations) was the result (Kowe et al., 2019). A Z-score above 1.96 or below −1.96 meant that there was a statistically significant hot spot or a statistically significant cold spot at a significance level of $p < 0.05$ (95% confidence interval) (Kowe et al., 2019). A Z-score near zero indicates no apparent spatial clustering (Kowe et al., 2019).

Table 18

Hot spot analysis (Getis-Ord Gi*) Statistical Criteria.

Category	**Z-score**	**P-value (probability) (%)**
Cold Spot	< − 2.58	p < 0.01 (99)
Cold Spot	< − 1.96	p < 0.05 (95)
Cold Spot	< − 1.65	p < 0.10 (90)
Not Significant	-	-
Hot Spot	> + 1.65	p < 0.10 (90)
Hot Spot	> + 1.96	p < 0.05 (95)
Hot Spot	> + 2.58	p < 0.01 (99)

According to Abdulhafedh, (2017) the standard formula that ArcGIS uses for Getis-Ord Gi statistic can be given as:

Equation 19. Getis-Ord Gi

$$G_i^* = \frac{\sum_{j=1}^{n} w_{ij}x_j - \overline{x}\sum_{j=1}^{n} w_{ij}}{S\sqrt{\frac{n\sum_{j=1}^{n} w_{ij}^2 - \left(\sum_{j=1}^{n} w_{ij}\right)^2}{n-1}}}$$

$$\overline{x} = \frac{\sum_{j=1}^{n} x_j}{n}$$

$$S = \sqrt{\frac{\sum_{j=1}^{n} x_j^2}{n} - \overline{x}^2}$$

Where x_i is the value of variable x at location *i;* x_j is the value of variable x at location *j;* w_{ij} are the elements of the weights matrix; and n is the number of observations. The values of *j* may equal *i* (Getis & Ord, 1992).

Results

Precipitation trends and Rainfall erosivity factor (R) during 1970 - 2015

According to the land extent of JBW, there is no significant spatial variability of the rainfall, even when the precipitation average was over 12.7mm in each rainfall station when compared by the four rainfall periods. However, as noticed in Figure 23 in the previous section, total annual maximum rainfall of around 300mm in Aguirre and around 500mm for both Guayama 2E and Jajome Alto stations were registered, averaging 22.8mm, 26.3, and 34.9mm, respectively. While previous research of Quiñones (2012) has focused on the importance of surface runoff as a source of freshwater to JBNERR, compared to groundwater discharges from the local aquifer, these results demonstrate rainfall exceeded 508 mm in three (3) instances, total monthly rainfall in Aguirre (1985, 1990, and 2003). That study provides insight into how rainfall events above 12.7mm enhance soil loss in JBW. Even when our results did not perfectly fit, these rainfall values compared to the historically found in this study period between 1970 and 2015, through the 90th percentile. However, a seasonal rainfall analysis was performed to identify the wettest months where soil erosion is expected to be higher. According to Ewel & Whitmore, (1973) and Zitello et al., (2008), Jobos Bay's has dry climate and relatively low seasonal rainfall, and surface runoff usually only occurs during the wettest months of the year, September through November.

The average monthly and annual rainfall results are shown in Table 19 and Figure 28. The months of May and October were the two peaks of mean monthly precipitation in 1970 – 1984, 1985 – 1999, and 2010 – 2015. The mean monthly precipitation ranges around 24 mm and 39 mm in May, and 21 mm and 49 mm in October for these periods. Meanwhile, September and November were the monthly precipitation peaks in 2000 - 2009, ranging between 31 mm and 52 mm in September, and 25 mm and 67 mm in November (Table 19). Consequently, December to April can be considered the five months of dry or low rainfall season because it is less than 30.0 mm mean monthly (Figure 28). Basically, this results aligned with Whitall et al., (2011); and Zitello et al., (2008), the wettest months are September to November in JBW. Although May and October exhibit different rainfall patterns, the results suggest that per millimeter (mm) of rain, these months show a higher erosivity than the rest of the months. Hence, from December until April can be considered the five months of low rainfall, and it can be inferred that the lowest erosivity per mm of rain occurs during these months in JBW. Interestingly, rainfall patterns are important to determine the harvest time and rotation in agriculture. To illustrate, the cane harvest period, known as “la zafra,” is a sugar harvesting and grinding , carried out mostly by temporary workers on a subcontract basis, depending on the area, the harvest takes place during the dry season (Wesseling et al., 2018). In Puerto Rico the summer period (July to September) is known as death time or “tiempo muerto” saw the labourers digging and cleaning drainage ditches, cane planting, weeding and cutting trees for new canefields (Ayala, 1994; Giusti-Cordero, 1996). As noted, in the example in sugarcane crops the dry season is time to harvest while the wet season is the time to dig, clean and plant. From August to November, only the colonia's

migrant labourers and agregados (tenant labourers) were hired (Giusti-Cordero, 1996). Then in November and December there was almost no work in the canefields: that was the heart of the dead time or the "winter" - "the invierno or invernazo, as we called it" (Giusti-Cordero, 1996).

Figure 28 The average annual rainfall ranged from 23.43 mm – 33.21 mm from 1970 to 1984, 22.44mm – 32.63mm from 1985 to 1999, 22.14mm – 39.72mm in 2000 – 2009, and from 23.21mm – 33.85 mm in 2010 – 2015 (Table 19). In general, the rainfall averages range from 22 mm to 40 mm being the Aguirre and Jajome Alto stations the less and higher average annual rainfall from 1970 – 2015. These results were expected, taking into consideration the watershed topographic profile. The Rio Seco (at the mouth) in the Northeast is the steepest area of the watershed, where Jajome station is closer to this area and where the most rainfall amount was registered during 1970 – 2015. However, rainfall is a dynamic triggering factor for soil loss and (might) present high spatial and temporal variability (Stefanidis et al., 2021), especially for agriculture activities. Thus, the effect of climate change on soil loss was evaluated through the monthly and annual precipitation condition performance for the historical frame 1970 to 2015.

Table 19

Annual and monthly precipitation means.

Station	Month												MAP (mm)
	01	02	03	04	05	06	07	08	09	10	11	12	
1970 - 1984													
Aguirre	15.4	16.0	13.5	19.0	20.8	20.6	22.5	23.4	27.5	33.3	25.4	13.9	23.4 ± 26.2
Guayama 2E	16.4	23.2	21.0	18.8	22.6	22.9	20.8	26.7	35.4	35.2	31.1	20.0	26.9 ± 28.7
Jajome alto	22.4	23.4	22.5	30.0	30.3	33.3	30.7	38.0	34.1	42.3	36.6	29.6	33.2 ± 30.2
1985 - 1999													
Aguirre	15.2	12.2	14.2	11.9	25.6	17.6	16.2	25.8	28.5	31.2	25.3	18.7	22.4 ± 26.6
Guayama 2E	19.0	20.2	15.4	19.8	25.2	16.7	24.6	23.9	31.3	29.2	27.0	21.1	24.6 ± 24.8
Jajome alto	48.4	24.2	22.6	30.6	33.6	29.0	27.2	32.9	33.7	45.2	34.2	25.5	32.6 ± 34.1
2000 - 2009													
Aguirre	12.3	28.9	17.8	18.7	24.3	16.7	22.4	17.5	31.3	22.7	25.5	15.7	22.1 ± 27.6
Guayama 2E	16.9	15.6	28.3	23.5	29.8	22.6	23.1	27.0	39.5	30.3	32.9	23.3	27.7 ± 34.3
Jajome alto	26.5	19.3	29.2	32.2	39.3	30.6	30.7	44.0	52.7	40.8	67.7	34.1	39.7 ± 37.6
2010 – 2015													
Aguirre	17.8	10.9	37.1	16.8	24.7	20.9	20.3	34.5	15.4	21.6	20.7	12.0	23.2 ± 24.9
Guayama 2E	17.9	15.1	15.8	19.9	27.8	25.5	28.3	31.4	28.7	24.2	27.7	16.0	26.1 ± 20.7
Jajome alto	22.3	26.7	23.2	22.9	37.7	31.8	36.5	44.7	33.9	49.7	29.7	22.8	33.9 ± 28.3

Note. MAP is the Mean Annual Precipitation in millimeter (mm) units and its standard deviation.

The months of May and October were the two peaks of mean monthly precipitation in 1970 – 1984, 1985 – 1999, and 2010 – 2015. The mean monthly precipitation ranges around 24 mm and 39 mm in May, and 21 mm and 49 mm in October for these periods. Meanwhile, September and November were the monthly precipitation peaks in 2000 - 2009, ranging between 31 mm and 52 mm in September, and 25 mm and 67 mm in November (Table 19). Consequently, December to April can

be considered the five months of dry or low rainfall season because it is less than 30.0 mm mean monthly (Figure 28). Basically, this results aligned with Whitall et al., (2011); and Zitello et al., (2008), the wettest months are September to November in JBW. Although May and October exhibit different rainfall patterns, the results suggest that per millimeter (mm) of rain, these months show a higher erosivity than the rest of the months. Hence, from December until April can be considered the five months of low rainfall, and it can be inferred that the lowest erosivity per mm of rain occurs during these months in JBW. Interestingly, rainfall patterns are important to determine the harvest time and rotation in agriculture. To illustrate, the cane harvest period, known as “la zafra,” is a sugar harvesting and grinding , carried out mostly by temporary workers on a subcontract basis, depending on the area, the harvest takes place during the dry season (Wesseling et al., 2018). In Puerto Rico the summer period (July to September) is known as death time or “tiempo muerto” saw the labourers digging and cleaning drainage ditches, cane planting, weeding and cutting trees for new canefields (Ayala, 1994; Giusti-Cordero, 1996). As noted, in the example in sugarcane crops the dry season is time to harvest while the wet season is the time to dig, clean and plant. From August to November, only the colonia's migrant labourers and agregados (tenant labourers) were hired (Giusti-Cordero, 1996). Then in November and December there was almost no work in the canefields: that was the heart of the dead time or the "winter" - "the invierno or invernazo, as we called it" (Giusti-Cordero, 1996).

Figure 28

Average monthly rainfall at climatic stations for Jobos Bay during 1970 - 2015.

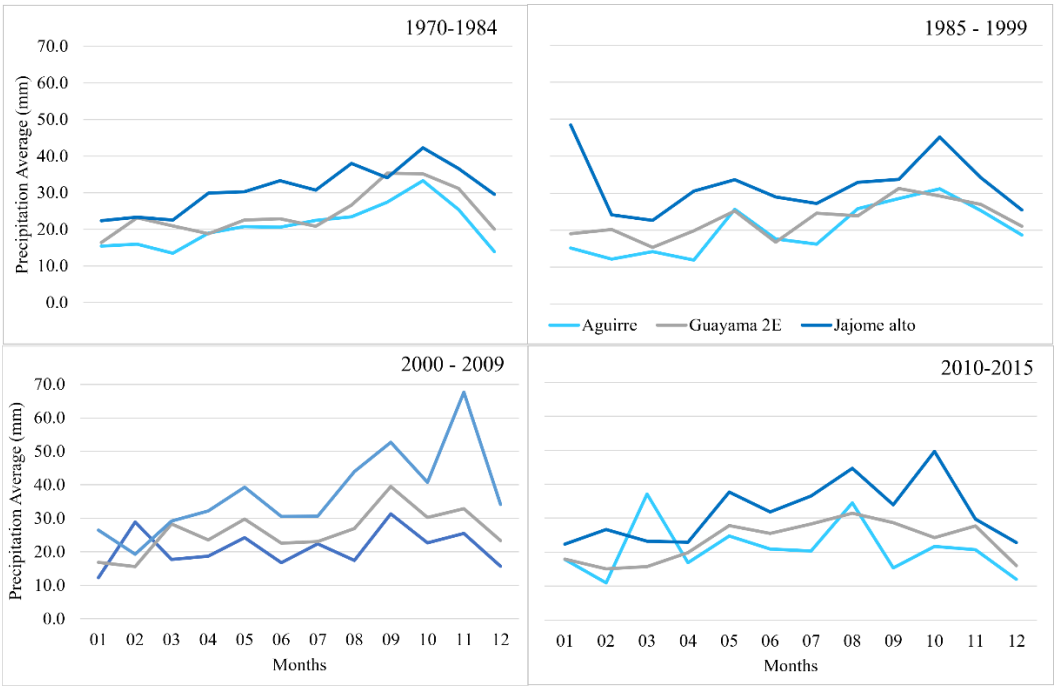

In terms of the erosivity factor, a weak spatial variation of R was observed, which was provided from three stations for 45 years. The spatiotemporal changes of the R-Factor are shown in Figure 29. The spatial variation of R significantly increases from the upper Northeast to the low-down northwest direction. During 1970 to 1984 rainfall period, R-Factor varied from 7,863.4 to 8,237.6 MJ*mm/ha*h. From 1985 – 1999, R factor range from 7,834.8 to 8,281.4 MJ*mm/ha*h. While from 2000 – 2009, R factor ranged from 7,939.3 to 8,408.3 MJ*mm/ha*h, and from 7,884.7 to 8,260.7 MJ*mm/ha*h during 2010 to 2015 rainfall period (Figure 29). Even when the highest erosivity factor were registered during 2000 to 2009 did not present a different erosivity factor pattern from the other rainfall periods. This spatial distribution is consistent with that of the rainfall pattern of JBW previously described and showed a clear distinction between the upper areas (with high R value) and the coastal areas (with low R value).

Certainly, a topographic influence was shown in the rainfall factor where the steepest areas are located near the Jajome station with the highest average annual rainfall and in the coastal areas is located near the rainfall Aguirre and Guayama stations with lowest average annual rainfall in JBW. This is explained by part of JBW's physical characteristics that are attributed to the presence of two of Puerto Rico's Central Interior Mountain Ranges to the north, La Cordillera Central and La Sierra de Cayey (Whitall et al., 2011). Hence, climate and erosion are linked to water movement into and through the soil, soil-water balance, and slope hydrology as well as the rainfalls events are an important influence on the rate of most erosion processes and are projected to increase in extreme rainfalls, which will play a critical role (Basher, Douglas, Elliott, Hughes, Jones, McIvor, Page, Rosser, & Tait, 2012). Literature shows that the erosive power of precipitation affects slope stability; the greater the increases of precipitation amount, the greater the soil loss (Basher et al., 2012). In this sense, much attention should be given to topography characteristics, and soils are usually relatively constant in the timescales of interest, whereas rainfall erosivity and vegetation vary greatly (Yin et al., 2015). The combination of all these factors was discussed later in the chapter.

Figure 29

Rainfall Erosivity Factor in JBNERR

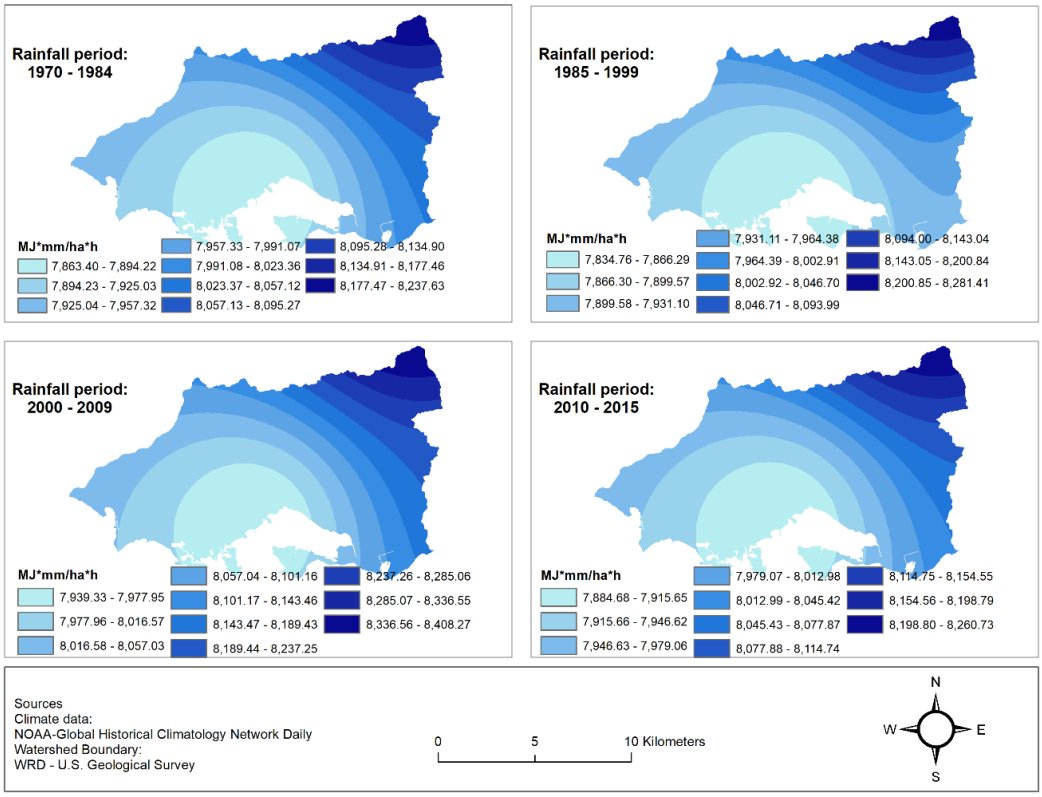

Soil Erodibility Factor (K)

The k values thru nomograph were calculated for each soil type by integrating soil analysis values in JBW and generalized through the soil map (Table 20). K-values ranges between 0.003 to 0.042 t*h/MJ*mm). Note that JBW has low K values. The K factor in SI units normally varies from near zero to about 0.1 (Weil & Brady, 2017), and highest k value was 0. 042 t*h/MJ*mm. Then, soils with high water infiltration rates commonly have K values of 0.025 or below, while more easily eroded soils with low infiltration rates have K factors of 0.04 or higher (Weil & Brady, 2017).

The lowest value of the factor K found at the southeast coast of JBW is 0.003. The soil type with the lowest k-value was Meros sand, whose surface texture is sand.

Sandy soils have low K values due to high infiltration rates and reduced runoff, and because sediment eroded from these soils is not easily transported (Ganasri & Ramesh, 2016). In JBW, sand and loamy sand were the surface texture of soil with the lowest Factor K values ranges 0.003 and 0.007 t*h/MJ*mm respectively. The K values of 0.003 and 0.007 are associated with low erodibility and having higher permeability according to the soil erodibility nomograph and the literature (Table 20).

Conversely, the highest value of the factor K is 0.042 t*h/MJ*mm found at the east and west of the watershed identified with the darker color in Figure 30. The k value of 0.042 t*h/MJ*mm is associated with less water infiltration and higher erodibility according to (Weil & Brady, 2017; Figure 30). The soil type with the highest k-value was Guamaní (Gm), with a surface texture of silty clay loam. Silt loam soils have moderate to high K values as the soil particles are moderately to easily detachable, infiltration is moderate to low producing moderate to high runoff, and the sediment is moderately to easily transport (Ganasri & Ramesh, 2016). While silt soils have the high K values as these soils crust readily, producing high runoff rates and quantities (Ganasri & Ramesh, 2016).

Overall, the surface texture with the greatest Factor K values ranges from 0.037 and 0.042 t*h/MJ*mm, are silty clay loam, then followed by the textures of sandy loam (0.032 t*h/MJ*mm) and clay loam (ranges from 0.026 and 0.032 t*h/MJ*mm). In general, clay soils have lower K values because they are more resistant to detachment compared to silt and silt loam soils. Since permeability measures the rate at which water percolates through the soil as a function of texture, structure, and composition. Therefore,

in JBW the higher values of the K factor are associated with the soils having moderate permeability and low to moderate erodibility in JBW.

Table 20

Soil types and Erodibility Factor for JBNERR.

Soil unit symbol	Soil unit name	Surface Texture	Factor K (t*h/MJ*mm)
Ad	Aguadilla loamy sand	Loamy sand	0.007
AmB	Amelia gravelly clay loam, 2 to 5 percent slopes	Gravelly clay loam	0.020
AmC2	Amelia gravelly clay loam, 5 to 12 percent slopes, eroded	Gravelly clay loam	0.020
An	Arenales sandy loam	Sandy loam	0.032
Ar	Arenales sandy loam, gravelly substratum	Sandy loam	0.032
CbF	Caguabo clay loam, 20 to 60 percent slopes	Clay loam	0.026
Ce	Cartagena clay	Clay	0.026
Cf	Catano loamy sand, 0 to 2 percent slopes	Loamy sand	0.007
ClB	Coamo clay loam, 2 to 5 percent slopes	Clay loam	0.032
Cm	Coastal beaches	Sand	0.007
Cn	Cobbly alluvial land	-	
DcE2	Daguao clay, 20 to 40 percent slopes, eroded	Clay	0.020
DeC2	Descalabrado clay loam, 5 to 12 percent slopes, eroded	Clay loam	0.032
DeE2	Descalabrado clay loam, 20 to 40 percent slopes, eroded	Clay loam	0.032
DgF2	Descalabrado and Guayama soils, 20 to 60 percent slopes, eroded	Clay loam	0.032
DrF	Descalabrado-Rock land complex, 40 to 60 percent slopes	Clay loam	0.032
FrA	Fraternidad clay, 0 to 2 percent slopes	Clay	0.022
FrB	Fraternidad clay, 2 to 5 percent slopes	Clay	0.022
Gm	Guamani silty clay loam	Silty clay loam	0.042

Soil unit symbol	Soil unit name	Surface Texture	Factor K (t*h/MJ*mm)
JaB	Jacana clay, 2 to 5 percent slopes	Clay	0.020
JaC2	Jacana clay, 5 to 12 percent slopes, eroded	Clay	0.020
MrB	Meros sand, 1 to 6 percent slopes	Sand	**0.003**
NaF	Naranjito silty clay loam, 40 to 60 percent slopes	Silty clay loam	0.037
NOTCOM	No Digital Data Available	-	
NOTPUB	Not Public Information	-	
PlB	Paso Seco clay, 0 to 5 percent slopes	Clay	0.026
Po	Poncena clay	Clay	0.022
PrC2	Pozo Blanco clay loam, 5 to 12 percent slopes, eroded	Clay loam	0.026
Rs	Rock land	Unweathered bedrock	
Sm	Saltwater marsh	Variable	
Tf	Tidal flats	Variable	
Ts	Tidal swamp	Variable	
Vc	Vayas silty clay, frequently flooded	Silty clay	0.037
Vs	Vives silty clay loam, high bottom	Silty clay loam	0.037
VvB	Vives clay, 2 to 7 percent slopes	Clay	0.032
W	Water		-

Figure 30

Erodibility Factor through Nomograph.

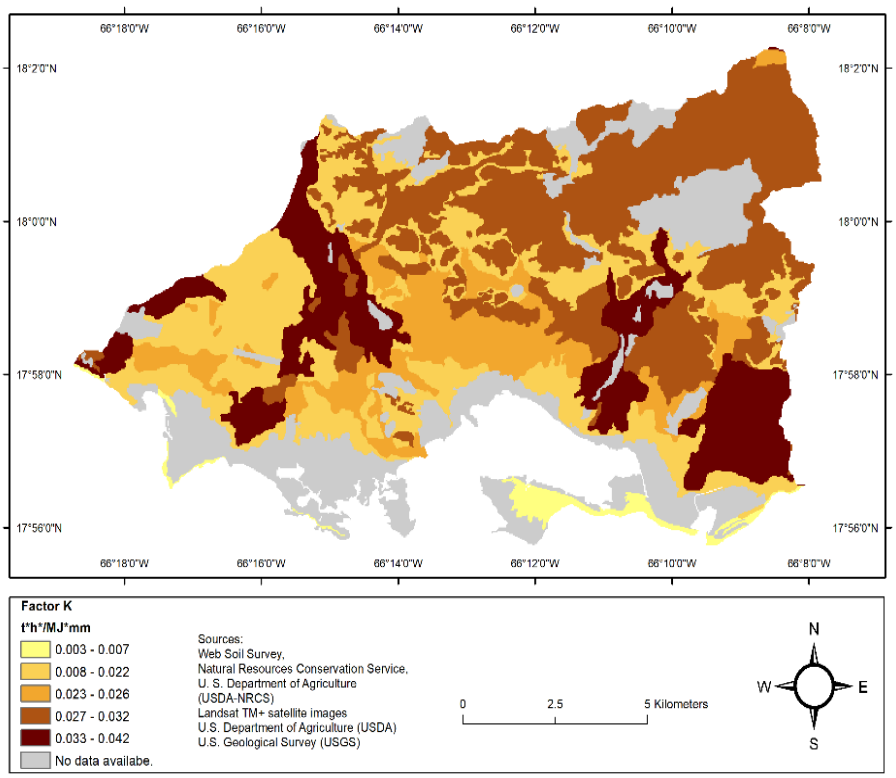

In sum, in JBW, most of the K-values range are explained due to its different topographies and a unique soil property. Even if the estimated values could be considered in error and the predicted soil loss may be far from exact, they are the best available data for at least assessing the erosion potential or relative erosion rates from different conditions (such as cover management or crop) or soils (Renard & Freimund, 1994). Soil erodibility is a key parameter for evaluating soil's susceptibility to erosion and is essential for erosion prediction and conservation planning (Wang, Zheng, Ro¨mkens, et al., 2013).

Topographic Factor (LS)

Important terrain characteristics influencing the mechanism of soil erosion are slope, length, aspect, and shape (Ganasri & Ramesh, 2016). Figure 31 illustrates the slope

length factor in JBW. The slope length range is between 0.34 – 612.42 meters long in this watershed. However, the shortest slope length is the most predominant compared to the longest slopes. The shortest slopes are found at the upper northwest of JBW. In Figure 31, a major concentration of this factor ranges between < 0.04 meters and 1.2 meters long. The length and steepness factors significantly influence the soil erosion processes (Aouichaty et al., 2021). The longer the slope, the greater the opportunity for accumulation and concentration of the runoff water (Weil & Brady, 2017).

Figure 31

Slope Length factor (Factor L) in JBW.

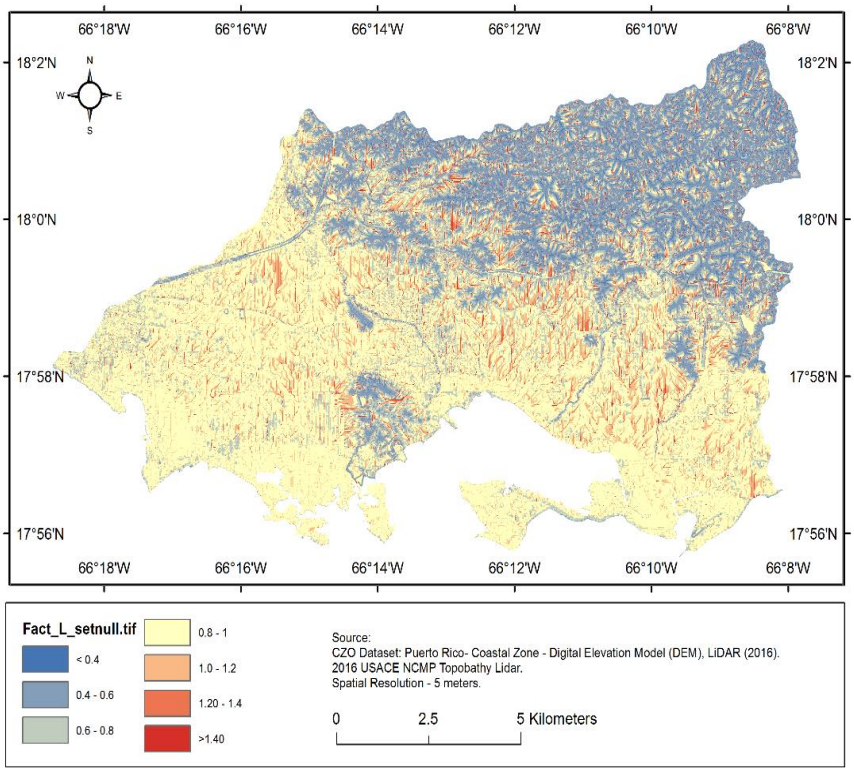

However, the effects of slope steepness have a greater impact on soil loss than slope length (Ganasri & Ramesh, 2016). Figure 32 illustrates the Steepness Factor (Factor S) in radians (a dimensionless SI unit for measuring angles). The slope was derived from

the Digital Elevation Model (DEM) with five (5) meters of spatial resolution. In JBW, the factor S ranges between 0.03 – 15.017 radians. The slopes with the greatest steepness and the shortest slope length are located at the upper northwest at the JBW. Nonetheless, the combination of Factor S and Factor L show the effect of the topographic factor on soil loss in JBW. Meanwhile, the longest and less steep slopes are located from the mid watershed zone thru the coast, especially at the southwest, where the cultivated lands are situated in JBW. According to Weil & Brady (2017), most sites cultivated to row crops have moderate rill to interrill erosion ratios, and on sites where this ratio is low, such as rangelands, more of the soil movement occurs by interrill erosion. On these sites, slope steepness (%) has a relatively greater influence on erosion, while the slope length has a relatively smaller influence (Weil & Brady, 2017).

Figure 32

Steepness Factor (Factor S).

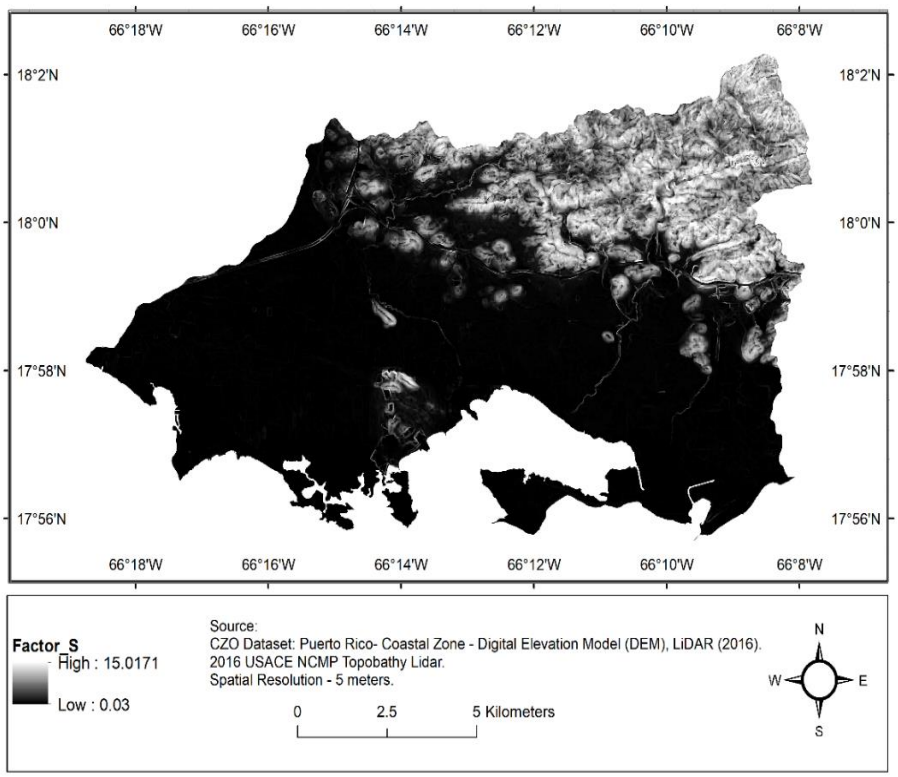

In terms of the unitless Factor LS, from the analysis, it was observed that the value of topographic factor (Factor LS) increases in a range of 0.03 – 1,920.23 as the flow accumulation and slope increase. This factor incorporated the flux of convergence impacts, which considered the runoff contribution from upstream to the downstream cells (de Mello et al., 2016b). In JBW, the Factor LS are concentrated between 0.03 flatter zones and 15.89 steeper zones (Figure 33). In JBW, the topographic factor shows that erosion-reducing effects of shortening slopes or reducing slope gradients are accounted for through the LS factor (Wischmeier & Smith, 1978). Similar results were also reported by Jahun et al. (2015). The combined effects of slope length and slope steepness give a good estimation of soil erosion rate. In this study area, the topography of this agricultural

watershed mostly favored more erosion at the upper northeast, but LULC should play an important role regarding the risk intensity and vulnerability of soil loss.

Figure 33

Factor LS for JBW.

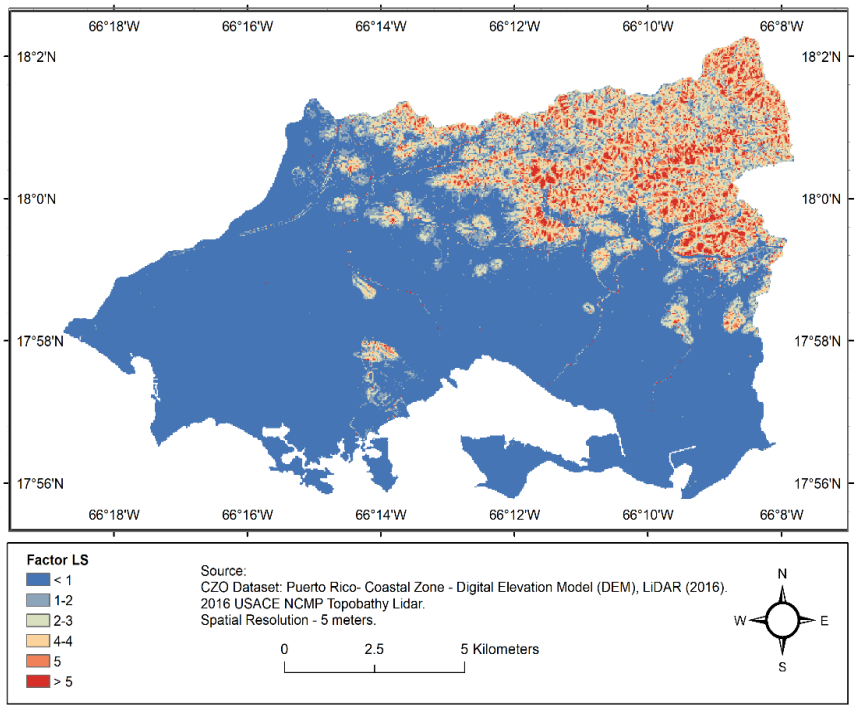

Land changes and Cover management factor (C)

The LULC reclassification maps of 1977, 1991, 2000, and 2010 are shown in Figure 34. LULC maps indicated a visible land transformation involving significant changes in cultivated lands and increased forest, pasture/grass, and urban development land. Therefore, a detailed land changes analysis was performed in chapter two for the forest, cultivated land, pasture/grass, urban development, and non-forest land classes. Land changes analysis was crucial to understand how soil loss might be accentuated through time, especially with cultivated land changes located at the lower and coastal regions in JBW. Hence vegetation cover that sustains the soil is one of the main factors

determining the land's response to rain events. In addition, vegetation intercepts raindrops and protects soils against the erosive action of water.

In agriculture, a significant decrease from 1977 to 1991 and 1991 to 2000 was identified as an increase between 2000 and 2010. According to the reclassification results, the forest was constantly the dominant land cover in the watershed's upper area in 1977 and 2010. Cultivated lands were mostly dominant in 1977 in sugar cane fields. In the meantime, the pasture/grass ranked third of the total area in 1977 and second place in 2010. However, in 1991 and 2000, pasture/grass ranked first. The urban development land gradually increased during the 33 years from 1977 to 2010, which is characteristic of the urbanization process in Puerto Rico during that time. Bare land remained, but its extension area is the smaller LULC class in JBW.

Figure 34

Land use/cover maps based on image classifications by year: (a) 1977; (b) 1991; (c) 2000; and (d) 2010.

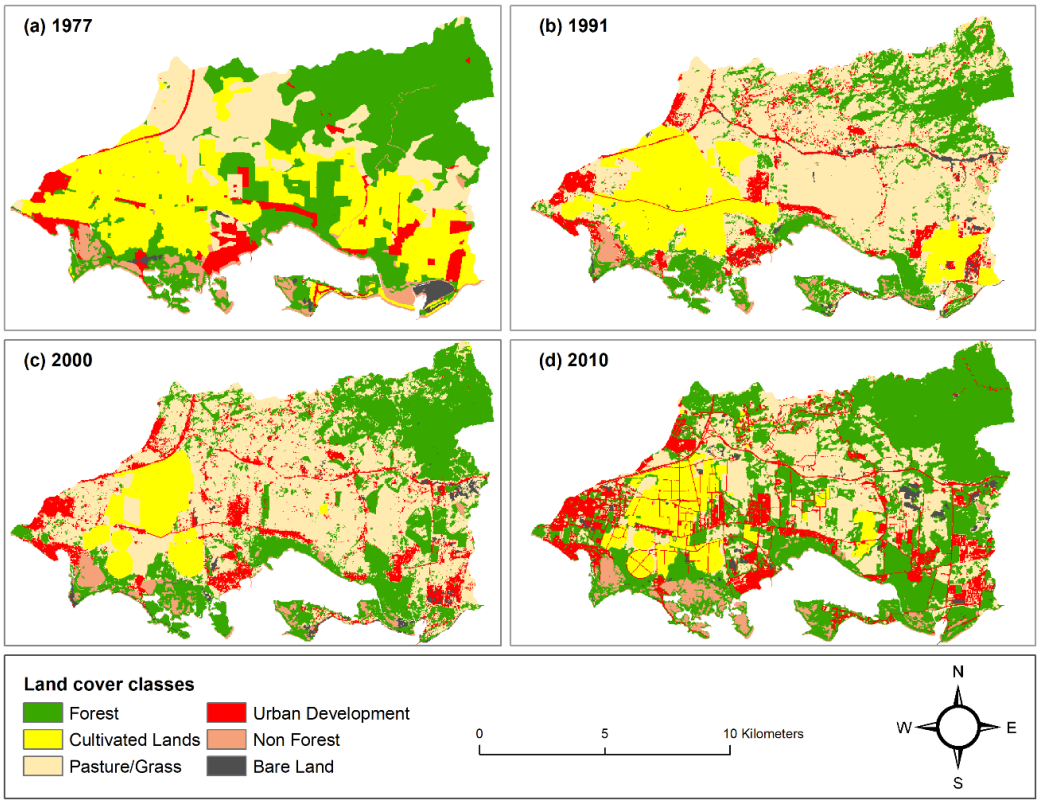

Table 21 shows the area covered by each LULC class with Factor C values each year. The highest percentage of LULC class from 1977 to 2010 ranges from 38.1% to 45.4%, forest with a Factor C value of 0.003. Forest increased 45.7% in 1991–2000 and 42.4% in 2000–2010 but markedly decreased 42.5% in the first period 1977–1991. Factor C represents the vegetation effectiveness as a protective cover for the soil against the impact energy of raindrops and the force of the runoff. Thus, it is expected that Forest has the lowest Factor C value after the non-forest class. Hence Non-Forest includes permanent water bodies; it is established that zero is the Factor C value.

Factor C for cultivated lands must be assigned based on the agricultural practices of the area. Nonetheless, previous studies in tropical areas and Puerto Rico used different Factor C value and averaged of 0.292 for Sugarcane crops and 0.164 for Plantains crops. Therefore, these Factor C values were set to sugarcane crops that were taking place in 1977 and 1991, and mainly plantains crop in 2000 and 2010 in JBW. Cultivated land decreased in JBW from 1977 to 2000, increased by 2010, and is still in the LULC class, which should be considered an indicator of poor soil protection. In effect, cultivated land decreased 41.0% and 55.5% to 1977–1991 and 1991-2000 respectively, and increased 16.2% in 2000-2010. These results suggest the possibility of high soil loss closer to the estuarine waters. Indistinctly cultivated lands decreased from 1977 to 2000 because it comprises a significant area extension in JBW. Factor C values for pasture are lower than cultivated lands, which might be explained because the grass is dense and runoff is very slow (about the slowest under any vegetative condition) (NRCS, 2002).

Furthermore, these results compare to Fu et al. (2006), where Factor C values for other LULC such as pasture and forest are generally lower than those for croplands with some exceptions, such as bare lands. Pasture areas acquire great importance because they significantly increased from 1977 to 2000, mainly due to abandoned agricultural areas. Specifically, from 1977 to 1991, pasture/grass nearly tripled in size with a net change of 167.3%. Contrary to 2000 to 2010, that pasture decreased by 44.7%, reducing its total land area three times. Bare lands, showed the highest Factor C value as theoretically assigned. Bare land covering between 1.1% and 1.4% remained stable from 1977 to 2010. By definition, C = 1 under standard fallow conditions, and as the surface cover is added to the soil, the C factor value approaches zero (Kelsey & Johnson, 2015). For

example, a C factor of 0.20 signifies that 20% of the amount of erosion will occur compared to continuous fallow conditions (Kelsey & Johnson, 2015).

Table 21

LULC percentage distribution and Factor C values.

LULC classes	Factor C	1977		1991		2000		2010	
		Area (km^2)	%	Area (km^2)	%	Area (km^2)	%	Area (km^2)	%
Forest	0.0027	52.1	38.1	29.9	21.9	43.6	31.9	62.1	45.4
***Cultivated Lands**	0.2921; 0.1642	43.3	31.7	25.5	18.6	11.3	8.3	13.2	9.6
Pasture/Grass	0.1304	24.3	17.8	65.0	47.5	63.0	46.1	34.8	25.4
Urban Development	0.02	8.9	6.5	11.1	8.1	13.1	9.6	19.2	14.0
****Non-Forest**	0	6.8	4.9	3.4	2.5	3.8	2.8	5.6	4.1
Bare land	1	1.5	1.1	1.9	1.4	2.0	1.4	1.9	1.4
Total	-	136.8	100	136.8	100	136.8	100	136.8	100

Note. *Factor C value of 0.40 was set to 1977 and 1991, and 0.346 for 2000 and 2010.
**Emergent Wetland, coastal and rock, and permanent water bodies are consolidated into non-forest class.
Source data from the Landsat TM+ satellite images, US Department of Agriculture (USDA), and US Geological Survey (USGS).

Figures 35, shows the spatial Cover Management Factor (C) distribution for 1977, 1991, 2000, and 2010. Cultivated lands were located at the lower areas, pasture was found mainly at the center area, while forest was predominant at the upper of JBW. As shown and described above, the higher the vegetation the lower Factor C value. According to Laboy et al. (2008), banana and plantain farms exist north of Mar Negro, outside JBNERR boundaries, extending toward plantain farms outside of the reserve boundaries, extending toward the higher, cooler mountain areas, and Pasturage is also a principal agricultural use. The end of the sugarcane cultivation era was 1994. After 1994, land-use change from monoculture to multi-culture also affected water delivery needs for

the new crops (Laboy et al., 2008). The results of Mohammed et al. (2021) proposed that changes in the inclination and LULC showed that soil erosion was larger on steeper slopes, and varied according to the rain amount. In this case as occurred in JBW, where the erosion processes are maximized by the steep slopes present in the higher sectors of the JBW, but the presence of Forest is abundant. In sum, the land cover having the higher C-factor value (low vegetation cover) subjected to the high rate of erosion. (Maury et al., 2019).

Figure 35

Cover Management Factor (C) maps based on Land cover and Land use reclassified images by year: (a) 1977; (b) 1991; (c) 2000; and (d) 2010.

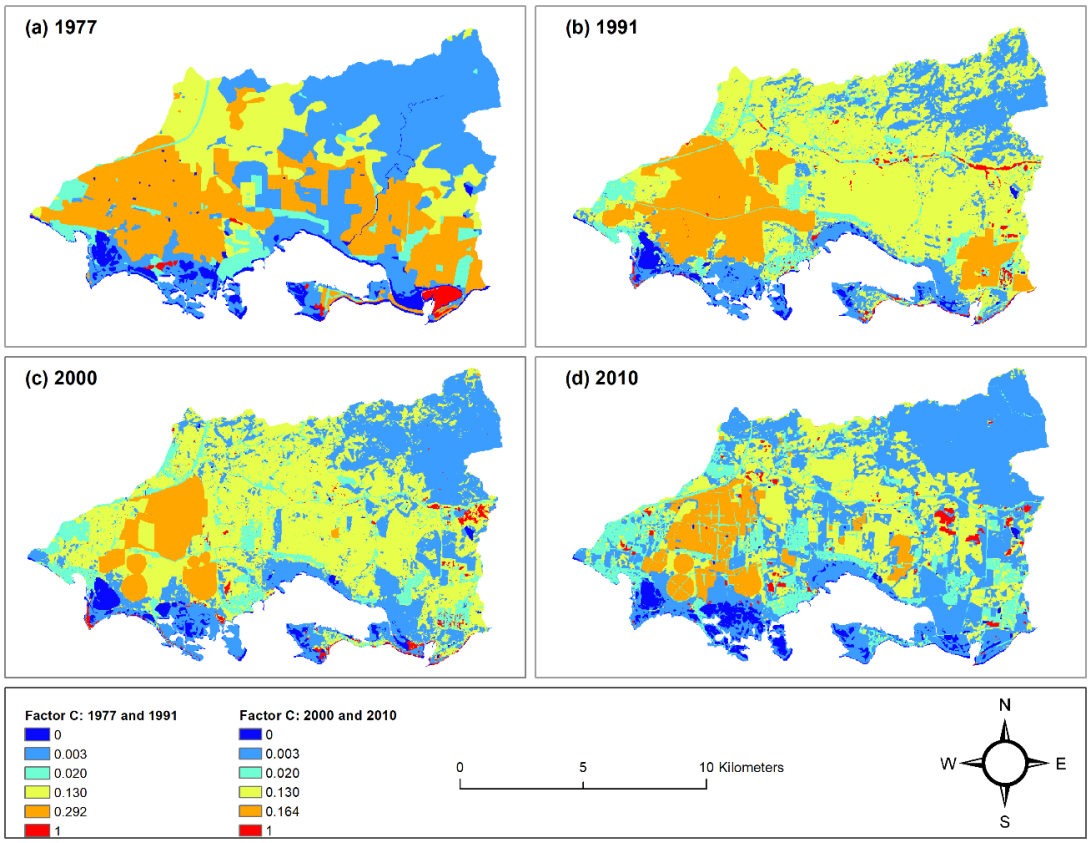

Conservation support practice factor (P)

For JBW, a value of 1 was set as the value for Factor P and thus occupied 100% of the watersheds, as set by previous studies in various watersheds in Puerto Rico, including JBW (Tania Del Mar López et al., 1998; Williams et al., 2011).

RUSLE

To estimate the annual average soil loss rate for the JBW in 1977, 1991, 2000, and 2010, the raster grids representing the RUSLE parameters were analyzed in GIS (Table 22). Overall, the annual average soil loss without for JBW was estimated to be 9.8 ton/ha/y in 1977, 16.0 ton/ha/y in 1991, 11.5 ton/ha/y in 2000 and, 8.7 ton/ha/y in 2010. Figure 36 offers a better appreciation of average annual soil loss about the calculation differences, trends, and magnitudes in JBW.

Table 22

The annual average soil loss rate for 1977, 1991, 2000, and 2010

Year	Average Soil Loss Rate (ton/ha/year)	Standard Deviation	Minimum	Maximum
1977	9.76	18.56	0	100
1991	16.07	27.99	0	100
2000	11.53	24.03	0	100
2010	8.72	21.44	0	100

Figure 36 shows the average soil loss in 1977, 1991, 2000, and 2010. The average soil loss was significantly greater in 1991 than in 1977, 2000, and 2010. Between 1977 and 1991, the average soil loss was 6.3 ton/ha/y greater 1991. In 1991, pasture grass represented 47.5% of JBW, remaining less forest extension area than in 1977 even when cultivated areas significantly decreased during the period. In addition, pasture/grass lands were in the middle watershed area, where the slopes are steep compared with the area

closer to the coast. Between 1991 to 2000, the average soil loss was 4.5 ton/ha/y greater 1991. However, between 2000 and 2010, the average soil loss was 2.8 ton/ha/y less in 2010. These results allow looking at the LULC influence on the soil loss process in JBW for 1977, 1991, 2000, and 2010. Even when cultivated lands were significantly greater in 1977 than in any other period, forest cover was also greater in 2010 compared to 1977. However, major attention should be given to pasture/grass areas because forest plays an important role in reducing erosion. However, pasture/grass combined with topographic factors seems to enhance soil loss, although cultivated land decreased during the study period. Considering that the rainfall erosivity factor did not present significant spatiotemporal changes; the erodibility and topographical factors remain consistent through time. Therefore, the cover management factor seems to be the main soil loss driver in JBW.

Figure 36

The annual average soil loss rate for 1977, 1991, 2000, and 2010.

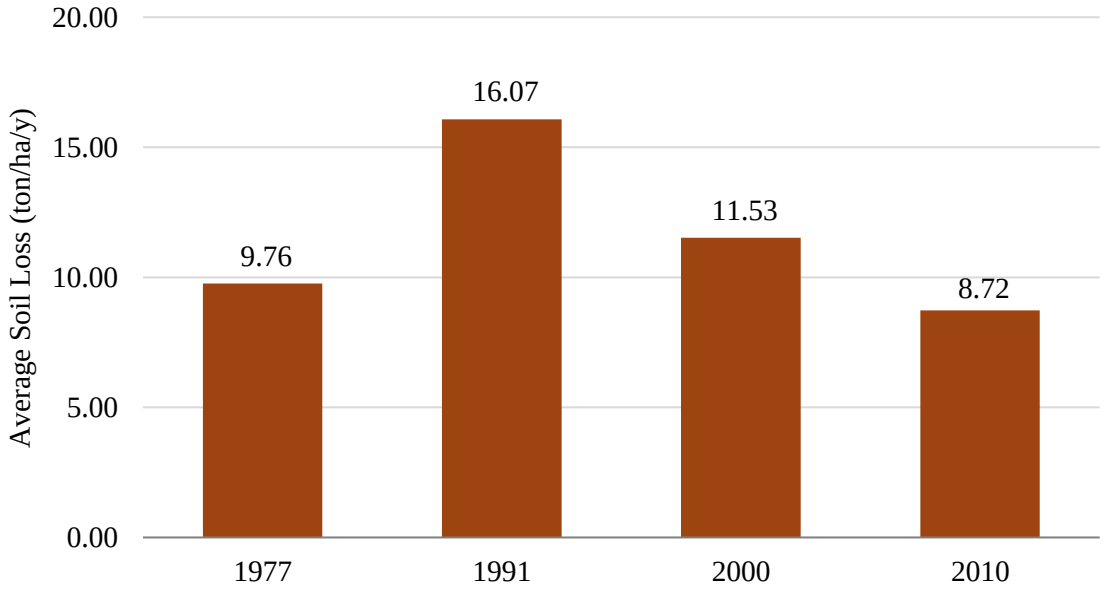

Table 23Table 23 and Figure 37 presents the average annual soil loss rate obtained for 1977, 1991, 2000, and 2010. The distribution of soil erosion risk classes showed that more than 40% of the watershed has slight soil loss, around 10% is slight to moderate, more than 13% was moderate, around 5% was moderate to high, and around 11% was very high from 1977 to 2010. However, in 1991 the soil erosion risk from moderate to very high was 45.6% (62.1 km^2), greater than 1977 with 39.9% (54.5 km^2), 2000 with 29.2% (39.8 km^2), and in 2010 with 20.9% (28.4 km^2). The highest soil loss values correlate with cover management and topographic factors. For example, the biggest Forest area cover was found in LULC 2010 raster with 45.4% and where the biggest slight soil erosion risk was found with 70.3% from the study period. The same results are illustrated in 1991 where the biggest area cover was pasture with 47.5% (65.0 km^2) and resulting with smallest slight soil loss with 43.0% compared with 1977, 2000 and 2010.

On the other hand, moderate soil erosion risk increased from 1977 to 1991, decreased from 1991 to 2010. Very High soil erosion risk resulted in 8.3% in 1977, 15.7% in 1991, 11.5% in 2000, and 8.8% in 2010, respectively. Special attention is pointed out in 1991 where high and very high erosion risk summed 19.9 %, while in 1977 was 14.1%, in 2000 it was 14.5%, and 10.9% in 2010. The very high soil erosion risk increased from 1977 to 1991 and decreased in 2000 and 2010 because forest area increased, cultivated lands decreased and changed from sugarcane to plantains, papaya, and other products. Previous found that Sugarcane crops worsens the soil loss more than plantains crops giving a major C value to sugarcane (Armour et al., 2009; Medeiros et al.,

2016; Morgan, 2005). Meanwhile, Pasture/Grass significantly increased from 1977 to 1991 and 2000 but decreased 20.7% between 2000 and 2010.

Table 23

Average annual soil loss rate by erosion type classifications for 1977, 1991, 2000, and 2010.

Soil Loss (ton/ha/yr)	**1977**		**1991**		**2000**		**2010**	
Type of erosion	**km^2**	**%**	**km^2**	**%**	**km^2**	**%**	**km^2**	**%**
Slight (0 - 2.5)	72.1	52.9	58.6	43.0	79.6	58.4	95.8	70.3
Slight to Moderate (2.5 - 5)	9.7	7.1	15.6	11.5	16.9	12.4	12.1	8.9
Moderate (5 - 10)	22.7	16.7	26.0	19.1	15.5	11.4	10.6	7.8
Moderate to High (10 - 15)	12.6	9.2	9.1	6.6	4.6	3.4	3.0	2.2
High (15 - 25)	7.8	5.8	5.7	4.2	4.1	3.0	2.8	2.1
Very high (25 - 100)	11.4	8.3	21.4	15.7	15.6	11.5	12.0	8.8

Figure 37

Soil erosion risk class by year in JBW.

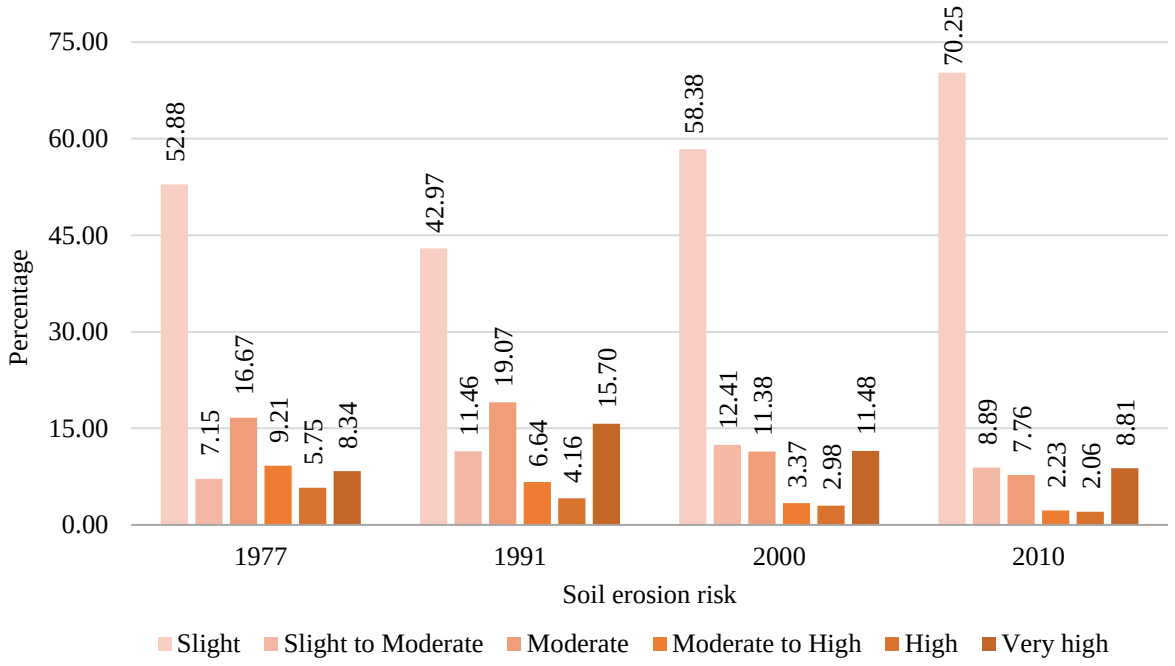

Figure 38 presents the spatial average annual soil loss rate and severity map of the Jobos Bay Watershed for conditions in 1977, 1991, 2000, and 2010. Overall, potential soil erosion risk and severity increase from the mid-upper Northeast to the lower reaches of the JBW catchment. Also, the very upper northeast area presented a minimal soil loss risk for the complete study period. However, surface erosion can vary spatially due to rainfall variability, topographic and morphological changes, soil types and characteristics, and human-induced disturbances (Farhan et al., 2013).

However, the spatial distribution showed that in 1977 the upper Northeast was the biggest area with slight to moderate soil erosion risk, while high and very high classes were found in the same area in 1991 and 2000 and decreased in 2010. This might be explained with Pasture/Grass in the upper areas of the watershed was greater in 1991 and

2000 than in 2010. Factor C values are greater for pasture/grass than forest, the slopes are steeper in this area, and rainfall activity was greater near the upper area compared with the lower watershed. In contrast, Forest recovery grew in areas classified as pasture/grass in 1991 and 2000. The soil erosion risk classification changed from very high to mainly slight or moderate to high. The less steep area of the watershed is located at the coast with slight, slight to moderate, and moderate to high potential soil erosion.

Nevertheless, special attention is given to the soil erosion risk at the lower area of JBW due to the cultivated lands located in this area. The soil erosion risk values associated with cultivated lands range from Moderate to Moderate to High, and High from 1977 to 2010. Very small areas were classified as high erosion risk in the Cultivated Lands class in 2000 and 2010. These findings can be mostly explained due to the gentle slopes that are related to slight to moderate potential soil loss in JBW.

Figure 38

Average annual soil loss rate and severity map of the Jobos Bay Watershed for conditions in 1977, 1991, 2000, and 2010.

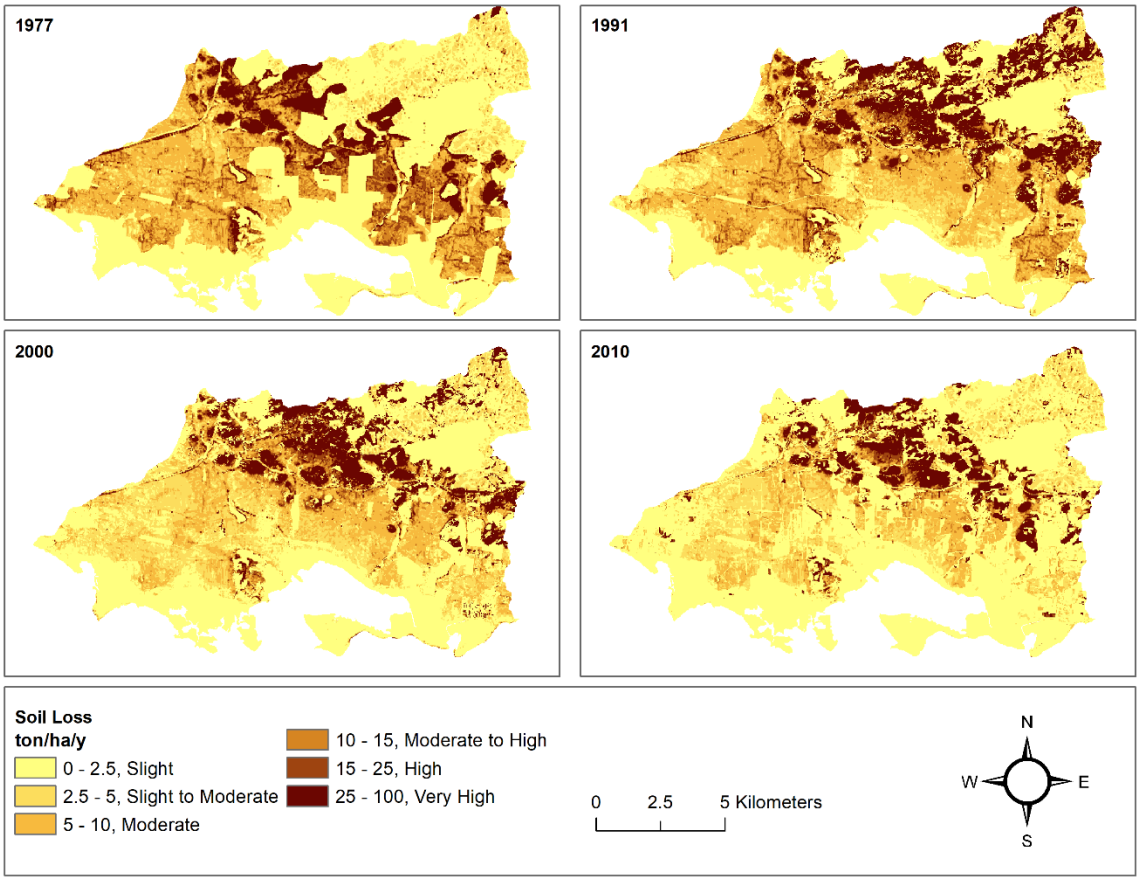

Hot Spot Analysis

Figure 39 illustrates the hotspots occurrence between 1977 and 2010 in JBW. The significant hot spots and cold spots of erosion rate differences are indicated with statistical confidence levels ranging from 90% ($p < 0.10$), 95% ($p < 0.05$), and 99% ($p < 0.01$). A high Z-score and small p-value indicate a significant hot spot (Kowe et al., 2019). On the other hand, a low negative Z-score and a small p-value indicate a significant cold spot (Kowe et al., 2019).

High positive Z-score values above 1.96 are mainly concentrated in the area classified as pasture/grass in JBW between 1977 – 1991, 1991 – 2000, and 2000 – 2010 with a 99% confidence level. The accumulated frequency of hotspots in the watershed was mainly found in the upper -Northeast between 1977 and 1991 due to the pasture land cover classified in 1991. As a result, the soil erosion risk was higher in 1991 compared to 1977. However, between 1991 and 2000, statistically significant cold spots had negative Z-scores (< -1.65 and < -2.58) that were taking place due to forest recovery. On the other hand, both periods presented a significant few hot spot from 90% - 99% of confidence closer to the coast in the middle of the watershed. It is explained because of the topographic factor. In other words, it is the steepest area compared with the rest of the coast. Between 2000 and 2010, a significant cold spot was dominant in the upper Northeast because forests continued to recover. The significant hot spot remained in the mid-watershed, where pasture/grass is the predominant land cover. Pasture is more prone to erosion than forest, whereas it has steep slopes. During this time, a hot spot was also identified in cultivated lands at the west of the study area.

From 1977 to 2010, hot spots related to soil loss confirmed that pasture/grass in steep areas are more vulnerable to soil loss, and cultivated land placed very close to the coast is also vulnerable to soil erosion. Since no previous research recorded high frequencies of soil loss hotspots in JBW during this period or before, this study showed a relationship between the topographic, cover management factors and the erosion hot spot distribution. In areas where Getis-Ord Gi* values are significantly different from the surroundings, they are considered neither hot spots nor cold spots identified as insignificant in the hot spot analysis because they are non-vegetation (Kowe et al., 2019).

Figure 39

Hot Spot occurrence corresponded to different statistical confidence (99%, 95%, and 90%) between 1977 and 2010 in JBW.

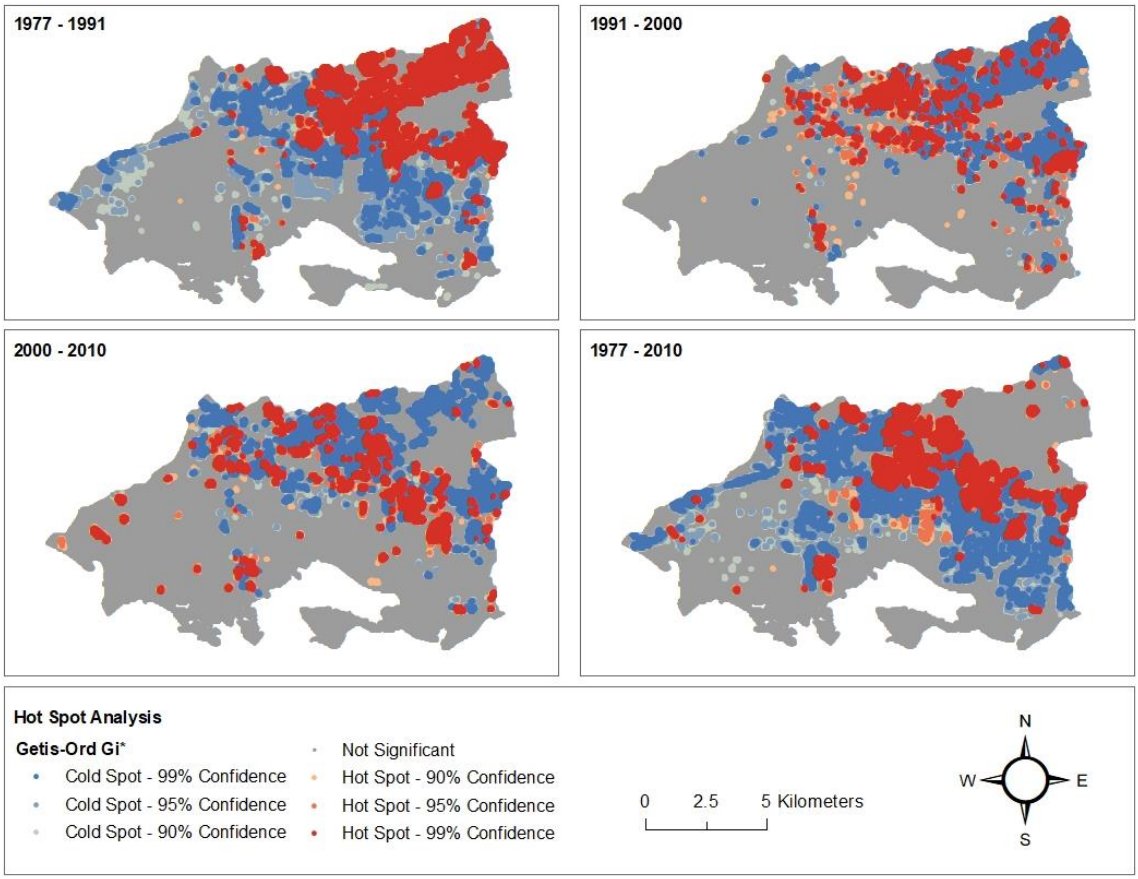

Discussion

The RUSLE is one of the most recognized erosion prediction models worldwide. The temporal and spatial patterns of soil erosion, rainfall erosivity, and land-use change from 1977 to 2010 were analyzed. However, the accuracy of RUSLE estimation depends on each factor's availability and quality of data. Therefore, the performance of available erodibility estimators thru RUSLE investigating the role of modified rainfall erosivity (R), soil erodibility (K), topographic factor (LS), and Cover Management Factor (C) on soil erosion in JBNERR were assessed.

The Factor R in RUSLE should be calculated using a maximum rainfall thirty minutes intensity (I_{30}), but only mean daily rainfall data were available for JBW from 1970 to 2015. Thus, this study used the Modified Rainfall Erosivity equation proposed by (Arnoldus, 1980) based on mean of monthly and annual precipitation. Another overcome limitation for Factor R calculations were the spatial distributions of the climatic stations over JBW. Only one station is located within the watershed and two climatic stations closest were conditioned by the data collection periods available to fulfill the research objectives. Nevertheless, a spatial IDW interpolation were performed given that the range of the average annual precipitation from these climatic stations were relatively small to lead discrepancies between interpolated and measured values. However, great validation resulted from the spatial regression analysis performed with the Factor R published by the Department of Commerce Department (DOC), NOAA, National Ocean Service (NOS), (2020). The model explained 99% of the variation within the data when regressed to R-Factor from NOAA. Therefore, the conversion factor was appropriate to estimate the annual rainfall erosivity factor.

The estimated R range from 7,834.8 to 8,408.3 MJ*mm/ha*h during 1970 to 2015. The highest R values represented an increase between 1970 and 2015. The R highest values between 1970 – 1984 was 8,237.63, between 1985 and 1999 was 8,281.41, between 2000 and 2009 was 8,408.27, and between 2010 and 2015 was 8,260.73 $MJ*mm*ha^{-1}*h^{-1}*y^{-1}$. However, the highest R-factor value was found between 2000 and 2009 because during this period more rainfall was registered compared to the other periods. The spatial variation of R increases following the Northeast to Northwest direction where the Rio Seco at the mouth is located, the steepest area of the watershed.

In addition, the station closest to the coast, Aguirre at 7.6 meters of elevation, represents the less rainfall erosivity resulting. In contrast, Guayama 2E station located at 21.9 meters of elevation ranked second, but Jajome station at 719.3 meters of elevation, the R-Factor, had the highest erosivity rainfall in every period. Nevertheless, a weak spatial variation of R was observed, which was provided from three stations for 45 years. In this sense, even when the Factor R was correct and the rainfall stations are located at different elevations, the spatial interpolation performed on precipitation data did not consider the topography of JBW. Even though data from this study does not reflect a significant rainfall variation among the three stations in 45 years, it does not mean that rainfall events in the 90th percentile cannot influence the soil erosion process.

The erodibility factor (K) is limited to the current data availability from the US Department of Agriculture, Natural Resources Conservation Service with the Soil Survey Staff to JBW as well as to Puerto Rico. The soil properties are associated with soils having low to moderate erodibility and low to moderate permeability in JBW. Overall, the surface texture with the greatest Factor K values is silty clay loam, then followed by the textures of sandy loam and clay loam. Since clay soils are unyielding to erode and sandy soils present higher permeability at which water percolates through the soil as a function of texture, structure, and composition allows to prevent soil loss.

The topographic factor was analyzed using the Digital Elevation Model (DEM) for Puerto Rico. This means that the Factor LS results were supported by the DEM accuracy and the cell size. In this study the best elevation source used was DEM has five (5) meters spatial resolution. From the topographic factor map, the slopes with the greatest steepness and the shortest slope length are located at the upper northwest at the

JBW. Because of the influence of different topographies, the flow accumulation and flow direction give insights into where deposition and where the soil erosion occurs. This LS-factor is concentrated between 0.03 the flatter zones and 1,920.23 the steeper zones, showing that erosion-reducing effects of shortening slopes or reducing slope gradients are accounted for through the LS factor as described by Wischmeier & Smith, (1978). Similar results were also reported by Jahun et al. (2015). The results also indicate that extended areas of steep slopes are prone to very high erosion than smaller extents, showing less proneness to erosion. But erosion rates are controlled by rainfall intensity, soil erodibility, slope, land cover, and management practices (Grau et al., 2003). In this sense, LULC considered on Factor C revealed important information to reject or accept that the steeper areas are more prone to erode.

The Cover Management Factor showed logical results after applying the averaged C values for each land-cover class, with a trend of increasing erosion with low vegetation. Considering that factor C is intended to reflect the effect of cropping and management practices on erosion rates, it is the most often used factor to compare the relative impacts of management options on conservation plans (Ndolo-Goy, 2015). As a result, the higher the vegetation the lower Factor C value, then greater Factor C values were set to cultivated lands class. Cultivated lands was located at the lower areas, pasture was found mainly at the center area, while forest was predominant at upper of JBW. These results suggest the possibility of higher soil loss closer to the estuarine waters because cultivated lands extension is very close to the coast. Since poor agriculture practices on cultivated lands are globally considered one of the major causes of land degradation, enhancing soil and threating coastal waters with inland pollutant (Harding et

al., 2014). Even though cultivated lands decreased from 1977 to 2000, they continue to be a significant extension of the area in JBW. According to Vijith et al. (2017) results the interpretation of distribution zones of high soil loss and vulnerability of terrain to erosion indicate that current land use practices are most influential in the RUSLE equation.

The forest is mainly found where the slopes are steeper, and rainfall activity was also greater near the upper. However, forest had the lowest Factor C value impacting the soil erosion risk classification. In sum, soil erosion is driven mainly by Factor C and is affected considerably by the Topographic Factor (LS) in JBW. Although, a Factor C limitation relies on the classification method accuracy used to derive the LULC rasters for JBW and if a refined classification methods are used to derive these LULC rasters, the annual average soil loss predicted in this study might be different. For example, it is hypothesized that if a refined classification method is applied for 1977 a higher soil loss rate should be expected because it has the biggest cultivated land area when compared with 1991, 2000 and 2010 LULC classes in JBW. Our results compare with Sharma et al. (2011) results where the transition of other LULC categories to cropland was most detrimental, while the forest was the most effective barrier to soil loss in an agricultural watershed in the tropical climate.

The implementation of soil and vegetation management (e.g., contour planting, no-till farming, and vegetative buffer strips) can reduce erosion by up to 99% (Labrière et al., 2015). In JBW, forest recovery from previous pasture as secondary forests would still be assets for conservation because in many instances, secondary forests provide conditions that help improve soil and water quality or which conserve genetic material, nutrients, moisture and/or soil organic matter (Brown & Lugo, 1990). Therefore,

considerable applied research on erosion control techniques has been done in the US and elsewhere. It can be grouped into two broad categories: (1) soil management techniques that improve infiltration rate, and (2) runoff management techniques that permit safe management/removal of surplus runoff (Lal, 1998). Also, Abdulkareem et al. (2019) to (1) proper protection and maintenance of previously installed temporary control measures when carrying out land clearing and grading, (2) during land clearing, smaller areas should be cleared and graded at a time giving emphasis on the potential erodibility of the soil in the location as well as the time it will take to stabilize the area upon completion of grading, (3) the dry season should be targeted as the best period for land clearing as well as soil cultivation and conservation practices should be employed instantly after land clearing, and (4) cleared vegetation and debris should never be deposited nor dumped in water bodies among other soil conservations and soil erosion control strategies.

Therefore, after calculating the different erosion factors, the estimated average annual soil loss ranges from 9.76 in 1977 to 8.72 in 2010 ton/ha/y being the year 2010 the smallest average soil loss rate. These results compared with partially urbanized (Coral Bay) and an undisturbed (Lameshur) coastal watershed in St. John, US Virgin Islands (USVI), where only 8.4 metric tons of soil loss from the Coral Bay watershed, and only 2.1 metric tons of soil loss for Lameshur Bay were modeled by RUSLE (Gudino-Elizondo et al., 2019). Gudino-Elizondo et al., (2019) that rural urbanization has important effects on stream flow composition and sediment yield in dry-tropical coastal watersheds because the human influence can be related to deforestation activities and the dissolutions of urban-derived materials such as industrial paint, asphalts, among others

construction materials. Hence, it is important to discuss RUSLE spatial variation of soil loss per year over JBW.

The predicted soil erosion rate variability from 1977 to 1991 in areas where pasture significantly increased in the upper and steeper areas. These results suggest that JBW has a slight to moderate potential soil loss in areas closer to the coast. This compares to the results of Williams et al., (2011), where JBW presented a higher erosivity potential that may cause more soil to be detached on steeper slopes and facilitate its transport from the watershed area. Similarly, these results are consistent with those obtained from other tropical watersheds of similar environmental characteristics investigated in Puerto Rico using the RUSLE model (López et al., 1998; Santiago, 2014; Williams et al., 2011). In the study was of López et al., (1998), the median rate of soil erosion in polygons of different land uses decreased in the following pattern: bare soil > open canopy forest > agriculture > pastures > less dense urban > closed-canopy forest > dense urban in Guadiana watershed.

In contrast, the study of Millward & Mersey (1999), the soil erosion rate estimated by RUSLE in tropical mountain watershed in Mexico presented extreme rate (~100 t/ha/y) during the wet season. Panagos et al. (2015) produced a soil erosion map for entire countries of the European Union and it was noted that the estimated soil loss rate varies from 0 to over 50 t/ha/y based on the terrain, vegetation and rainfall conditions existing in each country. Basically, tropical wet and dry climate is prevailing between 5° and 20° latitudes and receives less rainfall (Ghosal & Das Bhattacharya, 2020). Mainly in this type of climatic zone, rainfall occurs in a particular (i.e. single) season but the rest of the seasons becomes dry (Ghosal & Das Bhattacharya, 2020). The Erosion Vulnerability

Index (EVI) in the tropics showed a high risk categories occur throughout most of Southeast Asia, along the northern Andes, in the Caribbean and through most of Central America due to Agriculture, Grazing, Mining, and Development Risk Factors (Browning & Sawyer, 2021).

The comparison with soil erosion rates estimated in JBW and other parts of the world indicates the differential influence of various parameters on the rate of soil loss. Vijith et al. (2017) argues that it has been found that tropical regions which undergo severe terrain modifications in connection with plantation activities and timber logging become more vulnerable to erosion and can become hot spots for sediment production. Morgan (2005) argues that 10 ton/h/y is an appropriate boundary measure of soil loss over which agriculturists should be concerned. This categorization (slight to very high) is consistent with the model's role as a conservation management tool, where relative comparisons among land areas are more critical than assessing the absolute soil loss in a particular cell (Millward & Mersey, 1999). Other studies argues that although that a soil loss of 1 ton/y or less is considered tolerable soil erosion rate and in tropical areas the rate of soil formation is generally slow, a soil loss greater than 1 ton/h/y is regarded as irreversible soil erosion (Abdulkareem et al., 2019; Khosrokhani & Pradhan, 2014).

This study presented an increase of the area having slight annual soil erosion risk (< 2.5 ton/h/y) from 52.9% in 1977 to 70.3% in 2010. While areas having with high soil erosion risk (15 – 25 ton/h/y) decreased from 5.8% in 1977 to 2.1% in 2010. However, areas detected as very high soil erosion risk remained similar from 8.3% in 1977 to 8.8% in 2010. But special attention should point out in 1991 and 2000 where high and very high erosion risk summed 19.9 % and 14.5% and 10.9% in 2010. However, previous

studies found that sugarcane crops worsens the soil loss more than plantains crops giving a major C value to sugarcane (Armour et al., 2009; Medeiros et al., 2016; Morgan, 2005). In JBW sugarcane were taking place in 1991 and after 1993 the abandoned cultivated lands might affect the soil erosion until 2000 due to a lack of soil conservation practices. Vijith et al. (2017) argues that close examination of the spatial pattern of soil erosion vulnerable zone shows clustering particularly for the very high and critical soil erosion zones with some clusters being linear. Clustering of high and critical soil erosion zones is more common in the lower parts of the basin than the upper regions (Vijith et al., 2017), contrary to JBW.

Few recent studies analyze the results of soil loss by ordinal categories. However, a hot spot analysis by Getis-Ord Gi* is owing to the importance of LULC and the topographic factor influence on soil erosion process. The findings of hot spot analysis indicate and support the strong tendency for homogeneous areas such as forest and pasture to be spatially clustered. The results also suggest that areas with high soil loss risk are presented with the highest-level confidence hot spot and vice versa. This hot spot analysis helps understand where the areas are vulnerable to eroding spatially. Some studies suggest that Hot Spot Analysis by Getis-Ord Gi* promotes future work that could address the dynamics associated with gradual land transformations, such as urbanization, land cover changes, land degradation, and landscape fragmentation analysis (Abdulhafedh, 2017; Kowe et al., 2019; Mora et al., 2019). The most important result from the hot spot analysis is that there is no temporal either spatial consistency or that is because LULC classes areas where not consistent through the time. Thus, JBW as a tropical watershed naturally have a high risk to erosion, which is exacerbated by land use

change as argued by Browning and Sawyer, (2021). Tropical watersheds naturally have a high risk to erosion, which is exacerbated by land use change (Browning & Sawyer, 2021). As well as the tropical regions are prone to high erosion rates due to their consistently warm climate and prevalent rainfall both seasonally (higher latitudes) and year-round (near the equator) (Browning & Sawyer, 2021; Harding et al., 2014). For example, in terms of erosion and sediment transport the landscape is in a quasi-steady state from frequent disturbance by landslides or that the response to large disturbances like hurricanes as found in at Río Icacos at the east of Puerto Rico (Shanley et al., 2011). Río Icacos is a relatively pristine forested watershed with such a low channel gradient (Shanley et al., 2011), contrary to JBW which is a relative agricultural watershed. Therefore, this approach is essential to appreciate the model's predictive capabilities and identify where areas should be prioritized to implement best management practices.

Conclusion

This study used a GIS-based classic RUSLE model supported with Hot Spot Analysis by Getis-Ord Gi* statistic to map erosion hotspot areas in JBW. By analyzing soil erosion rates and soil loss risk in JBW in the past forty-six years, this study has shown how the cover management and topographic factors can, directly and indirectly, provides an insight into the cultivated land conversion. Furthermore, since cultivated lands presented moderate soil erosion risk, future pressure to expand agriculture within JBW might accentuate the rate of soil erosion. Based on this conclusion, future work on predicting and tracking cultivated land changes related to water and soil conservation should consider the soil type pattern and land use adjustment at the regional scale of soil conservation. Further research is needed for a more in-depth assessment and analysis to understand the relationship between soil erosion in upland areas and sedimentation in

Jobos Bay Estuary when extreme rainfall events occur (e.g., hurricanes, tropical storms). To that a sensitivity analysis about the Cover Management Factor (C factor), run the RUSLE model one standard deviation above the mean and one standard deviation below the mean are approaches to enhance the empirical model soil loss results. In addition, another recommendation is to summarize the RUSLE model for different regions and/or for LULC classes to have a more precise spatiotemporal soil loss appreciation. A deeper understanding will lead to employing conservation practices in the watershed and understanding the relationship between soil loss and its adjacent aquatic ecosystems' impact.

Concluding Remarks

Jobos Bay National Estuarine Research Reserve impacted by human activities, population increased from 1990 to 2010, land changes as growth in urban development because of conversion of cultivated lands to commercial or residential areas, and the preexistence industrial activities can potentially affect the soil erosion process in JBW. Since soil erosion is the response of the combination of climatic and physical factors, as well as the influence of the topographic factor and LULCC aspects, where LULCC is a consequence of human activities. This research has addressed several issues related to the accuracy and efficiency of dasymetric mapping methods, LULCC analysis throughout Transition Matrix methods, and on the Revised Universal Soil Loss Erosion equation model using pre-classified raster land cover dataset.

In Chapter I, I compared the performances of the IDM estimation model using the U.S. Census Bureau 1990, 2000, and 2010 census blocks population and housing count data and areas of the LULC classes in 1991, 2000, and 2010 respectively. In JBW the population and housing density value of each land cover were obtained in the three-class method. The IDM has shown to be a robust and effective method for enhancing areal interpolation and population mapping as reported in this chapter and other research (Fisher & Langford, 1995; Fisher & Langford, 1996b), but demands additional efforts based on geographic standardization. The IDM must further enhance its performance by overcoming its geographic delimitation differences when two or more censuses are used and facilitating comparison analysis. Then, it should recognize that there is a chance of inaccuracy in the census enumeration units, including errors in the satellite imagery process, or the population counts process might not be exact, impacting the performance of the proposed methods. Future research should address a common situation researchers

face using census data discrepancies in the boundaries of reporting units from a previous decennial census to another.

On the other hand, the accuracy of this method depends on how well the LULC data were classified. In this sense, our study could not delimit population and housing counts by residential land cover class because the land data classification was pre-classified as urban areas (including commercial, industrial, and residential areas). Thus a correct identification of residential areas in the satellite image should enhance the IDM mapping results. Another limitation to consider is using Land cover data with residential areas classification. If areas that are not residential are classified as residential, it will lower the mean population housing density of all residential areas contained within the source unit. To that, it is highly recommended to integrate land use data and validate the land uses in the field if possible. This recommendation will avoid the population and housing distribution from being placed in areas where it should not be present. Otherwise, higher accuracy in LULC classification is a desirable goal.

On the other hand, it is assumed that population densities are uniform among pixels of the same LULC class within each source unit, in this research, census block. As a result, abrupt changes of population density can be found at borders of source zones and those between different land use land cover (Kim, 2009). Therefore, the contrast of population density between two adjacent pixels with different land use land cover classes is mistakenly exaggerated (Kim, 2009). Two adjacent residential pixels may have much different population density values if those pixels fall into different source units because the binary dasymetric method does not account for the neighborhood effect (Kim, 2009). For example, one of the communities in JBW, Barrio Aguirre, is a residential area that

also contained a power energy plant and the Department of Natural Resources and Environment (DRNA, in Spanish), thus the population and even the housing densities cannot be uniform within the geographic (source) unit.

Moreover, IDM is considered one of the best methods used to generate a surface model that provides a more accurate representation of population. The accuracy in this study ranges from the MAE results, showed that population in 2010 was overestimated, particularly the blocks with larger geographical areas (e.g., blocks in the forest or pasture cover classes). Meanwhile, in 1990 and 2000 the population estimates were accurately calculated and distributed in the census blocks using the LULC re-classified images. The MAE for the housing units estimate was 0.03 in 1990, 0.04 in 2000, and 0.05 in 2010, showing the same situation in population estimates. Hence, a geographic unit standardization based on 2010 are recommended to make comparisons and further trends can be analyzed by integrating the Census 2020 population and housing data. According to Census 2020, total population decreased in Puerto Rico from 2010 to 2020. It is expected to see a population decreased within Jobos Bay Watershed Guayama is the fifth municipality with the highest population loss with 19.3% between 2010 and 2020. To that, it is highly recommended to analyze the sociodemographic characteristics and housing vacancy status to have a better understanding on anthropogenic activities taking place in the study area. Even more importantly investigate how the local community knowledge enriched the IDM results using LULC data as ancillary data. Consequently, a profound understanding on the sociodemographic and economic factors involved in land change processes is desired.

The LULC change explanations rely not only on socioeconomic activities but also on the environmental factors that play an important role, especially in forest recovery. The LULC at JBW has gone through changes like in urban development and corresponding conversion of agricultural lands to commercial, industrial, or residential areas as seen in Chapter 3. The land change trends in the watershed showed forest recovery and cultivated land conversion despite the significant importance as an agricultural watershed and as a natural reserve. The forest growth occurred as secondary forest from previous pastureland in the area. According to previous studies, secondary forest cover has increased in many tropical regions due to socioeconomic changes and abandonment of agricultural land and pastures (Flynn et al., 2010; Hecht & Saatchi, 2007; Rudel et al., 2000). The cultivated lands mostly decreased in the first two periods, 1977 – 1991 and 1991 – 2000, while urban areas were increasing as part of an economic shift in Puerto Rico.

Even when this study did not analyze how the land change trends and major environmental events like hurricane disturbance interact to determine the structure and composition of forests, it is recognized as part of the global driver of land changes. Future work is recommended to explore how hurricanes and land-use history impact forest recovery and the land in transitions due to the abandonment of agricultural land and pastures. In Puerto Rico, from 1991 to 2000, the island faced the following hurricanes: Hurricane Marilyn in 1995, Hurricane Hortense in 1996, and Hurricane Georges in 1998 (Metro de Puerto Rico, 2017). From 2000 to 2010, Hurricanes Frances in 2004, and Earl in 2010. After 2010, the major hurricanes were Hurricane Irma and Hurricane María, both in 2017. However, the secondary forests increase even if trees are

severely damaged, as occurs during storms or logging, because many species can resprout (Chazdon, 2003). Equally, studies on the effects of land-use history and hurricane disturbance on forest structure, composition, and recovery require long- term data sets, which span a broad range of land-use histories, since the space-for-time substitution do not necessarily predict the rate of change in forest dynamics (Chazdon et al., 2007; Flynn et al., 2010; Johnson & Miyanishi, 2008).

The most extensive form of major disturbance in JBNERR is the forest. At an islandwide scale, urbanization may reinforce forest expansion, because migration into urban areas is the main driver of land abandonment and subsequent forest regeneration (Grau et al., 2003). At a local scale, however, particularly in areas adjacent to the most intensively urbanized areas, an opposite pattern emerges: Low-density residential use invades forest (Grau et al., 2003). In addition, urban expansions occur over the most productive agricultural areas, a process that greatly reduces the island's capacity to re-adapt to an economy less dependent on external food sources (Grau et al., 2003).

This chapter has demonstrated the complexity of land changes analysis, to understand the demographics trends and further soil erosion risk at JBW. To support the observations made by Whitall et al., (2011), that even the great extension of vegetated lands may lead to the inaccurate conclusion that the JBW is a relatively pristine system. Recognizing that the current land change models are hampered by limited knowledge of the historical precedence for events (Runfola & Pontius, 2013). There are limitations to considered in future work regarding the classification systems for satellite images. This study used Landsat TM classified images. Even when the advantages of using classified land-cover images bring reducing the data volume, increasing computational efficiency,

strengthening representation of watersheds, and being able to employ data products in different scales (Wang, 2009). Additionally, land cover classification is also greatly facilitated by field work and supporting information such as other project results, research studies, soil surveys, crop information, topographic information, digital elevation models, or other land cover information or imagery (Lopez & Frohn, 2018). That means that the classification of land can be urban development, roads, water, forest, wetland, or bare land, was based on the prior investigator interests. Thus, it is recommended to apply or develop a LULC unsupervised or supervised classification system that specifically supports study objectives and to be compatible among different maps for specific time. The benefit of the LULC classification is construct history trends and changes by photographs or images of hydrological, vegetational, soil condition, or human activity data can be interpreted effectively (Lopez & Frohn, 2018). Therefore, in terms of land changes and demographics results, tackling the above-mentioned challenges and drifting the effects requires a great effort to know where intensity changes were shown, how changes occurred and why changes occurred. This was key to recognizing how soil erosion was responding to land changes in JBW.

In this sense Chapter 4 presents a soil erosion model in JBW for 1977, 1991, 2000, and 2010 through the Revised Soil Loss Equation (RUSLE) model. RUSLE was extended to determine soil erosion rates (in units of mass per area and time) under a large range of daily rainfall (1970 – 2015) and LULC data. Soil erosion is the response of the combination of climatic and physical factors, as well as the influence of the topographic factor and LULC changes, where LULC change might be in part a consequence of human activities. There is a significant contribution of this chapter because little research has

been done to quantitatively investigate the different demographic dynamics and biophysical drivers on LULCC and estimate the soil erosion rates over JBNERR area.

In JBW the predicted soil erosion rate variability from 1977 to 1991 in areas where pasture significantly increased in the upper and steeper areas. These results suggest that JBW has a slight to moderate potential soil loss in areas closer to the coast. JBW presented a higher soil loss risk on steeper slopes that cause more soil to be detached and facilitate its transports from the watershed area. However, the steepest area in the watershed was classified as forest, thus the mid-watershed area was mainly pasture and that area is steeper where cultivated lands are located. These results were consistent with those obtained from other tropical watersheds of similar environmental characteristics investigated in Puerto Rico using the RUSLE model (López et al., 1998; Santiago, 2014; Williams et al., 2011). The study of (López et al. (1998) found that the median soil erosion rates varied among the seven land uses decreasing in the following descending pattern: bare soil, open canopy forest, agriculture, pastures, less dense urban, closed-canopy forest, dense urban in Guadiana watershed.

Nonetheless, few recent studies analyze the results of soil loss through a hot spot analysis by Getis-Ord Gi*. This approach owing to the importance of LULC, and the topographic factor influence on soil erosion process and supports the strong tendency for homogeneous areas such as forest and pasture to be spatially clustered. The results also suggest that areas with high soil loss risk revealed by the RUSLE model are presented with the highest-level confidence hot spot and vice versa. Thus, the hot spot analysis helped to understand where the areas are more susceptible to spatially erode. Since some studies suggest that Hot Spot Analysis by Getis-Ord Gi* promotes future work associated

with land changes such as urbanization, land degradation due to high erosion rates (Abdulhafedh, 2017; Kowe et al., 2019; Mora et al., 2019) because this approach is essential to appreciate the model's predictive capabilities and identify where areas should be prioritized to implement best soil conservations and management practices.

Based on the argument that major anthropogenic drivers of erosion are land use and potentially climate change is occurring, both in a more intense precipitation and changes in air temperature (Borrelli et al., 2020; O'Neal et al., 2005; Yang et al., 2003). In addition, more in-depth assessment and analysis will be required to better understand the relationship between soil erosion in upland areas and how the estuary may be impacted when extreme rainfall events occur (e.g., hurricanes, tropical storms) (Williams et al., 2011). Thus, increases in soil erosion due to climate change are mainly induced by precipitation increase. Potential increases in rainfall erosivity may have the greatest impact by exacerbating effects of desertification, and poor land use practices on runoff and erosion (Edwards et al., 2019).

In terms of the global mean, changes in soil erosion in the 2090s are projected to increase by about 9% due to climate and about 5% due to land use (Belay & Mengistu, 2021; Yang et al., 2003). When the combined effect of LULC and climate change considered, the average annual soil loss rate was increased by 13.2% and 15.7% under different climate scenarios, respectively, which is much higher than the individual effects of LULC and climate change (Belay & Mengistu, 2021). In an urban setting, managers use different Best Management Practices (BMPs) to reduce and/or filter pollutants from stormwater runoff (Johnson et al., 2022). In agricultural areas, multiple practices are generally used together in conservation practice systems to conserve natural resources

and to abate pollutant losses from the landscape (Johnson et al., 2022). In forested areas, BMPs typically focus on reducing runoff and pollutant loads associated with silvicultural activities (Johnson et al., 2022).

Therefore, an increase in soil loss due to climate changes can affect the watershed's local ecosystems and can cause hydrological changes in streams originating from the watershed (Belay & Mengistu, 2021). Besides projections showing the complexity that soil erosion increases in the densest population areas due to land-use changes, also climate change induces a different pattern of erosion change (Yang et al., 2003). Because climate change is, expected on water quality and water temperatures, where both are likely to increase. In many areas of the US, changes in nonpoint loading of nutrients, sediment, and other pollutants from upland sources to water bodies will vary across locations and are closely linked to changes in precipitation (Johnson et al., 2022).

In Puerto Rico a climate change projection of 100-year (2000–2100) and a hydrologic analysis focused on the driest and wettest months of the year (i.e., February and September, respectively) in Puerto Rico (Harmsen et al., 2009). The results from this study are consistent with other studies which indicate that the rainy season will become wetter and the dry season will become drier in the tropical zones (Harmsen et al., 2009). The precipitation deficit during the dry season and relative crop yield reduction for a generic crop under climate change conditions, the agricultural sector's demand for water will increase because of the low soil moisture, which may lead to conflicts in water use (Harmsen et al., 2009). Relative crop yield reduction decreased during September and was associated with increasing precipitation excess (Harmsen et al., 2009). Hence, rainfall and soil properties are important generators of geologic soil erosion, human

activities can accelerate this natural process, by increasing soil loss from an area (Williams et al., 2011). At the global scale, changes in land surface properties associated with changes in vegetation can have impacts on continental and global atmospheric circulation, with possible large impacts on regional and continental climate (Verburg et al., 2011). Climate change will exacerbate the existing soil erosion problem and would need for vigorous proper conservation policies and investments to mitigate the negative impacts of climate change on soil loss (Belay & Mengistu, 2021). Understanding the potential impacts of projected climate change on soil erosion is critical for developing forward-looking, sustainable land management practices for these high-value coastal ecosystems (Edwards et al., 2019).

Hence, predicting the impact of future climate and LULC changes on soil erosion is very important to design appropriate land use planning and adaptation and mitigation measures under local and regional scales (Belay & Mengistu, 2021). This research project can be used as an educational instrument for the Puerto Rican community's education initiatives in JBW as well as the coastal managers use LULC data and maps to better understand the impacts of a natural phenomenon and human uses of the land. Maps and models can help managers assess urban growth and model water quality issues (NOAA, 2015). The results demostrate areas of high susceptibility to soil loss in response to climate and land changes providing quantitative outputs of expected housing units and human population distribution and densities, LULCC and soil erosion rates. Then it is recommended to continue to forest conservation in steeper upper and lowland coastal areas is key to decrease soil loss rates in any agricultural watershed preventing that major sedimentation loads and terrestrial pollutants reaches the estuaries. Forests reduce storm

runoff due to high rates of canopy interception (of precipitation) coupled with higher infiltration rates, and roots' stabilizing effects make the soil less vulnerable to erode (Johnson et al., 2022). On the other hand, in a landscape, systems of practices can reduce local and downstream pollution deliver where many practices function via physical, chemical, and biological processes that are dependent on weather and climate (Johnson et al., 2022). Similarly, selection of appropriate herbaceous species to maintain a healthy, vigorous ground cover will be effective in reducing surface erosion (Basher et al., 2012).

Therefore, the analyses applied in this research serve as tools to explore the complexity of social-ecological systems by integrating knowledge, theories, and approaches from different disciplines to evaluate possible scenarios developed with data mediate demographics. Likewise, the analyses provided knowledge advancement about tropical estuarine ecosystem and a new perspective to the Environmental Sciences research field with broad relevance to human impacts on coastal ecosystems. The research contributed to determining the magnitude of human population dynamics and land changes on soil loss and provided a baseline for assessing future actions by implementing sustainable land management practices and human uses of the landscape in JBNERR. In addition, it contributed to understanding the impact of land use in estuarine ecosystems and the effect they could have in a climate change scenario and contributed significantly to the advancement of coastal management.

Literature cited

Abdulhafedh, A. (2017). A Novel Hybrid Method for Measuring the Spatial Autocorrelation of Vehicular Crashes: Combining Moran's Index and Getis-Ord G_i[*] Statistic. *Open Journal of Civil Engineering*, *07*(02), 208–221. https://doi.org/10.4236/ojce.2017.72013

Abdulkareem, J. H., Pradhan, B., Sulaiman, W. N. A., & Jamil, N. R. (2019). Prediction of spatial soil loss impacted by long-term land-use/land-cover change in a tropical watershed. *Geoscience Frontiers*, *10*(2), 389–403. https://doi.org/10.1016/j.gsf.2017.10.010

Abel, J. R., & Deitz, R. (2014). Second District Highlights Las causas y consecuencias del descenso poblacional en Puerto Rico. *Current Issues in Economics and Finance*, *20*(4), 1–8. www.newyorkfed.org/research/current_issues

Aide, T. Mitchell, Zimmerman, J. K., Herrera, L., Rosario, M., & Serrano, M. (1995). Forest recovery in abandoned tropical pastures in Puerto Rico. *Forest Ecology and Management*, *77*(1–3), 77–86. https://doi.org/10.1016/0378-1127(95)03576-V

Aide, T.M., & Cavelier, J. (1994). Barriers to tropical lowland forest restoration in the Sierra Nevada de Santa Marta, Colombia. *Restoration Ecol.*, *2*, 219–229.

Aksoy, H., & Kavvas, M. L. (2005). A review of hillslope and watershed scale erosion and sediment transport models. *Catena*, *64*(2–3), 247–271. https://doi.org/10.1016/j.catena.2005.08.008

Almagro, A., Thomé, T. C., Colman, C. B., Pereira, R. B., Marcato Junior, J., Rodrigues, D. B. B., & Oliveira, P. T. S. (2019). Improving cover and management factor (C-factor) estimation using remote sensing approaches for tropical regions. *International Soil and Water Conservation Research*, *7*(4), 325–334. https://doi.org/10.1016/j.iswcr.2019.08.005

Almas, M., & Jamal, T. (1999). Use of RUSLE for Soil Loss Prediction During Different Growth Periods. *Pakistan Journal of Biological Sciences*, *3*(1), 118–121. https://doi.org/10.3923/pjbs.2000.118.121

Alo, C. A., & Pontius, R. G. J. (2008). Identifying systematic land-cover transitions using remote sensing and GIS: the fate of forests inside and outside protected areas of Southwestern Ghana. *Environment and Planning B: Planning and Design* , *35*, 280–295. https://doi.org/10.1068/b32091

Anaya, A. A., & Colon, E. J. (2014). *Erosión de suelo y mapa de riesgo para la cuenca del Río Grande de Añasco , Puerto Rico Erosión de suelo y mapa de riesgo para la cuenca del Río Grande de Añasco , Puerto Rico*. *February*, 0–8.

Angulo-Martínez, M., López-Vicente, M., Vicente-Serrano, S. M., & Beguería, S. (2009). Mapping rainfall erosivity at a regional scale: A comparison of interpolation methods in the Ebro Basin (NE Spain). *Hydrology and Earth System Sciences*,

13(10), 1907–1920. https://doi.org/10.5194/hess-13-1907-2009

Aouichaty, N., Bouslihim, Y., Hilali, S., Zouhri, A., & Koulali, Y. (2021). Influence of DEM resolution on the RUSLE model: Case of abandoned quarries in Settat province (Morocco). *E3S Web of Conferences*, *314*, 04004. https://www.e3s-conferences.org/articles/e3sconf/abs/2021/90/e3sconf_wmad2021_04004/e3sconf_wmad2021_04004.html

Apeti, D. A., Whitall, D. R., Pait, A. S., Dieppa, A., Zitello, A. G., & Lauenstein, G. G. (2012). Characterization of land-based sources of pollution in Jobos Bay, Puerto Rico: Status of heavy metal concentration in bed sediment. *Environmental Monitoring and Assessment*, *184*(2), 811–830. https://doi.org/10.1007/s10661-011-2003-0

Arce-Nazario, J. A. (2016). Translating land-use science to a museum exhibit. *Journal of Land Use Science*, *11*(4), 417–428. https://doi.org/10.1080/1747423X.2016.1172129

Armour, J. D., Hateley, L. R., & Pitt, G. L. (2009). Catchment modelling of sediment, nitrogen and phosphorus nutrient loads with SedNet/ANNEX in the Tully - Murray basin. *Marine and Freshwater Research*, *60*(11), 1091–1096. https://doi.org/10.1071/MF08345

Arnoldus, J. M. J. (1980). An approximation to the rainfall factor in the universal soil loss equation. In J. Wiley (Ed.), *Assessment of ersoion* (pp. 127–132). Chichester [Eng.], Boodt, M. de., Gabriels, D.

Asis, A. M., & Omasa, K. (2007). Estimation of vegetation parameter for modeling soil erosion using linear Spectral Mixture Analysis of Landsat ETM data. *Journal of Photogrammetry & Remote Sensing*, *62*, 309–324. https://doi.org/0.1016/j.isprsjprs.2007.05.013

Ayala, C. J. (1994). La nueva plantacion antillana (1898-1934). *OP. CIT. Revista Del Centro de Investigaciones Históricas de La Universidad de Puerto Rico, Recinto de Rio Piedras*, *8*, 121–165.

Basher, L., Douglas, G., Elliott, S., Hughes, A., Jones, H., McIvor, I., Page, M., Rosser, B., & Tait, A. (2012). *Impacts of climate change on erosion and erosion control methods – A critical review* (Vol. 4, Issue November). https://www.mpi.govt.nz/document-vault/4074

Batar, A. K., Watanabe, T., & Kumar, A. (2017). Assessment of land-use/land-cover change and forest fragmentation in the Garhwal Himalayan region of India. *Environments - MDPI*, *4*(2), 1–16. https://doi.org/10.3390/environments4020034

Belay, T., & Mengistu, D. A. (2021). Impacts of land use/land cover and climate changes on soil erosion in Muga watershed, Upper Blue Nile basin (Abay), Ethiopia. *Ecological Processes*, *10*(1). https://doi.org/10.1186/s13717-021-00339-9

Berihun, M. L., Tsunekawa, A., Haregeweyn, N., Meshesha, D. T., Adgo, E., Tsubo, M., Masunaga, T., Fenta, A. A., Sultan, D., & Yibeltal, M. (2019). Exploring land use/land cover changes, drivers and their implications in contrasting agro-ecological

environments of Ethiopia. *Land Use Policy*, *87*(May), 104052. https://doi.org/10.1016/j.landusepol.2019.104052

Beskow, S., Mello, C. R., Norton, L. D., Curi, N., Viola, M. R., & Avanzi, J. C. (2009). Soil erosion prediction in the Grande River Basin, Brazil using distributed modeling. *Catena*, *79*(1), 49–59. https://doi.org/10.1016/j.catena.2009.05.010

Bhatta, B. (2010). Avances in Geographic Information Science. Analysis of Urban Growth and Sprawl from Remote Sensing Data. In S. Balram & S. Dragicevic (Eds.), *Egyptian Journal of Remote Sensing and Space Science*. Springer. https://doi.org/10.1007/978-3-642-05299-6

Birdsey, R. A., & Weaver, P. L. (1987). *Forest Area Trends in Puerto Rico* (pp. 1–5). Res. Note SO-331, US Forest Service. https://www.srs.fs.usda.gov/pubs/rn/rn_so331.pdf

Bonilla, C. A., Reyes, J. L., & Magri, A. (2010). Water Erosion Prediction Using the Revised Universal Soil Loss Equation (RUSLE) in a GIS Framework, Central Chile. *Chilean Journal of Agricultural Research*, *70*(1), 159–169. https://doi.org/10.4067/s0718-58392010000100017

Borrelli, P., Robinson, D. A., Panagos, P., Lugato, E., Yang, J. E., Alewell, C., Wuepper, D., Montanarella, L., & Ballabio, C. (2020). Land use and climate change impacts on global soil erosion by water (2015-2070). *Proceedings of the National Academy of Sciences of the United States of America*, *117*(36), 21994–22001. https://doi.org/10.1073/pnas.2001403117

Brandeis, T. J., Escobedo, F. J., Staudhammer, C. L., Nowak, D. J., & Zipperer, W. C. (2014). *San Juan Bay Estuary Watershed Urban Forest Inventory. General Technical Report SRS–190.* www.srs.fs.usda.gov

Briggs, D. J., Gulliver, J., Fecht, D., & Vienneau, D. M. (2007). Dasymetric modelling of small-area population distribution using land cover and light emissions data. *Remote Sensing of Environment*, *108*(4), 451–466. https://doi.org/10.1016/j.rse.2006.11.020

Brown, D. G., Johnson, K. M., Loveland, T. R., & Theobald, D. M. (2005). Rural land-use trends in the conterminous United States, 1950-2000. *Ecological Applications*, *15*(6), 1851–1863. https://doi.org/10.1890/03-5220

Brown, S., & Lugo, A. E. (1990). Tropical secondary forests. *Journal of Tropical Ecology*, *6*(1), 1–32. https://doi.org/10.1017/S0266467400003989

Browning, T. N., & Sawyer, D. E. (2021). Vulnerability to watershed erosion and coastal deposition in the tropics. *Scientific Reports*, *11*(1), 1–11. https://doi.org/10.1038/s41598-020-79402-y

Buschbacher, R. J. (1986). Pasture Tropical Deforestation Development We can still conserve and rationally develop the largest remaining region of intact tropical forest. *American Institute of Biological Sciences*, *36*(1), 22–28.

Carter, M. R., Burns, L. A., Cavinder, T. R., Dugger, K. R., Fore, P. L., Hicks, D. B., Revells, H. L., Schmidt, T. W., & Agency, U. S. E. P. (1973). *Ecosystems analysis*

of the Big Cypress swamp and estuaries. http://www.science.fau.edu/biology/gawliklab/papers/CarterMRetal1973.pdf

Castro-Prieto, J., Martinuzzi, S., Radeloff, V. C., Helmers, D. P., Quiñones, M., & Gould, W. A. (2017). Declining human population but increasing residential development around protected areas in Puerto Rico. *Biological Conservation*, *209*, 473–481. https://doi.org/10.1016/j.biocon.2017.02.037

Center for Watershed Protection. (2008). *Guánica Bay Watershed Management Plan. A Pilot Project for Watershed Planning in Puerto Rico.*

Centro de Periodismo Investigativo. (2022, January 31). *Puerto Rico vive una acelerada aprobación de permisos de construcción en la costa - Ojo al Clima*. https://ojoalclima.com/puerto-rico-vive-una-acelerada-aprobacion-de-permisos-de-construccion-en-la-costa/

Chazdon, R. L. (2003). Tropical forest recovery: Legacies of human impact and natural disturbances. *Perspectives in Plant Ecology, Evolution and Systematics*, *6*(1–2), 51–71. https://doi.org/10.1078/1433-8319-00042

Chazdon, R. L., Letcher, S. G., Breugel, van M., Martínez-Ramos, M., Bongers, F., & Finegan, B. (2007). Chadzon et al 2007.pdf. *Phil. Trans. R. Soc.*, *362*, 273–289.

Chokkalingam, U., & De Jong, W. (2001). Secondary forest: A working definition and typology. *International Forestry Review*, *3*(1), 19–26.

Clark, M. L., Aide, T. M., & Riner, G. (2012). Land change for all municipalities in Latin America and the Caribbean assessed from 250-m MODIS imagery (2001-2010). *Remote Sensing of Environment*, *126*, 84–103. https://doi.org/10.1016/j.rse.2012.08.013

Coto, D., & Los Angeles Times. (2022, May 6). Combaten en PR construcción de viviendas en zonas prohibidas - Los Angeles Times. *Los Angeles Times*. https://www.latimes.com/espanol/internacional/articulo/2022-05-06/combaten-en-pr-construccion-de-viviendas-en-zonas-prohibidas

de Carvalho, D. F., Durigon, V. L., Antunes, M. A. H., de Almeida, W. S., & de Oliveira, P. T. S. (2014). Predicting soil erosion using Rusle and NDVI time series from TM Landsat 5. *Pesquisa Agropecuaria Brasileira*, *49*(3), 215–224. https://doi.org/10.1590/S0100-204X2014000300008

De Mello, C. R., Viola, M. R., Owens, P. R., De Mello, J. M., & Beskow, S. (2015). Interpolation methods for improving the RUSLE R-factor mapping in Brazil. *Journal of Soil and Water Conservation*, *70*(3), 182–197. https://doi.org/10.2489/jswc.70.3.182

de Mello, Carlos Rogério, Norton, L. D., Pinto, L. C., Beskow, S., & Curi, N. (2016a). Agricultural watershed modeling: a review for hydrology and soil erosion processes. *Ciencia E Agrotecnologia*, *40*(1), 7–25. https://doi.org/10.1590/S1413-70542016000100001

de Mello, Carlos Rogério, Norton, L. D., Pinto, L. C., Beskow, S., & Curi, N. (2016b).

Agricultural watershed modeling: a review for hydrology and soil erosion processes. In *Ciencia E Agrotecnologia* (Vol. 40, Issue 1, pp. 7–25). https://doi.org/10.1590/S1413-70542016000100001

de Oliveira, V. A., de Mello, C. R., Durães, M. F., & da Silva, A. M. (2014). Soil erosion vulnerability in the Verde River basin, southern Minas Gerais. *Ciencia e Agrotecnologia*, *38*(3), 262–269. https://doi.org/10.1590/S1413-70542014000300006

del Mar Lopez Marrero, T. (2003). THE STUDY OF LAND COVER CHANGE IN A CARIBBEAN LANDSCAPE: What Has Happened in Eastern Puerto Rico During the Last Two Decades?* Forest Service-International Institute of Tropical Forestry in Puerto. *Caribbean Studies*, *31*(2), 33. https://about.jstor.org/terms

Del Mar López, T., Aide, T. M., & Thomlinson, J. R. (2001). Urban expansion and the loss of prime agricultural lands in Puerto Rico. *Ambio*, *30*(1), 49–54. https://doi.org/10.1579/0044-7447-30.1.49

Del Mar López, Tania, Aide, T. M., & Scatena, F. N. (1998). The effect of land use on soil erosion in the Guadiana watershed in Puerto Rico. *Caribbean Journal of Science*, *34*(3–4), 298–307.

Deng, C. (2013). *Small-Area Population Estimation: an Integration of Demographic and Geographic Techniques* [University of Wisconsin Milwaukee]. https://dc.uwm.edu/cgi/viewcontent.cgi?article=1683&context=etd

Desmet, P. J. J., & Govers, G. (1996). A GIS procedure for automatically calculating the USLE LS factor on. *Journal of Soil and Water Conservation*, *51*(5), 427–433.

Dietz, J. L. (1986). Economic history of Puerto Rico : Institutional change and capitalist development. In *Princeton University Press*. Princeton University Press.

Djuwansah, M. R., & Mulyono, A. (2018). Assessment Model for Determining Soil Erodibility Factor in Lombok Island. *RISET Geologi Dan Pertambangan*, *27*(2). https://doi.org/10.14203/risetgeotam2017.v27.417

DNER. (2010). *Management Plan for the Jobos Bay National Estuarine Research Reserve, 2010 - 2015*. http://drna.pr.gov/historico/oficinas/arn/recursosvivientes/costasreservasrefugios/JobosBayManagementPlanFINALdecember.pdf

DOC, NOAA, NOS, O. (2020, June 4). *R-Factor for the Island of Puerto Rico - Datasets - NOAA Data Catalog*. NOAA's Ocean Service, Office for Coastal Management (OCM). https://data.noaa.gov/dataset/dataset/r-factor-for-the-island-of-puerto-rico1

Edwards, B. L., Webb, N. P., Brown, D. P., Elias, E., Peck, D. E., Pierson, F. B., Williams, C. J., & Herrick, J. E. (2019). Climate change impacts on wind and water erosion on US rangelands. *Journal of Soil and Water Conservation*, *74*(4), 405–418. https://doi.org/10.2489/jswc.74.4.405

Edwards, F. A., Massam, M. R., Cosset, C. C. P., Cannon, P. G., Haugaasen, T., Gilroy, J. J., & Edwards, D. P. (2021). Sparing land for secondary forest regeneration

protects more tropical biodiversity than land sharing in cattle farming landscapes. *Current Biology*, *31*(6), 1284-1293.e4. https://doi.org/10.1016/j.cub.2020.12.030

Eicher, C. L., & Brewer, C. A. (2001a). Cartography and Geographic Information Science Dasymetric Mapping and Areal Interpolation: Implementation and Evaluation Dasymetric Mapping and Areal Interpolation: Implementation and Evaluation. *Cartography and Geographic Information Science*, *28*(2), 125–138. https://doi.org/10.1559/152304001782173727org/10.1559/152304001782173727

Eicher, C. L., & Brewer, C. A. (2001b). Dasymetric Mapping and Areal Interpolation: Implementation and Evaluation. *Cartography and Geographic Information Science*, *28*(2), 125–138. https://doi.org/10.1559/152304001782173727

Elsenbeer, H., Cassel, K., & Tinner, W. (1993). A daily rainfall erosivity model for Western Amazonia. *Journal of Soil and Water Conservation*, *48*(5), 439–444. http://nbn-resolving.de/urn:nbn:de:kobv:517-opus-16962

Esri. (2019a). *Flow Accumulation—Help | ArcGIS Desktop*. http://desktop.arcgis.com/en/arcmap/latest/tools/spatial-analyst-toolbox/flow-accumulation.htm

Esri. (2019b). *Flow Direction—Help | ArcGIS Desktop*. http://desktop.arcgis.com/en/arcmap/latest/tools/spatial-analyst-toolbox/flow-direction.htm

Esri Community. (2012). *Flow direction values 1 - 255 | GeoNet*. GeoNet Flow Direction Values Discussions. https://community.esri.com/thread/52536

Estudios Técnicos Inc. (2014). *Plan Maestro de Acceso Público a las Costas de Puerto Rico*. https://doi.org/10.1017/CBO9781107415324.004

Estudios Técnicos Inc. (2017). *Jobos Bay Research Reserve Management Plan 2017-2022*. http://drna.pr.gov/wp-content/uploads/2017/08/Final-2017-2022-Jobos-Bay-Management-Plan.pdf

Estudios Tecnicos Inc. (2014). *Puerto Rico State Housing Plan Fiscal Years 2014-2018. ANNEX CC Government of Puerto Rico*. 78.

European Communities. (2001). *Manual of concepts on land cover and land use information systems*. http://europa.eu.int

Ewel, J. J., & Whitmore, J. L. (1973). The ecological life zones of Puerto Rico and the U.S.Virgin Islands. *Forest Service Research, December*, 72.

Fabricius, K. E. (2005). Effects of terrestrial runoff on the ecology of corals and coral reefs: Review and synthesis. *Marine Pollution Bulletin*, *50*(2), 125–146. https://doi.org/10.1016/j.marpolbul.2004.11.028

FAO. (1995). Forest Resources Assessment 1990 - Global Synthesis. In *Global Synthesis.* . http://www.fao.org/3/v5695e/v5695e00.htm

Farhan, Y., Zregat, D., & Farhan, I. (2013). Spatial Estimation of Soil Erosion Risk

Using RUSLE Approach, RS, and GIS Techniques: A Case Study of Kufranja Watershed, Northern Jordan. *Journal of Water Resource and Protection*, *05*(12), 1247–1261. https://doi.org/10.4236/jwarp.2013.512134

Ferro, V., Giordano, G., & Iovino, M. (1991). Isoerosivity and erosion risk map for sicily. *Hydrological Sciences Journal*, *36*(6), 549–564. https://doi.org/10.1080/02626669109492543

Ferro, V., Porto, P., & Yu, B. (1999). A comparative study of rainfall erosivity estimation for southern Italy and southeastern Australia. *Hydrological Sciences Journal*, *44*(1), 3–24. https://doi.org/10.1080/02626669909492199

Fisher, P F, & Langford, M. (1995). Modelling the errors in areal interpolation between zonal systems by Monte Carlo simulation. *Environment and Planning A*, *27*, 211–224. http://citeseerx.ist.psu.edu/viewdoc/download?doi=10.1.1.465.9635&rep=rep1&type=pdf

Fisher, Peter F., & Langford, M. (1996a). Modeling sensitivity to accuracy in classified imagery: A study of areal interpolation by dasymetric mapping. *Professional Geographer*, *48*(3), 299–309. https://doi.org/10.1111/j.0033-0124.1996.00299.x

Fisher, Peter F., & Langford, M. (1996b). Modeling sensitivity to accuracy in classified imagery: A study of areal interpolation by dasymetric mapping. In *Professional Geographer* (Vol. 48, Issue 3, pp. 299–309). https://doi.org/10.1111/j.0033-0124.1996.00299.x

Fletcher, J. E., Huber, A. L., Haws, F. W., & Clyde, C. G. (1977). *Runoff Estimates for Small Rural Watersheds and Development of a Sound Design method. Volume II, Recommendations for Preparing Design Manuals and Appendices B, C, D, E, F, G, & H* (Issue January). https://digitalcommons.usu.edu/water_rep/474/

Flynn, D. F. B., Uriarte, M., Crk, T., Pascarella, J. B., Zimmerman, J. K., Aide, T. M., & Caraballo Ortiz, M. A. (2010). Hurricane disturbance alters secondary forest recovery in Puerto Rico. *Biotropica*, *42*(2), 149–157. https://doi.org/10.1111/j.1744-7429.2009.00581.x

Foster, G. R., Mccool, D. K., Renard, K. G., & Moldenhauer, W. C. (1981). Conversion of the universal soil loss equation to SI metric units. *Journal of Soil Water Conservation*, *36*(6), 355–359. www.swcs.org

Fu, G., Chen, S., & Mccool, D. K. (2006). Modeling the impacts of no-till practice on soil erosion and sediment yield with RUSLE, SEDD, and ArcView GIS. *Soil & Tillage Research , 85*, 38–49. https://doi.org/10.1016/j.still.2004.11.009

Ganasri, B. P., & Ramesh, H. (2016). Assessment of soil erosion by RUSLE model using remote sensing and GIS - A case study of Nethravathi Basin. *Geoscience Frontiers*, *7*(6), 953–961. https://doi.org/10.1016/j.gsf.2015.10.007

Gao, Q., & Yu, M. (2017). Reforestation-induced changes of landscape composition and configuration modulate freshwater supply and flooding risk of tropical watersheds.

PLoS ONE, *12*(7), 14. https://doi.org/10.1371/journal.pone.0181315

Gao, Q., Yu, M., Liu, Y., Xu, H., & Xu, X. (2007). Modeling interplay between regional net ecosystem carbon balance and soil erosion for a crop-pasture region. *Journal of Geophysical Research: Biogeosciences*, *112*(4), 1–16. https://doi.org/10.1029/2007JG000455

García-Quijano, C. G., Poggie, J. J., Pitchon, A., & Del Pozo, M. H. (2015). Coastal Resource Foraging, Life satisfaction, and well-being in Southern Puerto Rico. *Journal of Anthropological Research*, *71*(2), 145–167.

García-Quijano, C., Poggie, J., Pitchon, A., del Pozo, M., & Alvarado, J. (2013). *The Coast's Bailout: Coastal Resource Use, Quality of Life, and Resilience in Southeastern Puerto Rico*.

García-Ruiz, J. M., Beguería, S., Nadal-Romero, E., González-Hidalgo, J. C., Lana-Renault, N., & Sanjuán, Y. (2015). A meta-analysis of soil erosion rates across the world. *Geomorphology*, *239*, 160–173. https://doi.org/10.1016/j.geomorph.2015.03.008

Getis, A., & Ord, J. K. (1992). The Analysis of Spatial Association by Use of Distance Statistics. *Geographical Analysis*, *24*(3), 189–206. https://doi.org/10.1111/j.1538-4632.1992.tb00261.x

Ghosal, K., & Das Bhattacharya, S. (2020). A Review of RUSLE Model. *Journal of the Indian Society of Remote Sensing*, *48*(4), 689–707. https://doi.org/10.1007/s12524-019-01097-0

Gibson, J., Li, C., & Boe-Gibson, G. (2014). Economic growth and expansion of China's urban land area: Evidence from administrative data and night lights, 1993-2012. *Sustainability (Switzerland)*, *6*(11), 7850–7865. https://doi.org/10.3390/su6117850

Giusti-Cordero, J. A. (1996). Labour, Ecology and History in a Puerto Rican Plantation Region: "Classic" Rural Proletarians Revisited. *International Review of Social History*, *41*(S4), 53–82. https://doi.org/10.1017/S0020859000114270

Gould, W. A., Wadsworth, F. H., Quiñones, M., Fain, S. J., & Álvarez-Berríos, N. L. (2017). Land use, conservation, forestry, and agriculture in Puerto Rico. *Forests*, *8*(7), 1–22. https://doi.org/10.3390/f8070242

Gould, W., Alarcón, C., Fevold, B., Jiménez, M., Martinuzzi, S., Potts, G., Quiñones, M., Solórzano, M., & Ventosa, E. (2008). The Puerto Rico Gap Analysis Project. Volume 1: Land cover, vertebrate species distributions, and land stewardship. *Gen. Tech. Rep. IITF-GTR-39.*, *March*, 165 p.

Govender, Y., & Thomlinson, J. R. (2010). Changes in landuse/landcover affect distribution and habitat of the land crab, Cardisoma guanhumi (Gecarcinidae, decapoda) in two estuaries in Puerto Rico. *Caribbean Journal of Science*, *46*(2–3), 258–266. https://doi.org/10.18475/cjos.v46i2.a14

Grau, H. R., Aide, T. M., Zimmerman, J. K., Thomlinson, J. R., Helmer, E., & Zou, X. (2003). The Ecological Consequences of Socioeconomic and Land-Use Changes in

Postagriculture Puerto Rico. *BioScience*, *53*(12), 1159. https://doi.org/10.1641/0006-3568(2003)053[1159:TECOSA]2.0.CO;2

Gudino-Elizondo, N., Kretzschmar, T., & Gray, S. C. (2019). Stream flow composition and sediment yield comparison between partially urbanized and undisturbed coastal watersheds—case study: St. John, US Virgin Islands. *Environmental Monitoring and Assessment*, *191*(11). https://doi.org/10.1007/s10661-019-7778-4

Hammer, R. B., Stewart, S. I., Winkler, R. L., Radeloff, V. C., & Vossa, P. R. (2004). Characterizing dynamic spatial and temporal residential density patterns from 1940-1990 across the North Central United States. *Landscape and Urban Planning*, *69*, 183–199. https://doi.org/10.1016/j.lmdurbplan.2003.08.011

Han, H., Yang, C., & Song, J. (2015). Scenario simulation and the prediction of land use and land cover change in Beijing, China. *Sustainability (Switzerland)*, *7*(4), 4260–4279. https://doi.org/10.3390/su7044260

Hansen, A. J. (2005). Rural landause trends in the conterminous united states, 1950a2000. *Ecological Applications : A Publication of the Ecological Society of America*, *15*(6), 1851–1863. https://doi.org/10.1071/WR97026

Harding, S. M., Wolff, M., Trewin, D., & Hunter, S. (2014). State of Tropic. In *The Counseling Psychologist* (Issue 1). https://doi.org/10.1177/0011000014564251

Harmsen, E. W., Miller, N. L., Schlegel, N. J., & Gonzalez, J. E. (2009). Seasonal climate change impacts on evapotranspiration, precipitation deficit and crop yield in Puerto Rico. *Agricultural Water Management*, *96*, 1085–1095. https://doi.org/10.1016/j.agwat.2009.02.006

Harvey, J. T. (2002). Estimating census district populations from satellite imagery: Some approaches and limitations. *International Journal of Remote Sensing*, *23*(10), 2071–2095. https://doi.org/10.1080/01431160110075901

Haylock, M., & Nicholls, N. (2000). Trends in extreme rainfall indices for an updated high quality data set for Australia, 1910-1998. *International Journal of Climatology*, *20*(13), 1533–1541. https://doi.org/10.1002/1097-0088(20001115)20:13<1533::AID-JOC586>3.0.CO;2-J

Hecht, S. B., & Saatchi, S. S. (2007). Globalization and forest resurgence: Changes in forest cover in El Salvador. *BioScience*, *57*(8), 663–672. https://doi.org/10.1641/B570806

Helmer, E. H. (2004). Forest conservation and land development in Puerto Rico. *Landscape Ecology*, *19*(1), 29–40. https://doi.org/10.1023/B:LAND.0000018364.68514.fb

Helmer, E. H., Ramos, O., López, T. D. M., Quinones, M., & Diaz, W. (2002). Mapping the forest type and land cover of Puerto Rico, a component of the Caribbean biodiversity hotspot. *Caribbean Journal of Science*, *38*(3–4), 165–183.

Helmer, H. E., & Ruefenacht, B. (2005). Cloud-Free Satellite Image Mosaics with Regression Trees and Histogram Matching. *Photogrammetric Engineering &*

Remote Sensing, *71*(9), 1079–1089. https://www.fs.fed.us/global/iitf/pubs/ja_iitf_2005_helmer001.pdf

Hernández, Y. A., Cornelis, W. M., González, H. M., Pérez, M. E. R., Brito, G. A., Suareza, J. D., & Gabriels, D. (2016). Rainfall Energy Characterization in Cuyaguateje Basin Erosion. *Cultivos Tropicales*, *37*(2), 56–71. https://doi.org/10.13140/RG.2.1.3287.1925

Hernando, D., & Romana, M. G. (2016). Estimate of the (R)USLE rainfall erosivity factor from monthly precipitation data in mainland Spain. *Journal of Iberian Geology*, *42*(1), 113–124. https://doi.org/10.5209/rev_JIGE.2016.v42.n1.49120

Holloway, S. R., Schumacher, J., & Redmond, R. L. (1997). People and place: dasymetric mapping using Arc/Info. *Missoula: Wildlife Spatial Analysis Lab*, 1–11.

Holt, J. B., Lo, C. P., & Hodler, T. W. (2004). Dasymetric Estimation of Population Density and Areal Interpolation of Census Data. *Cartography and Geographic Information Science*, *31*(2), 103–121. https://doi.org/10.1559/1523040041649407

Jahun, B. G., Ibrahim, R., Dlamini, N. S., & Musa, S. M. (2015). Review of Soil Erosion Assessment using RUSLE Model and GIS. *Journal of Biology, Agriculture and Healthcare*, *5*(9), 36–47.

Jia, P., & Gaughan, A. E. (2016). Dasymetric modeling: A hybrid approach using land cover and tax parcel data for mapping population in Alachua County, Florida. *Applied Geography*, *66*, 100–108. https://doi.org/10.1016/j.apgeog.2015.11.006

Johnson, E. A., & Miyanishi, K. (2008). Testing the assumptions of chronosequences in succession. *Ecology Letters*, *11*(5), 419–431. https://doi.org/10.1111/j.1461-0248.2008.01173.x

Johnson, T., Butcher, J., Santell, S., Schwartz, S., Julius, S., & Leduc, S. (2022). A review of climate change effects on practices for mitigating water quality impacts. *Journal of Water and Climate Change*, *13*(4), 1684–1705. https://doi.org/10.2166/wcc.2022.363

Junta de Planificación de Puerto Rico. (2019). *Plan de mitigación de Peligros Naturales. Municipio de Salinas. Versión Final.* http://cedd.pr.gov/Mitigacion/wp-content/uploads/2020/02/SALINA.pdf

Junta de Planificación de Puerto Rico. (2020). *Plan de mitigación de Peligros Naturales. Municipio de Guayama. Versión Final.* http://cedd.pr.gov/Mitigacion/wp-content/uploads/2020/02/SALINA.pdf

Kelsey, K., & Johnson, T. (2015). *DETERMINING COVER MANAGEMENT VALUES (C FACTORS) FOR SURFACE COVER BEST MANAGEMENT PRACTICES (BMPs).* http://citeseerx.ist.psu.edu/viewdoc/download?doi=10.1.1.486.4596&rep=rep1&type=pdf

Kennaway, T., & Helmer, E. (2007). The Forest Types and Ages Cleared for Land Development in Puerto Rico. *GIScience & Remote Sensing*, *44*(4), 356–382.

https://doi.org/10.2747/1548-1603.44.4.356

Kennish, M. J. (2002a). Environmental threats and environmental future of estuaries. *Environmental Conservation*, *29*(1), 78–107. https://doi.org/10.1017/S0376892902000061

Kennish, M. J. (2002b). Environmental threats and environmental future of estuaries. In *Environmental Conservation* (Vol. 29, Issue 1, pp. 78–107). https://doi.org/10.1017/S0376892902000061

Kennish, M. J. (2016). *Encyclopedia of Estuaries*. Springer Reference.

Khosrokhani, M., & Pradhan, B. (2014). Spatio-temporal assessment of soil erosion at Kuala Lumpur metropolitan city using remote sensing data and GIS. *Geomatics, Natural Hazards and Risk*, *5*(3), 252–270. https://doi.org/10.1080/19475705.2013.794164

Kim, H. H. (2009). *Intelligent Interpolation for Population Distribution Modeling* [University of Georgia]. https://getd.libs.uga.edu/pdfs/kim_hwa_hwan_200908_phd.pdf

Kowe, P., Mutanga, O., Odindi, J., & Dube, T. (2019). Exploring the spatial patterns of vegetation fragmentation using local spatial autocorrelation indices. *Journal of Applied Remote Sensing*, *13*(02), 1. https://doi.org/10.1117/1.jrs.13.024523

Kuzera, K., & Pontius, R. G. (2008). Importance of matrix construction for multiple-resolution categorical map comparison. *GIScience and Remote Sensing*, *45*(3), 249–274. https://doi.org/10.2747/1548-1603.45.3.249

Laboy-Nieves, E. N. (2009). Ecosystems and Environmental Health Human. In *Environmental Management, Sustainable Development and Human Health* (pp. 361–398). CRC Press, Taylor & Francis. https://doi.org/10.1017/CBO9781107415324.004

Laboy, E. N., Capellla, J., Robles, P. O., & González, C. M. (2008). *Jobos Bay Estuarine Profile: a National Estuarine Research Reserve*. https://coast.noaa.gov/data/docs/nerrs/Reserves_JOB_SiteProfile.pdf

Labrière, N., Locatelli, B., Laumonier, Y., Freycon, V., & Bernoux, M. (2015). Soil erosion in the humid tropics: A systematic quantitative review. *"Agriculture, Ecosystems and Environment," 203*, 127–139. https://doi.org/10.1016/j.agee.2015.01.027

Laflen, J. M., & Flanagan, D. C. (2013). The development of US soil erosion prediction and modeling. In *International soil and water conservation research* (Vol. 1, Issue 2, pp. 1–11). https://doi.org/10.1016/S2095-6339(15)30034-4

Lal, R. (1998). Soil erosion impact on agronomic productivity and environment quality. *Critical Reviews in Plant Sciences*, *17*(4), 319–464. https://doi.org/10.1016/S0735-2689(98)00363-3

Lal, R. (2001). Soil degradation by erosion. *Land Degradation and Development*, *12*,

519–539. https://doi.org/10.1002/ldr.472

Lam, N. S. N. (1983). Spatial Interpolation Methods: A Review. *The American Carthographer*, *10*(2), 129–150. http://www.geog.ucsb.edu/~kclarke/G232/Lam_1983.pdf

Lambin, E. F., Geist, H. J., & Lepers, E. (2003). Dynamics of Land-Use and Land-Cover Change in Tropical Regions. *Annual Review of Environment and Resources*, *28*, 205–241. https://doi.org/10.1146/annurev.energy.28.050302.105459

Lambin, E. F., Turner, B. L., Geist, H. J., Agbola, S. B., Angelsen, A., Bruce, J. W., Coomes, O. T., Dirzo, R., Fischer, G., Folke, C., George, P. S., Homewood, K., Imbernon, J., Leemans, R., Li, X., Moran, E. F., Mortimore, M., Ramakrishnan, P. S., Richards, J. F., … Xu, J. (2001). The causes of land-use and land-cover change: Moving beyond the myths. *Global Environmental Change*, *11*(4), 261–269. https://doi.org/10.1016/S0959-3780(01)00007-3

Langford, M., & Unwin, D. J. (1994). Generating and mapping population density surfaces within a geographical information system. *The Cartographic Journal*, *31*(1), 21–26. https://doi.org/10.1179/000870494787073718

Larsen, M. C., & Webb, R. M. T. (2009). Potential Effects of Runoff, Fluvial Sediment, and Nutrient Discharges on the Coral Reefs of Puerto Rico. *Journal of Coastal Research*, *25*(251), 189–208. https://doi.org/10.2112/07-0920.1

Lee, S., & Leigh, N. G. (2005). The role of inner ring suburbs in metropolitan smart growth strategies. *Journal of Planning Literature*, *19*(3), 330–346. https://doi.org/10.1177/0885412204271878

Lenth, B. A., Knight, R. L., & Gilgert, W. C. (2006). Conservation value of clustered housing developments. *Conservation Biology*, *20*(5), 1445–1456. https://doi.org/10.1111/j.1523-1739.2006.00491.x

Li, L., & Lu, D. (2016). Mapping population density distribution at multiple scales in Zhejiang Province using Landsat Thematic Mapper and census data. *International Journal of Remote Sensing*, *37*(18), 4243–4260. https://doi.org/10.1080/01431161.2016.1212422

Liping, C., Yujun, S., & Saeed, S. (2018). Monitoring and predicting land use and land cover changes using remote sensing and GIS techniques—A case study of a hilly area, Jiangle, China. *PLoS ONE*, *13*(7), 23. https://doi.org/10.1371/journal.pone.0200493

Lipp, E. K., Farrahà, S. A., & Rose, J. B. (2001). Assessment and Impact of Microbial Fecal Pollution and Human Enteric Pathogens in a Coastal Community. *Marine Pollution Bulletin*, *42*(4), 286–293. https://ac.els-cdn.com/S0025326X00001521/1-s2.0-S0025326X00001521-main.pdf?_tid=b9a8c47d-f88b-4ac1-b7ea-b8b6ec58a861&acdnat=1524159439_5f5675c1f411fdbc30456c0a99d6498d

Liu, J., Daily, G. C., Ehrlich, P. R., & Luck, G. W. (2003). Effects of household dynamics on resource consumption and biodiversity. *Nature*, *421*(January), 530–

533. https://doi.org/10.5772/64963

López Marrero, T. del M. (2003). The Study of Land Cover Change in a Caribbean Landscape: What Has Happened in Eastern Puerto Rico during the Last Two Decades? *Caribbean Studies*, *31*(2), 5–36. https://www.jstor.org/stable/pdf/25613406.pdf?ab_segments=0%2Fbasic_SYC-4801%2Ftest2&refreqid=search%3Ae58350da676c8f797afc3fbad5107312

Lopez, R. D., & Frohn, R. C. (2018). *Remote Sensing for Landscape Ecology. Monitoring, Modeling, and Assessment of Ecosysyems* (2nd. ed). CRC Press, Taylor & Francis Group.

Lu, D., Mausel, P., Brondízio, E., & Moran, E. (2004). Change detection techniques. *International Journal of Remote Sensing*, *25*(12), 2365–2401. https://doi.org/10.1080/0143116031000139863

Martinuzzi, S., Gould, W. A., Lugo, A. E., & Medina, E. (2009). Conversion and recovery of Puerto Rican mangroves: 200 years of change. *Forest Ecology and Management*, *257*(1), 75–84. https://doi.org/10.1016/j.foreco.2008.08.037

Martinuzzi, S., Gould, W. A., & Ramos González, O. M. (2007). Land development, land use, and urban sprawl in Puerto Rico integrating remote sensing and population census data. *Landscape and Urban Planning*, *79*(3–4), 288–297. https://doi.org/10.1016/j.landurbplan.2006.02.014

Maury, S., Gholkar, M., Jadhav, A., & Rane, N. (2019). Geophysical evaluation of soils and soil loss estimation in a semiarid region of Maharashtra using revised universal soil loss equation (RUSLE) and GIS methods. *Environmental Earth Sciences*, *78*(5). https://doi.org/10.1007/s12665-019-8137-z

Medeiros, G. de O. R., Giarolla, A., Sampaio, G., & Marinho, M. de A. (2016). Estimates of annual soil loss rates in the state of São Paulo, Brazil. *Revista Brasileira de Ciencia Do Solo*, *40*, 1–18. https://doi.org/10.1590/18069657rbcs20150497

Méndez-Lázaro, P., Muller-Karger, F. E., Otis, D., McCarthy, M. J., & Rodríguez, E. (2018). A heat vulnerability index to improve urban public health management in San Juan, Puerto Rico. *International Journal of Biometeorology*, *62*(5), 709–722. https://doi.org/10.1007/s00484-017-1319-z

Mennis, J. (2009). Dasymetric Mapping for Estimating Population in Small Areas. *Geography Compass*, *3*(2), 727–745.

Mennis, Jeremy. (2003). Generating Surface Models of Population Using Dasymetric Mapping. *Professional Geographer*, *55*(1), 31–42. https://doi.org/10.1111/0033-0124.10042

Mennis, Jeremy. (2009). Dasymetric mapping for estimating population in small areas. *Geography Compass*, *3*(2), 727–745. https://doi.org/10.1111/j.1749-8198.2009.00220.x

Mennis, Jeremy. (2015). Dasymetric Spatiotemporal Interpolation. *Professional Geographer*, *68*(1). https://doi.org/10.1080/00330124.2015.1033669

Mennis, Jeremy. (2016). Dasymetric Spatiotemporal Interpolation. *Professional Geographer*, *68*(1), 92–102. https://doi.org/10.1080/00330124.2015.1033669

Mennis, Jeremy, & Hultgren, T. (2006). Intelligent Dasymetric Mapping and Its Application to Areal Interpolation. *Cartography and Geographic Information Science*, *33*(3), 179–194. https://doi.org/10.1559/152304006779077309

Metro Puerto Rico. (2017, September 4). Tormentas y huracanes que pasaron por Puerto Rico. *Metro Puerto Rico*. https://www.metro.pr/pr/noticias/2017/09/04/tormentas-huracanes-pasaron-puerto-rico.html

Millward, A. A., & Mersey, J. E. (1999). Adapting the RUSLE to model soil erosion potential in a mountainous tropical watershed. *Catena*, *38*(2), 109–129. https://doi.org/10.1016/S0341-8162(99)00067-3

Mitsova, D., Esnard, A. M., & Li, Y. (2012). Using enhanced dasymetric mapping techniques to improve the spatial accuracy of sea level rise vulnerability assessments. *Journal of Coastal Conservation*, *16*(3), 355–372. https://doi.org/10.1007/s11852-012-0206-3

Mohammed, S., Alsafadi, K., Talukdar, S., Kiwan, S., Hennawi, S., Alshihabi, O., Sharaf, M., & Harsanyie, E. (2020). Estimation of soil erosion risk in southern part of Syria by using RUSLE integrating geo informatics approach. *Remote Sensing Applications: Society and Environment*, *20*(July), 100375. https://doi.org/10.1016/j.rsase.2020.100375

Mohammed, S., Hassan, E., Abdo, H. G., Szabo, S., Mokhtar, A., Alsafadi, K., Al-Khouri, I., & Rodrigo-Comino, J. (2021). Impacts of rainstorms on soil erosion and organic matter for different cover crop systems in the western coast agricultural region of Syria. In *Soil Use and Management* (Vol. 37, Issue 1). https://doi.org/10.1111/sum.12683

Mora, A. M., Saharjo, B. H., & Prasetyo, L. B. (2019). Integration of Gis and Remote Sensing for Hotspot Distribution Analysis in Berbak Sembilang National Park. *International Journal of Remote Sensing and Earth Sciences (IJReSES)*, *16*(1), 99. https://doi.org/10.30536/j.ijreses.2019.v16.a3194

Morgan, R. C. P. (2005). *Soil erosion and Conservation* (3rd ed.). Blackwell Publishing.

Moritz, S., & Bartz-Beielstein, T. (2017). imputeTS: Time Series Missing Value Imputation in R. *The R Journal*, *9*(1), 12. https://journal.r-project.org/archive/2017/RJ-2017-009/RJ-2017-009.pdf

Moritz, S., Sardá, A., Bartz-Beielstein, T., Zaefferer, M., & Stork, J. (2015). Comparison of different Methods for Univariate Time Series Imputation in R. *Cologne University of Applied Sciences*, 20. www.th-koeln.de

Ndolo-Goy, P. (2015). *GIS-Based Soil Erosion Modeling and Sediment Yield of The N'Djili River Basin, Democratic Republic of Congo* [Colorado State University]. https://doi.org/10.1145/3132847.3132886

Nearing, M. A., Xie, Y., Liu, B., & Ye, Y. (2017). Natural and anthropogenic rates of soil

erosion. *International Soil and Water Conservation Research*, *5*, 77–84. https://doi.org/10.1016/j.iswcr.2017.04.001

NOAA. (2013). National coastal population report: Population trends from 1970 to 2010. In *NOAA State of the Coast Report Series*. http://stateofthecoast.noaa.gov

NOAA Office for Coastal Management (NOAA/OCM). (2009). *C-CAP Land Cover, Jobos Bay, Commonwealth of Pueto Rico 2007 | ID: 48288 | InPort*. C-CAP Land Cover, Jobos Bay, Commonwealth of Pueto Rico 2007. https://inport.nmfs.noaa.gov/inport/item/48288

NOAA Office for Coastal Management (NOAA/OCM). (2017). *C-CAP Land Cover, Puerto Rico, 2010 | ID: 48301 | InPort*. C-CAP Land Cover, Puerto Rico, 2010. https://inport.nmfs.noaa.gov/inport/item/48301

Noticias Salinas. (2022, March 24). Recursos Naturales sabía de las irregularidades en Bahía de Jobos en Salinas - Noticias Salinas. *Noticias Salinas*. https://www.noticiasdesalinas.com/recursos-naturales-sabia-de-las-irregularidades-en-bahia-de-jobos-en-salinas/

NRCS. (2002). *Field Office Technical Guide Section I-General Resource References-Erosion Prediction: RUSLE C Factors*. https://efotg.sc.egov.usda.gov/references/Agency/NY/Archived_RUSLE_Cover_Mgmt_Conditions_130228.pdf

O'Neal, M. R., Nearing, M. A., Vining, R. C., Southworth, J., & Pfeifer, R. A. (2005). Climate change impacts on soil erosion in Midwest United States with changes in crop management. *Catena*, *61*(2-3 SPEC. ISS.), 165–184. https://doi.org/10.1016/j.catena.2005.03.003

Ochoa, P. A., Fries, A., Mejía, D., Burneo, J. I., Ruíz-Sinoga, J. D., & Cerdà, A. (2016). Effects of climate, land cover and topography on soil erosion risk in a semiarid basin of the Andes. *Catena*, *140*, 31–42. https://doi.org/10.1016/j.catena.2016.01.011

Osaragi, T., & Aoki, Y. (2006). A Method for Estimating Land Use Transition Probability Using Raster Data Considerations about apatial unit of transition, fixed state. In H. J. P. Leeuwen, Jos P. van Timmermans (Ed.), *Innovations in Design & Decsion Support Systems in Architecture and Urban Planning*. Springer. https://cumincad.architexturez.net/system/files/pdf/ddss2006-hb-69.content.pdf

Osei-Twumasi, A., & Falconer, R. A. (2014). Diffuse Source Pollution Studies in a Physical Model of the Severn Estuary, UK. *Journal of Water Resource and Protection.*, *6*(6), 1390–1403. https://doi.org/10.4236/jwarp.2014.615128

Ozsahin, E., Duru, U., & Eroglu, I. (2018). Land use and land cover changes (LULCC), a key to understand soil erosion intensities in the Maritsa Basin. *Water (Switzerland)*, *10*(3). https://doi.org/10.3390/w10030335

Ozsoy, G., & Aksoy, E. (2015). Estimation of soil erosion risk within an important agricultural sub-watershed in Bursa, Turkey, in relation to rapid urbanization. *Environmental Monitoring and Assessment*, *187*(7), 1–14.

https://doi.org/10.1007/s10661-015-4653-9

Panagos, P., Borrelli, P., Meusburger, K., Alewell, C., Lugato, E., & Montanarella, L. (2015). Estimating the soil erosion cover-management factor at the European scale. *Land Use Policy*, *48*, 38–50. https://doi.org/10.1016/j.landusepol.2015.05.021

Paroissien, J. B., Darboux, F., Couturier, A., Devillers, B., Mouillot, F., Raclot, D., & Le Bissonnais, Y. (2015). A method for modeling the effects of climate and land use changes on erosion and sustainability of soil in a Mediterranean watershed (Languedoc, France). *Journal of Environmental Management*, *150*(May), 57–68. https://doi.org/10.1016/j.jenvman.2014.10.034

Parry, R. (1998). Agricultural Phosphorus and Water Quality: A U.S. Environmental Protection Agency Perspective. *Journal of Environment Quality*, *27*(2), 258. https://doi.org/10.2134/jeq1998.00472425002700020003x

Peña, E. N. (2012). *Using Census Data, Urban Land-cover Classification, and Dasymetric Mapping to measure Urban Growth of the lower Rio Grande Valley, Texas* (Issue December).

Pérez, D. Y. (2022, April 6). *Los 20 propietarios en Salinas que DRNA tiene en la mira – NotiCel – Noticias de Puerto Rico* . https://www.noticel.com/top-stories/gobierno/20220406/los-20-propietarios-en-salinas-que-drna-tiene-en-la-mira/

Pôças, I., Cunha, M., & Pereira, L. S. (2011). Remote sensing based indicators of changes in a mountain rural landscape of Northeast Portugal. *Applied Geography*, *31*, 871–880. https://doi.org/10.1016/j.apgeog.2011.01.014

Pontius, R. G., & Cheuk, M. L. (2006). A generalized cross-tabulation matrix to compare soft-classified maps at multiple resolutions. *International Journal of Geographical Information Science*, *20*(1), 1–30. https://doi.org/10.1080/13658810500391024

Pontius, Robert G, Shusas, E., & Mceachern, M. (2004). Detecting important categorical land changes while accounting for persistence. *Agriculture, Ecosystems and Environment*, *101*, 251–268. https://doi.org/10.1016/j.agee.2003.09.008

Prasannakumar, V., Vijith, H., Abinod, S., & Geetha, N. (2012). Estimation of soil erosion risk within a small mountainous sub-watershed in Kerala, India, using Revised Universal Soil Loss Equation (RUSLE) and geo-information technology. *Geoscience Frontiers*, *3*(2), 209–215. https://doi.org/10.1016/j.gsf.2011.11.003

Prasetyo, L. B., Dharmawan, A. H., Nasdian, F. T., & Ramdhoni, S. (2016). Historical Forest fire Occurrence Analysis in Jambi Province During the Period of 2000 – 2015: Its Distribution & Land Cover Trajectories. *Procedia Environmental Sciences*, *33*(April), 450–459. https://doi.org/10.1016/j.proenv.2016.03.096

PRWRERI. (2013). *Final Project Report Detailed Land Use and Habitat Inventory, 2012 of the Jobos Bay National Estuarine Research Reserve Watershed*. http://geodec.com/jbnerr2012/final_report_JBNERR2012.pdf

Puyravaud, J. P. (2003). Standardizing the calculation of the annual rate of deforestation. *Forest Ecology and Management*, *177*(1–3), 593–596.

https://doi.org/10.1016/S0378-1127(02)00335-3

Qiu, F., Sridharan, H., & Chun, Y. (2010). Spatial autoregressive model for population estimation at the census block level using LIDAR-derived building volume information. *Cartography and Geographic Information Science*, *37*(3), 239–257. https://doi.org/10.1559/152304010792194949

Qiu, F., Zhang, C., & Zhou, Y. (2012). The development of an areal interpolation ArcGIS extension and a comparative study. *GIScience and Remote Sensing*, *49*(5), 644–663. https://doi.org/10.2747/1548-1603.49.5.644

Quinn, J. M., & Stroud, M. J. (2002). Water quality and sediment and nutrient export from New Zealand hill-land catchments of contrasting land use Water quality and sediment and nutrient export from New Zealand -land catchments of contrasting land use. *New Zealand Journal of Marine and Freshwater Research*, *36*(2), 409–429. https://doi.org/10.1080/00288330.2002.9517097

Quiñones, F. (2012). *Importancia de la escorrentía superficial como fuente de Agua fresca a la reserva jobanerr de la bahia de jobos en salinas, puerto rico, en comparacion a las descargas de agua subterránea del acuifero local*.

Radeloff, V. C., Hagen, A. E., Voss, P. R., Field, D. R., & Mladenoff, D. J. (2000). Exploring the spatial relationship between census and land-cover data. *Society and Natural Resources*, *13*(6), 599–609. https://doi.org/10.1080/08941920050114646

Ramachandra, T. V, & Kumar, U. (2004). Geographic Resources Decision Support System for land use, land cover dynamics analysis. *FOSS/GRASS Users Conference*, 12–14. http://ces.iisc.ernet.in/energy/Welcome.html

Ramos-Scharrón, C. E., Torres-Pulliza, D., & Hernández-Delgado, E. A. (2015). Watershed- and island wide-scale land cover changes in Puerto Rico (1930s-2004) and their potential effects on coral reef ecosystems. *Science of the Total Environment*, *506–507*, 241–251. https://doi.org/10.1016/j.scitotenv.2014.11.016

Ratnayake, N. P., Sampei, Y., Tokuoka, T., Suzuki, N., & Ishida, H. (2005). Anthropogenic impacts recorded in the sediments of Lunawa, a small tropical estuary, Sri Lanka. *Environmental Geology*, *48*(2), 139–148. https://doi.org/10.1007/s00254-005-1232-3

Rawat, J. S., & Kumar, M. (2015). Monitoring land use/cover change using remote sensing and GIS techniques: A case study of Hawalbagh block, district Almora, Uttarakhand, India. *Egyptian Journal of Remote Sensing and Space Science*, *18*, 77–84. https://doi.org/10.1016/j.ejrs.2015.02.002

Red State Data Center de Puerto Rico (SDC-PR). (2021, August 12). Guánica perdió 29% de su población según el Censo 2020. Comparativa de los Censos Decenales 2010-2020, indica también que 74 de los 78 Municipios perdieron al menos 5 % de su población en la pasada década. *Instituto de Estadísticas de Puerto Rico*, 5.

Renard, K. G., Foster, G. R., Weesies, G. A., McCool, D., & Yoder, D. (1997). *Predicting Soil Erosion by Water: A Guide to Conservation Planning with the*

Revised Universal Soil Loss Equation (RUSLE). USDA, Agriculture Handbook (703). https://www.ars.usda.gov/ARSUserFiles/64080530/rusle/ah_703.pdf

Renard, Kenneth G, & Freimund, J. R. (1994). Using monthly precipitation data to estimate the R-factor in the revised USLE. *Journal of Hydrology*, *157*, 287–306. https://eurekamag.com/pdf/002/002728247.pdf

Renard KG, Foster GR, Weesies GA, McCool DK, Y. D. (1997). *Predicting soil erosion by water: A guide to conservation planning with the Revised Universal Soil Loss Equation*. U.S. Department of Agriculture, Agriculture Handbook No. 703. https://doi.org/DC0-16-048938-5 65–100.

Renschler, C. S., Mannaerts, C., & Diekkruger, B. (1999). Evaluating spatial and temporal variability in soil erosion risk--rainfall erosivity and soil loss ratios in Andalusia, Spain. *Catena*, *34*(3–4), 209–225. https://doi.org/10.1016/S0341-8162(98)00117-9

Rodríguez-Velázquez, V., & Sosa-Pascual, O. (2022, March 22). *Centro de Periodismo Investigativo | Negligencia local y federal propicia crimen ambiental en la Bahía de Jobos en Salinas | Centro de Periodismo Investigativo*. https://periodismoinvestigativo.com/2022/03/negligencia-local-y-federal-propicia-crimen-ambiental-en-la-bahia-de-jobos-en-salinas/

Rojas-González, A. M. (2008). Soil erosion calculation using remote sensing and GIS in Río Grande de Arecibo watershed, Puerto Rico. *American Society for Photogrammetry and Remote Sensing - ASPRS Annual Conference 2008 - Bridging the Horizons: New Frontiers in Geospatial Collaboration*, *2*(March 2008), 595–600. http://www.scopus.com/inward/record.url?eid=2-s2.0-84868683037&partnerID=tZOtx3y1

Rudel, T. K., Perez-Lugo, M., & Zichal, H. (2000). When Fields Revert to Forest: Development and Spontaneous Reforestation in Post-War Puerto Rico. *Professional Geographer*, *52*(3), 386–397. https://doi.org/10.1111/0033-0124.00233

Runfola, D. S. M., & Pontius, R. G. (2013). Measuring the temporal instability of land change using the Flow matrix. *International Journal of Geographical Information Science*, *27*(9), 1696–1716. https://doi.org/10.1080/13658816.2013.792344

Ryan, K. E., Walsh, J. P., Corbett, D. R., & Winter, A. (2008). A record of recent change in terrestrial sedimentation in a coral-reef environment, La Parguera, Puerto Rico: A response to coastal development? *Marine Pollution Bulletin*, *56*(6), 1177–1183. https://doi.org/10.1016/j.marpolbul.2008.02.017

Saha, S. K. (2003). WATER AND WIND INDUCED SOIL EROSION ASSESSMENT AND MONITORING USING REMOTE SENSING AND GIS. *Satellite Remote Sensing GIS Application in Agricultural Meteorology*, 317–330. http://www.wamis.org/agm/pubs/agm8/Paper-15.pdf

Salazar-Ortiz, M., & Cuevas, E. (2017). Land Use and Land Management during the Past Century Determine Mangrove Dynamics in Northwestern Puerto Rico: the Case of the Maracayo Mangrove. *Journal of Environmental Science and Engineering B*, *6*,

593–623. https://doi.org/10.17265/2162-5263/2017.12.002

Salinger, M. J., & Griffiths, G. M. (2001). Trends in New Zealand daily temperature and rainfall extremes. *International Journal of Climatology*, *21*(12), 1437–1452. https://doi.org/10.1002/joc.694

Santiago, I. J. A. (2014). Erosión y Aumento en Inundabilidad en el Municipio de Río Grande. In *PRCR - Geospatial Science and Technology* (Vols. 2010–2019, Issue 1, p. 7). Polytechnic University of Puerto Rico. http://hdl.handle.net/20.500.12475/776

Schroeder, J. P. (2017). Hybrid areal interpolation of census counts from 2000 blocks to 2010 geographies ☆. *Computers, Environment and Urban Systems*, *62*, 53–63. https://doi.org/10.1016/j.compenvurbsys.2016.10.001

SDC-PR. (2021, April 26). *PR | State Data Center*. Población Total de Puerto Rico - Censo Decenal 2020. https://censo.estadisticas.pr/

Shalaby, A., & Tateishi, R. (2007). Remote sensing and GIS for mapping and monitoring land cover and land-use changes in the Northwestern coastal zone of Egypt. *Applied Geography*, *27*, 28–41. https://doi.org/10.1016/j.apgeog.2006.09.004

Shanley, J. B., McDowell, W. H., & Stallard, R. F. (2011). Long-term patterns and short-term dynamics of stream solutes and suspended sediment in a rapidly weathering tropical watershed. *Water Resources Research*, *47*(7), 1–11. https://doi.org/10.1029/2010WR009788

Sharma, A., Tiwari, K. N., & Bhadoria, P. B. S. (2011). Effect of land use land cover change on soil erosion potential in an agricultural watershed. *Environmental Monitoring and Assessment*, *173*(1–4), 789–801. https://doi.org/10.1007/s10661-010-1423-6

Simms, A., Woodroffe, C., & Jones, B. (2003). Application of RUSLE for erosion management in a coastal catchment, southern NSW. *Faculty of Science-Papers*, *2*(July), 678–683. http://ro.uow.edu.au/cgi/viewcontent.cgi?article=1034&context=scipapers

Sleeter, R., & Gould, M. D. (2007). *Geographic information system software to remodel population data using dasymetric mapping methods* (Issue tm 11c2). http://purl.access.gpo.gov/GPO/LPS106635

Smith, S. K., Nogle, J., & Cody, S. (2002). A regression Approach to Estimate the Average Number of Persons per Household. *Demography*, *39*(4), 697–712.

Soil Survey Staff, Natural Resources Conservation Service, U. S. D. of A. W. S. S. (2019). *Web Soil Survey - Getting Started*. USDA-NRCS. https://websoilsurvey.sc.egov.usda.gov/app/gettingstarted.htm

Sorichetta, A., Hornby, G. M., Stevens, F. R., Gaughan, A. E., Linard, C., & Tatem, A. J. (2015). High-resolution gridded population datasets for Latin America and the Caribbean OPEN SUBJECT CATEGORIES » Geography » Malaria » Sustainability » Environmental sciences Background & Summary. *Scientific Data*,

2(150045). https://doi.org/10.1038/sdata.2015.45

Stefanidis, S., Alexandridis, V., Chatzichristaki, C., & Stefanidis, P. (2021). Assessing soil loss by water erosion in a typical mediterranean ecosystem of Northern Greece under current and future rainfall erosivity. *Water (Switzerland)*, *13*(15). https://doi.org/10.3390/w13152002

Stevens, F. R., Gaughan, A. E., Linard, C., & Tatem, A. J. (2015). Disaggregating census data for population mapping using Random forests with remotely-sensed and ancillary data. *PLoS ONE*, *10*(2), 1–22. https://doi.org/10.1371/journal.pone.0107042

Su, M. D., Lin, M. C., Hsieh, H. I., Tsai, B. W., & Lin, C. H. (2010). Multi-layer multi-class dasymetric mapping to estimate population distribution. *Science of the Total Environment*, *408*(20), 4807–4816. https://doi.org/10.1016/j.scitotenv.2010.06.032

Suppiah, R., & Hennessy, K. J. (1998). Trends in total rainfall, heavy rain events and number of dry days in Australia, 1910-1990. *International Journal of Climatology*, *18*(10), 1141–1164. https://doi.org/10.1002/(SICI)1097-0088(199808)18:10<1141::AID-JOC286>3.0.CO;2-P

Syphard, A. D., Stewart, S. I., Mckeefry, J., Hammer, R. B., Fried, J. S., Holcomb, S., & Radeloff, V. C. (2009). Assessing housing growth when census boundaries change. *International Journal of Geographical Information Science*, *23*(7), 859–876. https://doi.org/10.1080/13658810802359877

Takada, T., Miyamoto, A., & Hasegawa, S. F. (2010). Derivation of a yearly transition probability matrix for land-use dynamics and its applications. *Landscape Ecology*, *25*(4), 561–572. https://doi.org/10.1007/s10980-009-9433-x

Teferi, E., Bewket, W., Uhlenbrook, S., & Wenninger, J. (2013). Understanding recent land use and land cover dynamics in the source region of the Upper Blue Nile, Ethiopia: Spatially explicit statistical modeling of systematic transitions. *Agriculture, Ecosystems and Environment*, *165*, 98–117. https://doi.org/10.1016/j.agee.2012.11.007

Telemundo Puerto Rico. (2022, March 23). *Construyen casas con piscina y muelles en Reserva Estuarina en Salinas – Telemundo Puerto Rico*. https://www.telemundopr.com/noticias/puerto-rico/construyen-casas-con-piscina-y-muelles-en-reserva-estuarina-en-salinas/2319149/

Titus, J.G.; Anderson, K.E.; Cahoon, D.R.; Gesch, D.B.; Gill, S.K.; Gutierrez, B.T.; Thieler, E.R.; Williams, S. J. (2009). The First State of the Coastal Cycle Sensitivity to Carbon Report Sea-Level Rise : Focus on Mid-Atlantic Region. In *Synthesis and Assessment Product 4.1 Report by the U.S. Climate Change Science Program and the Subcommittee on Global Change Research* (Issue January 2009).

Tobler, W. R. (1979). Smooth pycnophylactic interpolation for geographical regions. *Journal of the American Statistical Association*, *74*(367), 519–530. https://doi.org/10.1080/01621459.1979.10481647

Torres-Rojo, J. M., Magaña-Torres, O. S., & Moreno-Sánchez, F. (2016). PREDICTION OF LAND USE CHANGE/FOREST COVER IN MEXICO TROUGH TRANSITION PROBABILITIES. *Agrociencia*, *50*(6), 769–785. http://www.scielo.org.mx/pdf/agro/v50n6/1405-3195-agro-50-06-00769-en.pdf

Traini, C., Menier, D., & Proust, J.-N. (2008). The Vilaine River estuary in the Bay of Biscay: Insight into geomorphologic controls on estuarine sedimentation. *Geophysical Research Abstracts*, *10*, 5. https://doi.org/EGU2008-A-05586

Tripathi, S., Subedi, R., & Adhikari, H. (2020). Forest Cover Change Pattern after the Intervention of Community Forestry Management System in the Mid - Hill of Nepal : A Case Study. *Remote Sensing*, *12*(2756), 18. https://doi.org/10.3390/rs12172756

Turner, II B. L., Skole, D., Sanderson, S., Fischer, G., Fresco, L., Leemans, R., Graetz, D., Kitamura, T., Liu, Y., Martinelli, L., Milanova, E., Norse, D., Okoth-Ogendo, H. W. O., Parry, M., Pritchard, L., Strezpek, K., Veldkamp, T., Kanger, M., Morais, J., & Czulinski, A. (1995). *Land-Use and Land-Cover Change Science/Research Plan; IGBP Report No.35 and HDP Report No.7*.

Turner, Ii B L, Lambin, E. F., & Reenberg, A. (2007). The emergence of land change science for global environmental change and sustainability. *PNAS*, *104*(52), 20666–20671. www.pnas.orgcgidoi10.1073pnas.0704119104

U.S. Census Bureau. (2020). *Visualizaciones publicadas mediante los State-by-State Visualizations of Key Demographic Trends From the 2020 Census. Resultados Censo 2020 para Puerto Rico y sus Municipios* . https://www.census.gov/library/stories/state-by-state.html

US Census Bureau. (2012). *Censo de Población y Vivienda del 2010, Recuentos de Población y Unidades de Vivienda, CPH-2-53SP, Puerto Rico*. https://censo.estadisticas.pr/sites/default/files/Decenal/cph-2-53sp_Recuentos de Población y Unidades de Vivienda.pdf

US Census Bureau. (2022). *Census Bureau Tables: Five Years Community Survey 2020. Total Population and total Housing Units, 2020.* https://data.census.gov/cedsci/table?g=0500000US72057%240600000,72123%240600000&y=2010&d=DEC Summary File 1

USDA-NRCS. (n.d.). *Prime & Other Important Farmlands Definitions | NRCS Caribbean Area*. Retrieved April 29, 2021, from https://www.nrcs.usda.gov/wps/portal/nrcs/detailfull/pr/soils/?cid=nrcs141p2_037285

USDA-NRCS. (2019). *Custom Soil Resource Report for Humacao Area, Puerto Rico Eastern Part*.

Vallebona, C., Pellegrino, E., Frumento, P., & Bonari, E. (2015). Temporal trends in extreme rainfall intensity and erosivity in the Mediterranean region: a case study in southern Tuscany, Italy. *Climatic Change*, *128*(1–2), 139–151. https://doi.org/10.1007/s10584-014-1287-9

Verburg, P. H., Neumann, K., & Nol, L. (2011). Challenges in using land use and land cover data for global change studies. *Global Change Biology*, *17*(2), 974–989. https://doi.org/10.1111/j.1365-2486.2010.02307.x

Vijith, H., Seling, L. W., & Dodge-Wan, D. (2017). Estimation of soil loss and identification of erosion risk zones in a forested region in Sarawak, Malaysia, Northern Borneo. *Environment, Development and Sustainability*, *20*(3), 1365–1384. https://doi.org/10.1007/s10668-017-9946-4

Viqueira, R. R. A. (2018). *Implementation of the Guánica Bay Watershed Management Plan*.

Wang, B., Zheng, F., & Guan, Y. (2016). Improved USLE-K factor prediction: A case study on water erosion areas in China. *International Soil and Water Conservation Research*, *4*(3), 168–176. https://doi.org/10.1016/j.iswcr.2016.08.003

Wang, B., Zheng, F., Ro¨mkens, M. J. M., & Ro¨mkens, R. (2013). Comparison of soil erodibility factors in USLE, RUSLE2, EPIC and Dg models based on a Chinese soil erodibility database. *Acta Agriculturae Scandinavica Section B ? Soil and Plant Science*, *63*(1), 69–79. https://doi.org/10.1080/09064710.2012.718358

Wang, B., Zheng, F., & Römkens, M. J. M. (2013). Comparison of soil erodibility factors in USLE, RUSLE2, EPIC and Dg models based on a Chinese soil erodibility database. *Acta Agriculturae Scandinavica Section B: Soil and Plant Science*, *63*(1), 69–79. https://doi.org/10.1080/09064710.2012.718358

Wang, C., Gao, Q., Wang, X., & Yu, M. (2016). Spatially differentiated trends in urbanization, agricultural land abandonment and reclamation, and woodland recovery in Northern China. *Scientific Report*, *6*, 12. https://doi.org/10.1038/srep37658

Wang, C., Yu, M., & Gao, Q. (2017). Continued Reforestation and Urban Expansion in the New Century of a Tropical Island in the Caribbean. *Remote Sensing*, *9*(7), 731. https://doi.org/10.3390/rs9070731

Warne, A. G., Webb, R. M. T., & Larsen, M. C. (2005). Water, Sediment, and Nutrient Discharge Characteristics of Rivers in Puerto Rico , and their Potential Influence on Coral Reefs. In *Scientific Investigations Report 2005-5206*.

Weichselbaum, J., & Papathoma, M. (2005). Sharpening census information in GIS to meet real-world conditions – the case for Earth Observation. *WIT Transactions on Ecology and the Environment*, *84*, 143–152.

Weil, R. R., & Brady, N. C. (2017). *The Nature and Properties of Soils* (15th ed.). Pearson Education Limited.

Wesseling, C., Crowe, J., Peraza, S., Aragón, A., & Partanen, T. (2018). *Trabajadores de la caña de azúcar* (p. 14). OISIS. www.oiss.org/estrategia/IMG/pdf/6-Cana.pdf

Whitall, D., Bauer, L. J., Sherman, C., Edwards, K., Mason, A., Pait, T., & Caldow, C. (2013). *Baseline Characterization of Fish Communities and Associat- ed Benthic Habitats in the Guánica Bay Region of Southwest Puerto Rico* (Vol. 169).

Whitall, D. R., Costa, B. M., Bauer, L. J., Dieppa, A., & Hile, S. D. (2011). *A Baseline Assessment of the Ecological Resources of Jobos Bay, Puerto Rico*. http://aquaticcommons.org/14763/1/jobosbaybaseline.pdf

Williams, N. B., Dixon, B., & Johnson, A. (2011). Estimating soil loss from two coastal watersheds in Puerto Rico with RUSLE. *Interdisciplinary Environmental Review*, *12*(2), 108. https://doi.org/10.1504/ier.2011.040243

Wischmeier, W. H., & Smith, D. D. (1978). Predicting rainfall erosion losses. *Agriculture Handbook No. 537*, *537*, 285–291. https://doi.org/10.1029/TR039i002p00285

Wischmeier, W., Smith, D. D., Wischmer, W. H., & Smith, D. D. (1978). Predicting rainfall erosion losses: a guide to conservation planning. In *U.S. Department of Agriculture Handbook No. 537* (pp. 1–69). https://doi.org/10.1029/TR039i002p00285

Wright, J. K. (1936). A Method of Mapping Densities of Populatrion with Cape Cod as an Example. *Geographical Review*, *26*(1), 103–110. https://doi.org/10.4157/grj.12.378

Wu, S. S., Qiu, X., & Wang, L. (2005). Population estimation methods in GIS and remote sensing: A review. *GIScience and Remote Sensing*, *42*(1), 80–96. https://doi.org/10.2747/1548-1603.42.1.80

Xie, Y., Liu, B., & Nearing, M. A. (2002). Practical Thresholds for Separating Erosive and Non-Erosive Storms. *Transactions of the American Society of Agricultural Engineers*, *45*(6), 1843–1847. https://doi.org/10.13031/2013.11435

Yang, D., Kanae, S., Oki, T., Koike, T., & Musiake, K. (2003). Global potential soil erosion with reference to land use and climate changes. *Hydrological Processes*, *17*(14), 2913–2928. https://doi.org/10.1002/hyp.1441

Yin, S., Xie, Y., Liu, B., & Nearing, M. A. (2015). Rainfall erosivity estimation based on rainfall data collected over a range of temporal resolutions. *Hydrol. Earth Syst. Sci*, *19*, 4113–4126. https://doi.org/10.5194/hess-19-4113-2015

Yogani, G., & Thomlinson, J. R. (2010). Changes in landuse/landcover affect distribution and habitat of the land crab, Cardisoma guanhumi (Gecarcinidae, decapoda) in two estuaries in Puerto Rico. *Caribbean Journal of Science*, *46*(2–3), 258–266. https://doi.org/10.18475/cjos.v46i2.a14

Yu, B., & Rosewell, C. J. (1996). An assessment of a daily rainfall erosivity model for New South Wales. *Australian Journal of Soil Research*, *34*(1), 139–152. https://doi.org/10.1071/SR9960139

Yuan, Y., Jiang, Y., Taguas, E. V., Mbonimpa, E. G., & Hu, W. (2015). Sediment loss and its cause in Puerto Rico watersheds. *Soil*, *1*(2), 595–602. https://doi.org/10.5194/soil-1-595-2015

Zandbergen, P. A., & Ignizio, D. A. (2010). Comparison of Dasymetric Mapping Techniques for Small-Area Population Estimates. *Cartography and Geographic Information Science*, *37*(3), 199–214. https://doi.org/10.1559/152304010792194985

Zhang, B., Zhang, Q., Feng, C., Feng, Q., & Zhang, S. (2017). Understanding land use and land cover dynamics from 1976 to 2014 in Yellow River Delta. *Land*, *6*(1), 1–20. https://doi.org/10.3390/land6010020

Zitello, A. G., Whitall, D. R., Dieppa, A., Christensen, M. E., Monaco, M. E., & Rohmann, S. O. (2008). Characterizing Jobos Bay, Puerto Rico : A watershed modeling analysis and monitoring plan. In *NOAA Technical Memorandum NOS NCCOS 76*. http://data.nodc.noaa.gov/coris/library/NOAA/CRCP/project/20189/Jobos_Bay_CEAPHiRes.pdf Online version in PDF (14.92 MB)

Zoraghein, H., Leyk, S., Ruther, M., & Buttenfield, B. P. (2016). Exploiting temporal information in parcel data to refine small area population estimates. *Computers, Environment and Urban Systems*, *58*, 19–28. https://doi.org/10.1016/j.compenvurbsys.2016.03.004